

AN INTRINSIC SEDIMENT TRACING METHOD USING NATURAL QUARTZ- AND FELDSPAR LUMINESCENCE

A FEASIBILITY STUDY AT THE SAND ENGINE MEGA-NOURISHMENT, TER HEIJDE,
THE NETHERLANDS.

MASTER THESIS

ing. Paul D. Notenboom
MSc. student Coastal Engineering
Delft University of Technology

Sunday, 16 June 2013



*Master Thesis in fulfilment of the requirements for the degree of Master of
Science in Coastal Engineering at Delft University of Technology*

Graduation Committee:

Prof.dr.ir. M.J.F. Stive

Delft University of Technology, dept. of Coastal Engineering

Prof.dr.ir. J. Wallinga

Wageningen University, dept. Soil Geography and Landscape and NCL)

Dr.ir. J.S.M. van Thiel de Vries

Delft University of Technology and Deltares

Dr. T. Reimann

Delft University of Technology and NCL

Daily supervision

M.A. de Schipper MSc.

Delft University of Technology

Daily supervision

'Imagination is more important than knowledge. For knowledge is limited to all we now know and understand, while imagination embraces the entire world, and all there ever will be to know and understand.'

- **Albert Einstein**

Voor mijn opa,
~ **Nicolaas Tuk** ~
1937 – 2012

Page left blank intentionally

PREFACE & ACKNOWLEDGEMENTS

This thesis report marks the final step in obtaining the Master's degree in Hydraulic Engineering, specialization Coastal Engineering at the faculty of Civil Engineering and Geosciences engineering; Delft University of Technology (DUT), Delft, the Netherlands. This project is performed in cooperation with the Netherlands Centre for Luminescence dating (NCL); Wageningen University (WUR), Wageningen, the Netherlands.

The master thesis and feasibility on the development of a new intrinsic luminescence tracing method is closely related to a post-doc research funded by the NWO (Rubicon Grant) executed by geographer Dr. Tony Reimann (*Title: Past coastal sediment-system dynamics in South Holland and the implication of this for present and future coastal change*). The research focuses on the applicability of luminescence in Geo-technical (Geo-morphology) studies to study as sediment-system dynamics.

Two persons have been constantly involved with the project and learned me more than I did ever imagine I would do. They both helped me finish this complex and multidisciplinary thesis report and for that, it is not more than appropriate to thank both Tony Reimann and Matthieu de Schipper for their daily support, thoughts and friendship. I would also like to thank the remainder of my graduation committee; Marcel Stive for being the chairman of my graduation committee, Jakob Wallinga for his support and letting me use the facilities at the NCL and Jaap van Thiel de Vries for his support during this project.

Not the least I like to thank my parents as well as my family for always supporting me in pursuing every endeavour I take. In addition, my friends I like to thank them for their part, in particular: Erwin, Gertjan, Mark and Rob. Moreover, I like to thank Christina, Romee and everyone else that I might have forgotten to mention!

Paul Notenboom

Strijen, June 2013

Page left blank intentionally

ABSTRACT

The goal of a sediment tracer is to give quantitative or relative feedback on (coastal) morphological changes or track either sediment or other particles (e.g. contaminations) in sediment dynamic environments. A sediment tracer is a visible or invisible marked (sediment) grain that is artificially injected or is present in-situ. This Master Thesis main objective is a feasibility study and the development of a new type of sediment tracer. This sediment tracer focuses on the intrinsic luminescence properties of the quartz and feldspar minerals as a measure for sediment transport.

Utilizing an intrinsic property as tracer has a number of advantages over the use of artificial or natural tracers. First the tracer is a guaranteed match to its environment in terms of transport and interaction within the sediment system. The use of artificial tracers is especially problematic in large study areas, because the deploy scope depends on the quantity of injected material to the environment it is placed in. Natural tracers (partly) deal with this problem, since they make use of in-situ material. An example is the utilization of naturally occurring radionuclides. However, they don't account for internal dynamics that can provide insight in the transport history from the original source to the position of deposition. Hence natural tracers are mostly used for provenance studies.

Luminescence is the latent light that is emitted by a mineral after it is stimulated by a source of heat or light. It is a well described phenomenon in sediment grains and the mechanics have a simple analogy to a battery that is charged and uncharged (i.e. luminescence signal is accumulate and depleted). The accumulation of a luminescence signal is triggered by ionizing radiation, which is the product of naturally decaying radioactive isotopes during prolonged burial. The depletion occurs when the grains are exposed to heat or daylight. The rate at which the signal depletes depends on the daylight conditions as well as the depth of immersion in water. This makes every sediment grain a possible data recorder for its own (day)light exposure history or deposition- /erosion history, put in terms of morphology. We hypothesized that the degree of daylight exposure, hence the depletion of luminescence signal during transport, could represent the distance- and/or mode (aeolian, water lain etc.) of transport.

Luminescence is measured in an equivalent dose in Grays. There are a multitude of stimulation methods to recover an equivalent dose from sediment, moreover are each of these methods are coupled to unique luminescence properties. Usually these stimulation methods are tested separately on either a quartz or a feldspar sample. In this thesis we have developed a new protocol to simultaneously retrieve a range of signals (blue light-, (post infrared) infrared light- and thermal stimulation) from a polymineral sample of mixed quartz and feldspar grains. This *Polymineral Multi Signal Single Aliquot Regenerative* protocol, PMS-SAR for short, proved to be representative for separate measurements of quartz and feldspar. Next, we have conducted controlled daylight exposure- or bleaching experiments to investigate the bleaching behaviour per signal. We found that each signal has a unique dynamic bleaching rate and range that differs approximately one order of magnitude.

To test the feasibility as a sediment tracer we have been applying the PMS-SAR luminescence protocol and the results of the bleaching experiments in a test case at the Sand Engine, a mega-nourishment at the Dutch coast. An intensive monitoring campaign at the Sand Engine pilot project has provided bathymetry- and hydrological data. With this data a model is made to investigate the historical evolution of a sand spit that arose at the North-eastern tip of the Sand Engine after construction. Next luminescence measurements were conducted on selected sediment samples taken on the Sand Engine to see whether the results are in accordance with the historical evolution.

The luminescence measurement results from the Sand Engine samples were then reflected upon the bleaching curves to give us the Equivalent Exposure Time (EET). The measurement results reveal an average increase in EET value for the different signals with distance from the first core position, which is consistent with our expectations. In addition to this we could also make a clear distinction between the presumably water lain transported samples and the aeolian sample. These distinct observations reveal the true potential of a multi signal luminescence technique and the use of it in morphological studies. However, these observation were made with very straight forward assumptions, hence to get a more accurate picture that can by appointed to morphological evolution and processes in mega-nourishment additional experiments are recommended.

SAMENVATTING

Het doel van een sediment traceermethode is een kwantitatieve terugkoppeling te geven op morfologische veranderingen of het traceren van sediment of andere deeltjes (e.g. contaminaties) in een dynamische omgeving. Een sediment tracer is een zichtbaar of onzichtbaar gemarkeerde sediment korrel die kunstmatig geïnjecteerd wordt of in-situ aanwezig is in het studie gebied. Het doel van deze Master Thesis is om een haalbaarheid studie verrichten naar een nieuw ontwikkelde traceermethode. Dit nieuwe type tracer werkt op basis van de in kwarts en veldspaat aanwezige intrinsieke luminescentie eigenschappen.

Het gebruik van een intrinsieke eigenschap als traceermethode heeft een aantal voordelen ten opzichte van kunstmatige- of natuurlijk tracers. Het gebruik van kunstmatige tracers is vooral een probleem in omvangrijke onderzoeksgebieden omdat het toepassingsbereik van de tracers afhankelijk is van de hoeveelheid geïnjecteerd traceermateriaal op de omgeving. Het gebruik van natuurlijke tracers lost dat probleem deels op, doordat er gebruik wordt gemaakt van natuurlijk in-situ materiaal. Een voorbeeld hiervan is het gebruik van natuurlijk voorkomende radionuclides. Hoewel natuurlijk tracers uitermate geschikt zijn voor het gebruik in sediment herkomst studies, bezitten ze geen interne dynamiek die een maatstaf kan zijn voor de transport geschiedenis tussen de bron en de afzettingspositie.

Luminescentie is het latente licht dat wordt uitgezonden door een mineraal nadat deze door een bron van warmte of licht wordt gestimuleerd. Dit fenomeen is welbekend en onderzocht, het mechaniek van luminescentie kan worden vergeleken met een op- en afladende batterij (d.w.z. het accumuleren en vervolgens verminderen van het luminescentie signaal). De accumulatie van het luminescentie signaal begint met ioniserende straling als gevolg van natuurlijk vervallend radioactieve isotopen gedurende lange van licht afgeschermd periodes zoals bij begraving. Het verminderen of geheel verwijderen van het signaal gebeurt zodra het sediment wordt blootgesteld aan warmte en/of licht. De snelheid waarmee dit gebeurt is afhankelijk van zowel de licht condities als de mate waarin het sediment is ondergedompeld. Dit maakt van elke sediment korrel een mogelijke data recorder voor de mate van blootstelling aan licht of in morfologische termen de sedimentatie/erosie geschiedenis. Wij nemen aan dat deze vermindering van luminescentie signaal representatief kan zijn voor de getransporteerde afstand en uiteindelijk ook de manier waarop het sediment is getransporteerd.

Het gemeten signaal wordt uitgedrukt in een equivalente dosis in Grays. Er is een verscheidenheid aan stimulatie methodes om deze equivalente dosis in sediment te meten, daarnaast is elke stimulatie methode gekoppeld aan unieke luminescentie eigenschappen. Wij hebben voor dit project een nieuw protocol ontwikkeld dat gelijktijdig en hele reeks aan signalen kan meten van verschillende stimulatie methodes (blauw-, (postinfrarood) infrarood licht en warmte) uit een gemengd polymineraal monster. Hier waar normaal gesproken de metingen gescheiden worden gedaan op gezuiverde kwarts en veldspaat monsters. Dit polymineraal multi signaal protocol (PMS-SAR) bleek na verscheidene experimenten in staat om resultaten te reproduceren vergelijkbaar aan dat van gescheiden metingen. Vervolgens zijn er gecontroleerde blootstellingsexperimenten gedaan om per signaal het blootstellingsgedrag te bepalen. Vanuit deze experimenten kunnen we concluderen dat elk signaal een uniek blootstellingsgedrag toont die enkele orders grote van elkaar verschillen.

Om de haalbaarheid te achterhalen van een sediment traceertechniek gebruikmakend van het PMS-SAR protocol in combinatie met de blootstellinggegevens is een test casus gedaan op de Zand motor, een mega suppletie pilot project aan de Nederlandse kust. Een intensieve monitor campagne heeft ons voorzien in topografische- en hydrologische gegevens. Met deze gegevens is er een model opgesteld om de historische evolutie van de aan de Noord oostelijke zijde ontstane zandspit te onderzoeken. Vervolgens zijn er luminescentie metingen verricht op geselecteerde sediment boringen en een eolisch monster die genomen zijn ter hoogte van de zandspit. Dit om te onderzoeken of de luminescentie waardes een beeld vormen in overeenstemming met de geobserveerde evolutie.

De resultaten van de luminescentie metingen van de geselecteerde Zand motor monsters zijn vervolgens gespiegeld aan het blootstellinggedrag om ons een Equivalente Blootstellingtijd (EET) op te leveren. In de resultaten hiervan kunnen we goed een oplopende trend van meerdere signaal EET waardes met vermoedelijk transport afstand onderscheiden. Daarnaast kunnen we ook een duidelijk verschil onderscheiden tussen ondergedompeld- en eolisch getransporteerde monsters. Deze waarnemingen zijn in de lijn der verwachting en gaan daar zelfs aan voorbij omdat de trends zo goed zichtbaar blijken. Deze observatie onthult het werkelijke potentie van deze intrinsieke luminescentie sediment traceertechniek. Moet daar bij worden aangemerkt dat deze observaties zijn gebaseerd op relatief simpele aannames, om een beter beeld te kunnen krijgen van morfologische processen bij mega suppleties worden verdere experimenten zeer sterk aangeraden.

TABLE OF CONTENTS

Preface & Acknowledgements	ii
Abstract	iii
Samenvatting	iv
I. Chapter 1: Introduction	1
1.1 Research background.....	3
1.1.1 Artificial tracers	3
1.1.2 Natural tracers	3
1.1.3 Natural luminosity sediment tracing.....	4
1.2 Relevance of the project	5
1.3 Research question & objectives	5
1.4 Readers guide	6
II. Chapter 2: Luminescence physics	7
2.1 Luminescence in sediments.....	8
2.1.1 History	8
2.1.2 Quartz, feldspar and Polymineral	8
2.2 Physical background.....	9
2.2.1 Trapping, storage & eviction.....	10
2.3 Luminescence research.....	12
2.3.1 Luminescence sediment tracing technique	12
2.3.2 Bleaching behaviour	14
2.3.3 Environmental bleaching.....	15
III. Chapter 3: Sand Engine site & Field data	17
3.1 Sand Engine pilot project	18
3.2 Bathymetric monitoring	19
3.2.1 Bathymetry measurements	19
3.2.2 Bathymetry observations.....	20
3.3 Sediment sampling	22
3.3.1 Sediment core boring.....	22
3.3.2 Sample strategy.....	23
3.3.3 Aeolian sample	27
3.3.4 Sedimentology	27
IV. Chapter 4: Luminescence measurements	29
4.1 Signal measurement.....	30
4.1.1 Sample preparation.....	31
4.2 Luminescence measurement protocol.....	31
4.2.1 Polymineral Multi-Signal Single Aliquot Regenerative dose protocol (PMS-SAR)33	
4.3 Performance test of PMS-SAR protocol	35
4.4 Sand Engine luminescence results.....	36
4.4.1 Signal characteristics	37
4.4.2 Bleaching experiment.....	39
4.4.3 Effective Exposure Time (EET)	41

V.	Chapter 5: Application synthesis	43
	5.1 Luminescence signal analysis.....	44
	5.1.1 Equivalent Exposure Time (EET) results	44
	5.1.2 Sediment source.....	45
	5.1.3 Transport distance	47
	5.1.4 Mode of transport.....	49
	5.2 Discussion	51
	5.2.1 Capabilities	51
	5.2.2 Pitfalls.....	52
	5.2.3 Feasibility.....	52
VI.	Chapter 6: Conclusion & Recommendations	53
	6.1 Conclusion.....	54
	6.2 Recommendations.....	54
	References	56
	List of figures	59
	List of tables	60
	Appendix 1: Summary recent studies	61
	Appendix 2: Core sample details	62
	Appendix 3: Polymineral performance test	64
	Appendix 4: Core sample measurements	65
	Appendix 5: bleaching experiment measurements	67

CHAPTER 1: INTRODUCTION



UNDERSTANDING COASTAL SEDIMENT TRANSPORT DYNAMICS IS OF GREAT IMPORTANCE FOR DESIGNING MEGA NOURISHMENTS, FOR EXAMPLE THE 'SAND ENGINE' NEAR TER HEIJDE, THE NETHERLANDS. THE 'SAND ENGINE' PILOT PROJECT IS CLOSELY MONITORED USING BATHYMETRY MEASUREMENTS AND AERIAL PHOTOGRAPHS. HOWEVER, THESE DO ONLY PROVIDE BOTTOM ELEVATION INFORMATION ON A MONTHLY RESOLUTION. TO STUDY THE RELATIVE CHANGES A SEDIMENT TRACING TECHNIQUE IS DEVELOPED USING THE INTRINSIC LUMINESCENCE PROPERTIES OF SEDIMENT AT A LATER STAGE AN APPLICATION TEST IS CONDUCTED TO TEST THE FEASIBILITY. FIRST AN INTRODUCTION WILL BE MADE INTO SEDIMENT TRACERS.

The Sand Engine in July 2011¹

¹ Rijkswaterstaat / Joop van Houdt

Coastal morphology is a contemporary part of more general morphology, which translates into the study of shape or the shaping of. Coastal morphology in particular focuses on the interaction between water and sediment and the resulting changes on the coasts. Monitoring changes in the landscape is one of the prime subjects in morphologic research. In the natural landscaping of deltas, estuaries and beaches water plays a dominant role because of its eroding power. Especially in areas where interactions with waves, tidal currents or any fast flowing stream for that reason the landscaping power of water becomes strongly visible. Most natural landscaping timescales are in the order of centuries-millennia. However, anthropogenic intervention changes the landscapes much faster, mining operation for example have a big impact on the landscaping.

Countless studies have been conducted on the processes that govern the dynamics of sediment bodies under hydrodynamic or aeolian loads. Still no study can describe or understand fully what happens to the morphology during e.g. a short energetic event like a storm or long(er) term changes. Monitoring coastal morphology on a large scale proves to be a very difficult or even impossible task. The monitoring of coast is mainly based on bathymetry measurements with echo sounding type techniques. The biggest downside of this type of monitoring is the fact that it will only show absolute changes in the coastal profile at the moment of monitoring if compared with earlier measurements. Most sediment studies are based on these absolute changes. However, absolute change can hardly distinguish provenance or relative changes.

Sediment tracing or particle tracking are methods that can give quantitative or relative feedback on (coastal) morphological changes. The goal of a sediment tracer is to visualize or track sediment or other particles (e.g. contaminations) in sediment dynamic environments. A sediment tracer is a visible or invisible marked (sediment) grain that is artificially injected or is present in-situ. In a test case the Sand Engine mega-nourishment (3.1) will be utilized to test a new development in sediment tracing.

Sediment tracing is mainly used to study provenance, in other words to investigate sources and sinks of sediment within a dynamic system. The second one is erosion process tracing, this focuses on the erosion and sedimentation of riverbeds or coastal beaches. The tracer must meet certain criteria in order for it to properly represent and interact with the environment (see Table I-1).

No.

- | | |
|----|---|
| 1. | The tracer hydraulic and bio-organic properties mimic those of the sediment of interest, and therefore the tracer is transported in the same fashion as native sediment |
| 2. | The tracer does not change properties through time (at least over the timescales of interest) and can be monitored |
| 3. | The tracer does not manifestly change the transporting system in any way |

Table I-1: Assumptions on the use of tracers in particle tracing studies (after Foster 2000)

One of the earliest experiments with particle tracers for scientific purposes is the brickbat study of Richardson (1902) on long shore transport of gravel on Chesil Beach, UK. However, it was not until the 1950s and early 1960s that serious development of tracing technique took place, starting with the development of radioactive tagged particles (Black et al. 2007). Development of tracers as well as particle tracking has experienced a resurgence of interest and application by geologists, hydrologists, oceanographers and engineers principally as a result of the arrival of new, innovative manufacturing and measurement techniques (Black et al. 2007). However, the techniques in existence today do not provide a fully 100% representation of natural properties, in terms of density and grain-shape and also being hazard free. These properties as grains size etc. matter because they are governing for the sediment transport dynamics.

Sediment tracer studies suffer from many practical problems as where to sample for a good representative sample or the ratio of injected mass to study area (i.e. having a too small injection mass compared to the study site will result in a dilution problem, were the tracer becomes the needle in the haystack). Still difficult and laborious (artificial) sediment tracer studies are still employed for lack of a better alternative for monitoring e.g. bed load transport (White 1998).

1.1 Research background

Tracers can be generally divided into two categories, one being the artificial tracers and the other being natural tracers. Artificial tracers need to be injected into the study environment as where natural tracers involve properties of in-situ material e.g. natural magnetism, natural colour differences etc. The tracing and measuring of elements like natural radionuclides are brought under intrinsic tracers as most of these radionuclides are enclosed in the sediment material.

1.1.1 Artificial tracers

There are several types of artificial tracers. The simplest yet effective artificial tracers are dyed grains of sediment. Synthetic artificial tracers as (fluorescent) coated glass beads (Ventura et al. 2001) or coloured plastics (Grasso et al. 2011) (Figure I-1) are an example of more advanced artificial tracers. Keeping grain extrinsic properties (e.g. grain size, roughness etc.) and the intrinsic properties (e.g. specific weight) equal is crucial for the accuracy of the tracer in representing the environmental sediment transport conditions. This is one of the major difficulties of using artificial sediment tracers. There is a very complex interaction and composition of particles at a coastal site; in fact, no sediment grain is the same.

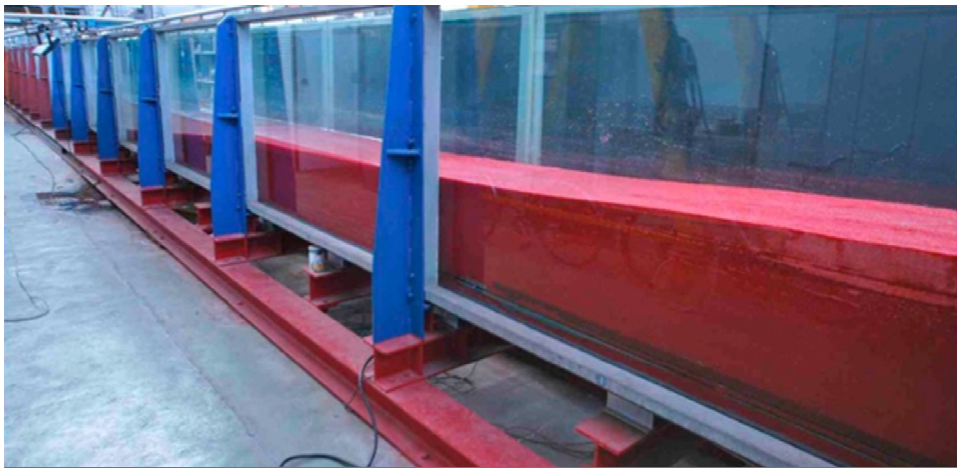


Figure I-1: Coloured plastic tracers in an experimental flume (www.florentgrasso.com)

The use of dyed sediment requires a relatively large ratio of injected material i.e. dyed sediment to the environment that is studied. In river systems the study area is controlled by the water edges. However, estuaries or coastal areas are not bound at the seaside, therefore giving less control over the sediment tracing material. This is one of the main reasons why the latter kind of tracers are more commonly used in river and estuary studies. The employability of an artificial sediment tracer in coastal environments is as such limited due to the rapid dilution of tracer material. Another disadvantage of using artificial tracers is the potential negative environmental impact of dyed- or synthetic material.

1.1.2 Natural tracers

Tracers using in-situ sediment are called natural tracers. Natural tracers can depend on visible properties of sediment e.g. grain size, natural colour etc. or markers that coexist with the sediment (e.g. specific types of elements). Compared to artificial tracers making use of the in-situ sediment deals partially with the problem of dilution since there is no dependence on the input of material. However, with natural tracers it is important to know in which quantities they exist on the study site, the durability against weathering during sediment transport (see Table I-1, point 2) and if these tracers wear down could this be quantified or related to the morphology

Natural sediment tracing techniques with environmental radionuclides, e.g. natural occurring radioactive isotopes as ^{137}Cs , $^{210}\text{Pb}_{\text{ex}}$, ^7Be and ^{40}K (found in feldspars) are used to investigate mobilization and transport of fine sediments in river catchment areas (Walling 2003).

Another natural tracing technique uses multiple naturally occurring geochemical elements to act as tracers. Geochemical tracers proved its importance in identifying and tracing sediment (e.g. Fu et al. 2006 in an Australian coastal catchment). The problem with these radionuclide tracers is that they do not always appear in the same quantity at every site and the interpretation of these tracers is also very complex because the elements are dynamically independent from each other, rather than act as a single entity.

Environmental magnetism is a technique that uses the internal magnetic properties of mineral as tracers. Examples of environmental magnetism in a sediment provenance studies are by Rotman et al. (2008) in a managed realignment shore or e.g. studies studying soil erosion with (synthetic) magnetic tracers (Van der Post et al. 1995, Ventura et al. 2001). Environmental magnetism is the closed to a full field based sediment-tracing technique today, since most grains are to some degree magnetic or contain magnetic minerals. However, in most environments the natural magnetic properties are too low to detect by modern detectors. For an accurate result the use of synthetic magnetic tracers with far more magnetic is a must, thus referring back to an artificial tracer and the dilution problem.

1.1.3 Natural luminosity sediment tracing

In this study we are focussing on an intrinsic property of sediment: luminescence. Luminescence is closely related to environmental radionuclides. Radionuclides as well as cosmic radiation are the prime sources exciting a luminescence signal in sediment, how this is related and the general physics of luminescence are described in Chapter 0. Using the natural luminosity as a tracing technique was first proposed by Forman (1990). He studies the retreat of a glacier by analysing the (thermal) luminescence properties of glacial sediment at Spitsbergen, Svalbard.

The main application of sediment luminescence until recent has been the dating of sediments like quartz and feldspar for geological and archaeological purposes. Usually luminescence is used to determine depositional ages for geological or archaeological layers in the age range of 10 to 300.000 years. In this study, the technique will be applied as a measure for very recent sediment transport within a mega-nourishment, where typical timescales are in the order of days to weeks or even shorter depending on the forcing dynamic at the bed level. Its feasibility will be both tested for its provenance monitoring capabilities as well as erosion process tracing.

The choice of luminescence measurement method depends on which aspect/property of sediment is studied and to what goal. Luminescence in natural minerals can either be stimulated by heat (Thermo luminescence, TL) or light (Optically Stimulated Luminescence, OSL). Furthermore, the luminescence can be measured from a bulk luminescence signal of multiple-grain (MG) subsamples (termed aliquot) or single grains (SG).

One of the first suggestions to use (quartz) luminescence for sediment tracing in coastal processes was by Rink (1999). Since then there have been a number of papers and studies trying to utilise luminescence as a light-sensitive indicator in sediment transport research. Recently, Keizars et al. (2008) proposed to utilise the natural residual thermoluminescence (NRTL) of quartz as a method for the analysis of sand transport along a beach stretch of 20 km in the St. Joseph Peninsula, Florida, USA. They found empirical relations between the NRTL signal of samples along the coast and daylight exposure experiments. Liu et al. (2011) apply both TL and OSL for the monitoring of long shore movement of nourished sands with feldspar luminescence and relates both outcomes to each other. Clear conclusions from this paper are that TL is preferred for long-term near shore studies because it is less sensitive to sunlight exposure. Where OSL is more sensitive to sunlight exposure and thus is preferred for short-term (event scale) sediment transport studies in a limited area.

Another recent study by Sawakuchi et al. (2012) uses quartz OSL sensitivity of single-grains as a proxy for storm activity on the southern Brazilian coast during the late Holocene (6000 years ago – present). The study was preceded by studies studying the provenance of different rock sources of sediment culminating along the same coastal stretch originating from one supplying river and depositional history (e.g. erosion and sedimentation cycles) of quartz grains by using

thermoluminescence sensitivity as proxy for repetitive erosion-transport-deposition cycles (Sawakuchi et al. 2008, Sawakuchi et al. 2011). They found, taken into account earlier conclusions on the difference in sensitivity of sediments in dependence of their source rock, that the difference in depositional sedimentary history (read: high or low OSL sensitivity) shows a discrimination between transport under fair- or storm conditions of sediments along the coast. More details on these three studies can be found in Appendix 1.

All three studies are good examples of luminescence applied to sediment transport and provenance analysis, though not definite, the combination of both shows great potential and just as much room for more research. This study an experimental luminescence protocol will be developed in order to enhance measurements with quartz OSL, feldspar IRSL and TL measurements. With this protocol it will be possible to read short-term to long-term processes at the same time, hence enhancing the dynamic measure range of sediment tracing. This will also involve a daylight exposure experiment to relate luminescence values to morphological processes. The Sand Engine will act as a unique natural laboratory and monitoring program from which we can derive a 'known' depositional history feedback on the luminescence results. This provides the ideal conditions to study for the first time the (full) potential of luminescence sediment tracing. Ultimately the goal is to map and monitor (coastal) morphological changes using this luminescence tracing technique.

1.2 Relevance of the project

As it was said, the concept of sediment tracing has been around since a century. It is one of the few ways in distinguishing provenance or relative morphological changes in a sediment dynamic environment. However, in pursuing this endeavour it became obvious from the first experiments over a hundred years ago that the implementation can be a very complex affair. Referring back to the three main requirements of a good tracer (Table I-1) a luminescence-based tracer fulfils all of them. Using the luminescence properties of sediments has a number of advantages in comparison to artificial tracers or natural tracers. Luminescence, as an intrinsic property, exists in the most common minerals found on earth (feldspar and quartz). Feldspar and quartz account for >90% of the coastal sediment at sandy beaches. Thus, most of the particles at a beach can potentially be used for sediment tracing. The techniques and theories for measuring luminescence are well investigated. These tracer technique, unlike artificial tracers or other natural tracers, shares 100% natural properties with the surrounding sediment in terms of density, grain-shape and the interaction between, also they are unlimited available and hazard-free. Tracers of this kind provide a guaranteed hazard-free application and do not need any pre-study treatment(s) like irradiation or dying.

However, luminescence needs more research and development before one could use it with certainty and apply it to any sediment dynamic environment. In 1.1.3 some recent studies have applied luminescence in an effort to reveal details in the sediment transport of a specific area. Each one applies slightly different luminescence approach (i.e. signal, research purpose etc.). Between the studies the (morphological) timescales do also differ or there is no indication of them at all. More detailed research and more complex theories have to be developed would luminescence be used as a common tool by (coastal) morphology researchers.

1.3 Research question & objectives

There is great potential for the appliances of luminescence as a sediment tracing technique. However, there are many questions surrounding the exact way to apply the technique in morphological processes in the order of months to years. From earlier works of Liu et al. 2011, a difference between signals (OSL and TL) can be assumed to relate to differences in sedimentary history. In this project luminescence measurements will simultaneous comprehend blue, (post-infrared) infrared stimulated OSL, as well as TL. Addressing the possibility to make and monitor distinctions between different morphological processes.

Quartz OSL signals decrease very fast under daylight exposure during sediment transport. However, under same exposure conditions the TL decreases much slower in signal. The idea is that this post-IR stimulated signals have an intermediate signal decrease character and with this a more detailed fingerprint of the sedimentary history of a sample can be made. Eventually these differences can be ascribed to transport distance, different modes of transport, sedimentation/erosion cycles or e.g. improve the quantification of sediment provenance. With the research goals mentioned above a research question can be defined as:

Could a multi signal luminescence protocol be applied as an accurate technique for tracing sediment particles and sedimentary transport history at a mega nourishment ?

To answer this question some objectives are listed:

- Analyse and gather (pre-luminescence testing) monitoring data to reconstruct where, at what time and under which conditions the retrieved samples were likely to have been deposited and how far it was transported before;
- Develop a luminescence protocol that comprehends quartz OSL, feldspar IRSL, feldspar post-IR IRSL and TL stimulation in order to simultaneously monitor short-term, mid-term and long-term coastal sedimentary processes;
- Extend the gathered data results by this protocol to make a distinction between e.g. transport distance, mode of transport etc. Are there confident patterns that relate to monitoring data and theory;
- Evaluate the feasibility of luminescence as a tool to understand sediment-system transport dynamics in mega nourishments.

In this thesis the performance of a multi luminescence signal protocol is explored. On top of this a sediment transport study using luminescence is looking at the morphological changes in the 'Sand Engine' near Ter Heijde, the Netherlands from its completion in November 2011 until sediment sampling in May/June 2012. During this period the Sand engine was closely monitored to support ongoing and future research. A new protocol as well as a practical application at the Sand Engine will be assessed in this thesis.

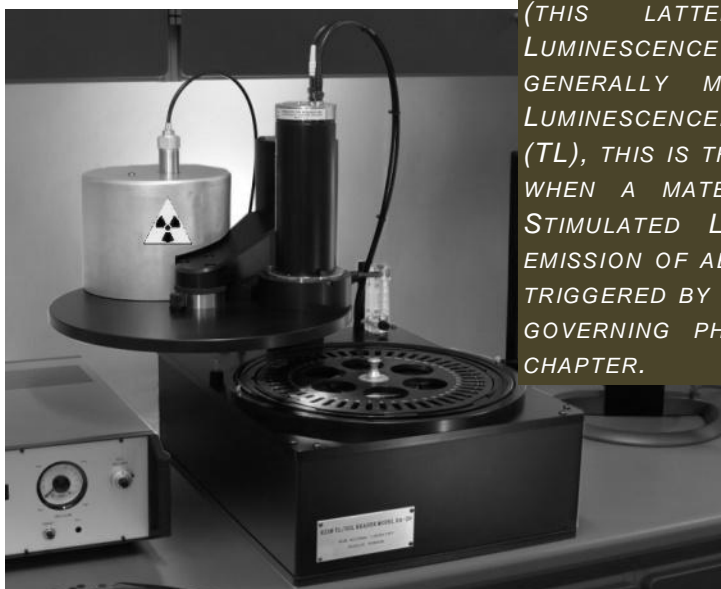
The master thesis and feasibility study is closely related to a post-doc research funded by the NWO (Rubicon Grant) executed by geographer Dr. Tony Reimann (Title: ***Past coastal sediment-system dynamics in South Holland and the implication of this for present and future coastal change***). The research focuses on studying the applicability of luminescence in Geo-technical (Geo-morphology) studies like sediment-system dynamics. The work is a collaboration between the Delft University of Technology (DUT) sections of Hydraulic Engineering and Applied Physics more specific Coastal Engineering and the Netherlands Centre for Luminescence dating (NCL).

1.4 Readers guide

The thesis will start with the introduction on the general physics behind luminescence in sediments (Chapter II). The second part is the analysis of the observed morphology in the 'Sand Engine' mega-nourishment as well discuss the collection/selection of field data for the luminescence measurements (Chapter III). The next part on luminescence will be based on experimental tests done in the NCL lab to find and improve a protocol satisfying the hypothesis as well as the daylight exposure experiment (Chapter IV) Finally the application feasibility will analysed and discussed (Chapter V) to end with conclusions and recommendations (Chapter VI).

CHAPTER 2: LUMINESCENCE PHYSICS

LUMINESCENCE IN GENERAL MEANS THE EMISSION OF LIGHT OUT OF A SOLID MATERIAL WITHOUT REACHING ITS GLOWING TEMPERATURE (THIS LATTER IS CALLED INCANDESCENCE). LUMINESCENCE IN GEO-SCIENTIFIC STUDIES GENERALLY MAKE USE OF TWO TYPES OF LUMINESCENCE. KNOWING, THERMOLUMINESCENCE (TL), THIS IS THE RE-EMISSION OF ABSORBED LIGHT WHEN A MATERIAL IS HEATED AND OPTICALLY STIMULATED LUMINESCENCE (OSL) THERE THE EMISSION OF ABSORBED LIGHT OUT OF MATERIAL IS TRIGGERED BY MEANS OF LIGHT STIMULATION. THE GOVERNING PHYSICS WILL BE TREATED IN THIS CHAPTER.



Luminescence Reader (© Risø National Laboratory, Denmark)

Luminescence is an intrinsic property of mineral grains and is stored within its internal structure. This luminescence property is most commonly used as a tool to determine when mineral grains were last exposed to daylight before burial, providing insight in the age of an archaeological artefact or geological site. The two commonly used luminescence techniques are Thermoluminescence (TL) and Optically Stimulated Luminescence (OSL). In the case of TL heat is used to stimulate the luminescence signal out of the mineral grains. OSL uses visible light to stimulate the luminescence signal out of the mineral grains. Thermoluminescence (TL) or Optically Stimulated Luminescence (OSL) are most commonly used for dating pottery or sediments. Currently, the vast majority of geo-scientific luminescence research is about improving the dating accuracy and precision as well as extending the age range of TL and OSL dating (Wintle, 2008). However recent luminescence studies (see 1.1.3) propose the potential use of luminescence on a wider range of applications e.g. sand transport dynamics. In that case the focus moves to other aspects of luminescence e.g. signal decay (bleaching) or behaviour of TL- and OSL signals (2.3.2).

2.1 Luminescence in sediments

The general physical mechanism driving the production of luminescence can be described in three steps: trapping, storage and eviction (see 2.2.1). These are triggered by the decay of naturally occurring radioactive isotopes. Subsequently more information is given on the luminescence applications and the new application and environmental aspects (see 2.3).

2.1.1 History

Thermoluminescence was developed in the 1960's for dating ancient pottery (e.g. Aitken et al. 1964). From the late 1970's this was expanded to dating geological sediments (e.g. Wintle and Huntley 1979b). For the TL signal to be completely reset to zero, heat is needed. In a baking process of pottery enough heat is generated to reset the TL signal. In a natural geological setting TL is zeroed due to daylight exposure, which is less effective zeroing the luminescence signal. Optically Stimulated Luminescence (OSL) as a tool for dating sediments was first proposed by Huntley et al. (1985). The main advantage of OSL is that the resetting of these signals during daylight (e.g. sediment transport) is an order of magnitude faster than TL signals (Godfrey-Smith et al., 1988). This zeroing is crucial for accurately determining depositional ages in most sedimentary environments.

2.1.2 Quartz, feldspar and Polymineral

Most luminescence studies make use of two types of minerals: quartz and feldspar(s). In a typical coastal sandy beach environment such as the Dutch coast both minerals will make up for >95% of all material. Depending on the degree of weathering and supply of sediments (e.g. river outflow) the most abundant mineral in a coastal sediment system is quartz. Typical for quartz is that most grains are translucent and are neither easily weathered nor sensitive to chemicals. In Figure II-1 a microscopic picture is given of a luminescence test sample in which grains of both quartz and feldspar are highlighted.

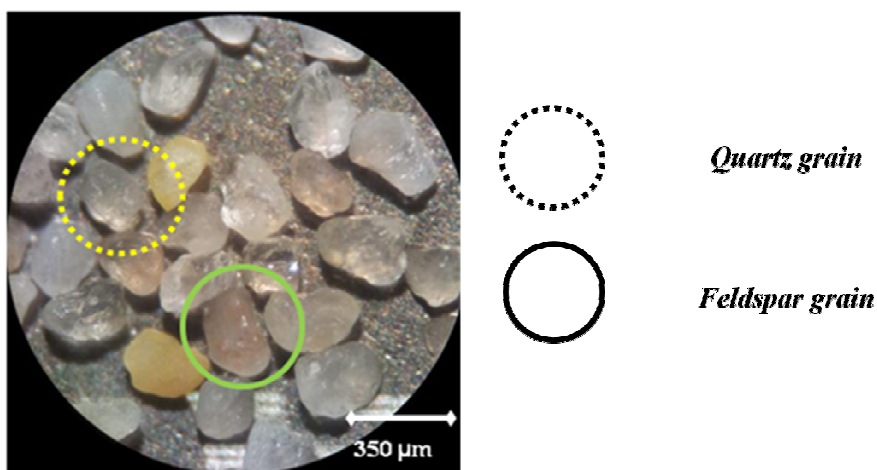


Figure II-1: Microscopic picture of minerals (luminescence test sub-sample)

The effective bleaching time (time to deplete a signal due to exposure to light) is a decisive factor for choosing which mineral to use in a particular luminescence study (Wallinga 2002). Quartz bleaches significantly faster under full day light conditions than feldspar (Godfrey-Smith et al. 1988). However, the opposite might be true for stimulation under an altered light-spectrum (wavelength). This is the case when a sample is bleached under submerged conditions where part of the light-spectrum is absorbed (Hansen et al. 1999, Sanderson et al 2007).

Feldspars exist in various types. Most important for luminescence research are the potassium-rich (^{40}K) feldspars, because they produce a brighter and more stable luminescence signal compared to other feldspars. The feldspars, however, are less robust against weathering and tend to have locked in contaminations of other materials and have a more inhomogeneous crystal structure than quartz. This implies that feldspar luminescence measurements are more affected by undesirable signal contributions.

The preparation of subsamples consisting out of pure quartz- or feldspar involves sieving, several chemical treatment steps and density separation of the minerals (4.1.1). To avoid this last laborious step(s), polymineral sub-samples are examined, containing both the quartz- and feldspar fractions. However, this cannot be done without adapting the measurement procedure. Therefore for one sediment sample the performance of this polymineral approach including a newly developed measurement protocol is compared with conventional measurements with density separated quartz and feldspars sub-samples (see 4.3).

2.2 Physical background

Four types of radiation contribute to the accumulation of luminescence signals in sediment. These four are the alpha particles, beta particles (electrons), gamma rays and to some degree the cosmic radiation. Their respective contribution depends on the penetration power of radiation per type into the mineral. An illustration of these four types is given with an indication of the penetration depth (Figure II-2); here also a distinction is made between cosmic, external and internal origins. The existence of this radiation is due to the decay of small quantities naturally occurring radioactive isotopes e.g. Thorium-232, Uranium-238 or Potassium-40. The biggest contribution inducing a luminescence signal is arising from beta particles (β) and gamma rays (γ). However, alpha particles (α) don't have enough penetration power, hence they are only affecting the outer rim of mineral grains. Cosmic radiation accounts for approximately 10% of the total radiation that affects the sample.

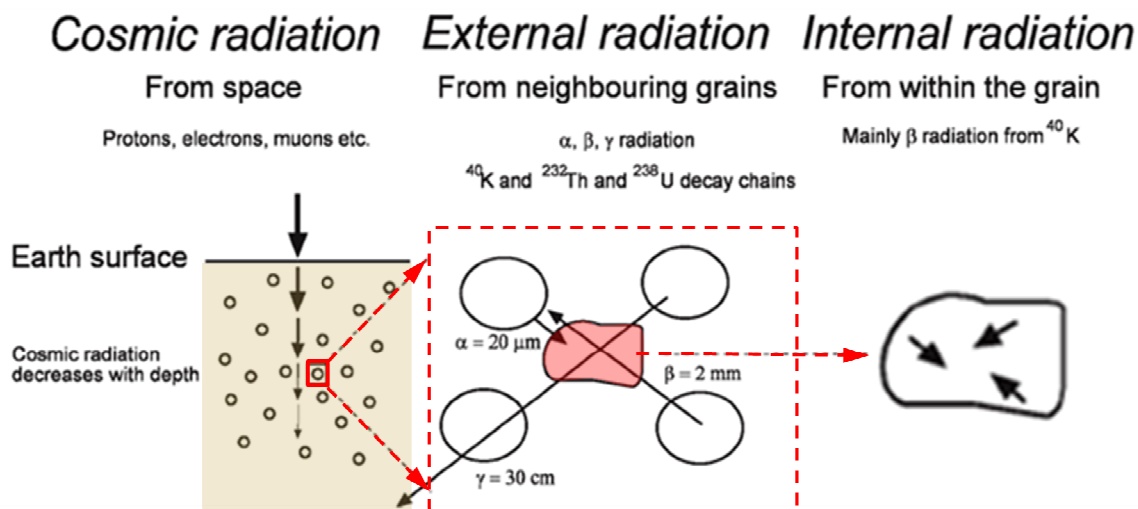


Figure II-2: Different components contributing to accumulation of luminescence signal (modified from Preusser et al. 2008)

2.2.1 Trapping, storage & eviction²

The luminescence production in minerals can be ascribed in a three step physical process: Trapping, storage and eviction. This process is started by the decay of naturally occurring radioactive isotopes. Radioactive decay or radioactivity is an ionisation energy. Ionization energy describes the amount of energy that is needed to remove an electron from an atom or molecule. The basic luminescence mechanism is that this ionising radiation (**irradiation**) causes the excitation of electrons within the crystal lattice of a mineral, leading to electrons at higher energy states (Preusser et al. 2008). This is easiest explained in an energy level diagram. This energy level diagram is also called the 'band gap model'. In Figure II-3 two such diagrams show first the trapping- (irradiation) and the storage step, the second diagram in

Figure II-4 shows the eviction process. The valance band represents an energy level range in which electrons move around a local atom and cannot move throughout the crystal. However, the conduction band in this model is where electrons, when given enough energy, can move delocalized from their atom and freely throughout the crystal. Electrons exiting the valance band, travelling through the band gap into the conduction band, cause a charge deficit or hole in the valance band to appear. Because of the energy equilibrium this charge deficit within the crystalline structure forms a recombination centre or luminescence centre denoted with a 'L' in the band-gap. An electron in the conduction band loses energy whilst travelling that at some point the energy level is reduced such that a travelling electron falls back into the band gap. In a perfect crystal this electron would always fall back into the valance band. However, most naturally occurring crystals are inhomogeneous or doped with other elements causing the existence of luminescence traps. Some of the electrons will get caught or 'trapped' in these luminescence traps (denoted with 'T' in the energy level diagram) in the band-gap.

² Based on Preusser et al. 2008

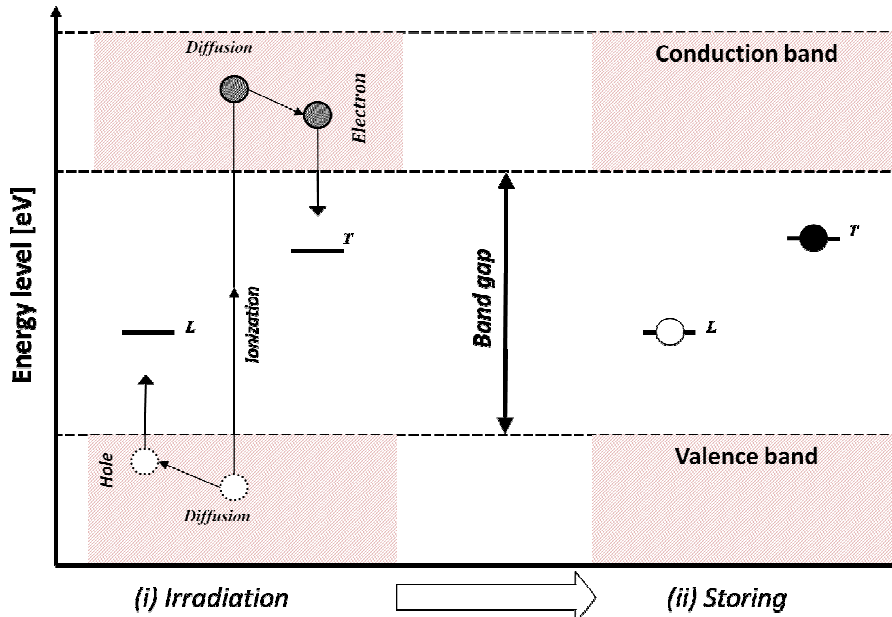


Figure II-3: Energy level diagram (modified from Aitken 1998)

Repetitive cycles gradually produce more trapped electrons in the mineral. These electrons are **stored** there until the mineral is stimulated with a certain energy to release the charge. This is what happens during luminescence measurements. This release of trapped electrons is called **eviction** (Figure II-4). Eviction can be induced in the mineral when either exposing it to heat (TL) or light (OSL). Electrons that are evicted from their traps move back up into the conduction band, because of the addition of energy. Eventually these electrons will fall back into the band-gap recombining in the luminescence centre (that was the result of the charge deficit) that was created during the irradiation process. As a product of this recombination process light photons are emitted (luminescence). When light is the source of stimulation the light that is emitted as a result of the recombination process will have a shorter wavelength. Shorter light wavelength are higher in energy than longer wavelengths. This shortening of the wavelength is due larger energy difference between recombination centre and conduction band than between the traps and conduction band .

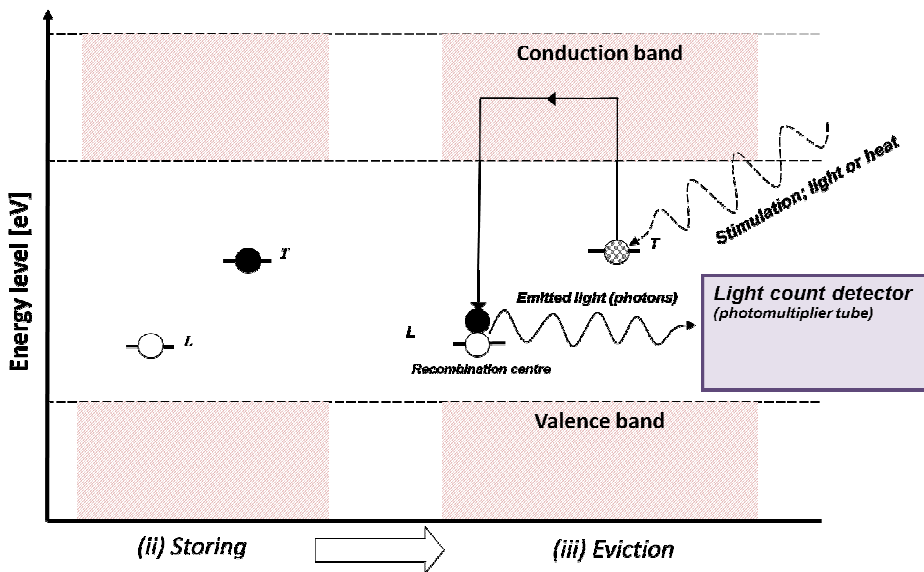


Figure II-4: Energy level diagram (modified from Aitken 1998)

These photons are measured during a luminescence measurement and form a measure for the charging and ultimately the total burial time of the sediment. For more details and information

the reader is referred to more specialized literature on luminescence production in sediments (e.g. Aitken 1998, Wallinga 2002, Preusser et al. 2008).

2.3 Luminescence research

Most luminescence research is focussed on improving dating applications of sediments or archaeological artefacts. The age of a sample is determined on the basis of the ratio between total during burial accumulated luminescence signal and the rate in which this accumulation took place. This accumulation rate or dose rate is determined by measuring the concentration of natural occurring radioactive isotopes in the sample (^{238}U , ^{232}Th , ^{40}K) and considering the contribution of ionizing cosmic radiation (cosmic dose rate).

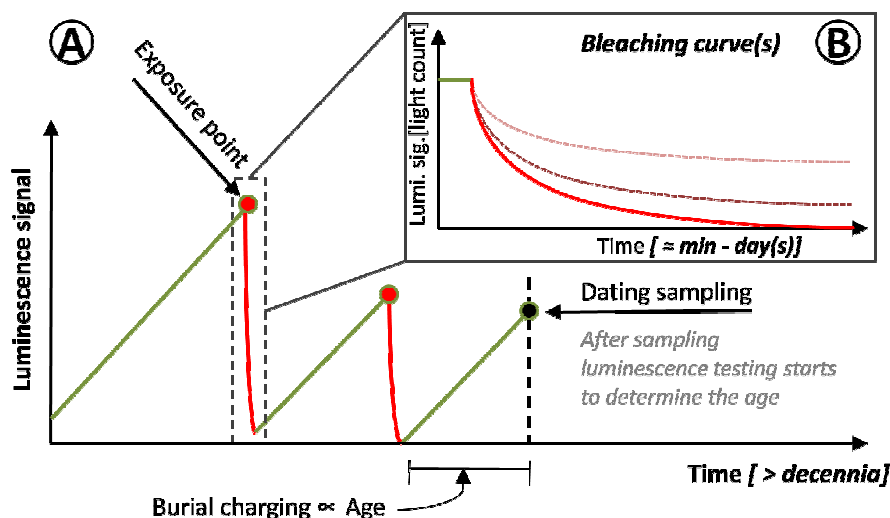


Figure II-5: Schematic sediment age determination. (A) Burial cycles; accumulation and resetting. (B) Example of bleaching curve(s) during exposure.

In Figure II-5 a schematic example of a sedimentary history that shows luminescence accumulation (green) versus zeroing (red) events. The accumulation rate is several orders of magnitude slower than the signal zeroing. For an accurate age determination this signal should be fully zeroed pre-burial since the age is proportional to the accumulated luminescence signal. A residual dose from partial bleaching could possibly cause an overestimate the sediments' age.

2.3.1 Luminescence sediment tracing technique

The coastal zone is a constantly changing environment. In Figure II-6 an overview is given of coastal sedimentary- and morphology phenomena and their scales. In the overview the aspect(s) of the Sand Engine is categorized in between rips/dunes and sand bars. However, the Sand Engine mega-nourishment is rather an anthropogenic or human intervention than a natural phenomena such as sand bars. These temporal- and spatial scales are much faster than typical geological landscapes (centuries – millennia) on which most (coastal) luminescence dating application are used (e.g. Reimann & Tsukamoto 2012; <500 years).

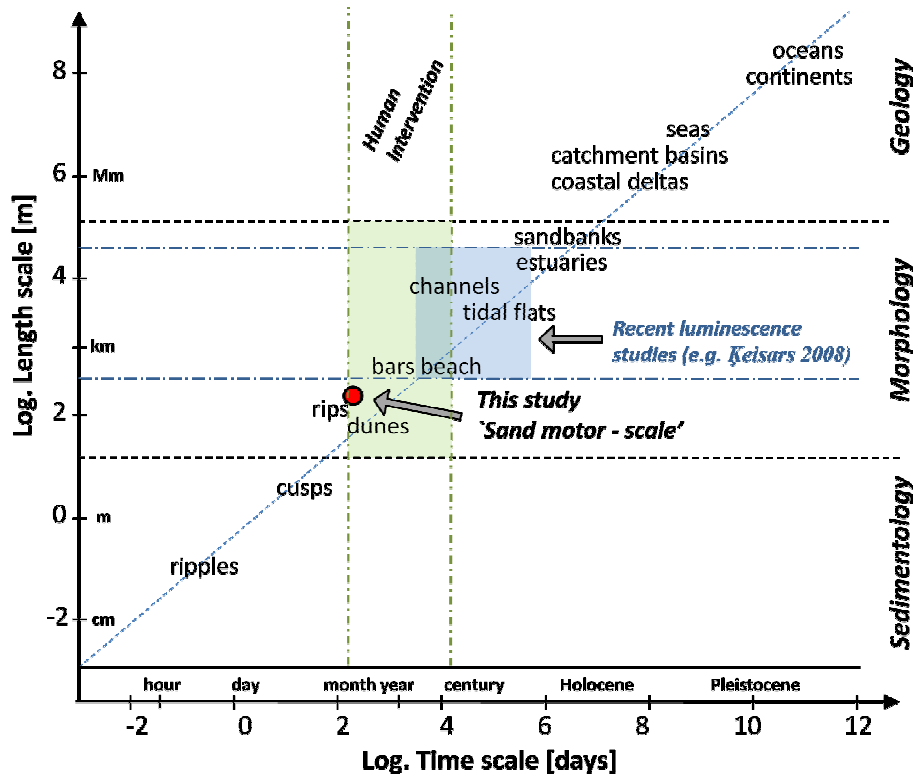


Figure II-6: Coastal phenomena time- and length scales (Modified from Dronkers 2005)

The temporal scales (weeks to months) of coastal morphological changes are minimally an order of magnitude faster than the average resolution of luminescence dating which is in the order of years (e.g. Ballarini et al., 2003). Thus, compared to conventional age calculation studies, luminescence dating is not suitable to investigate these morphological changes we are interested in. However, as seen in the insert of Figure II-5, there is a luminescence process that acts on a much shorter temporal scale, pointing out the bleaching process of signal in sediments. The concept for a luminescence tracer technique is based on this bleaching process.

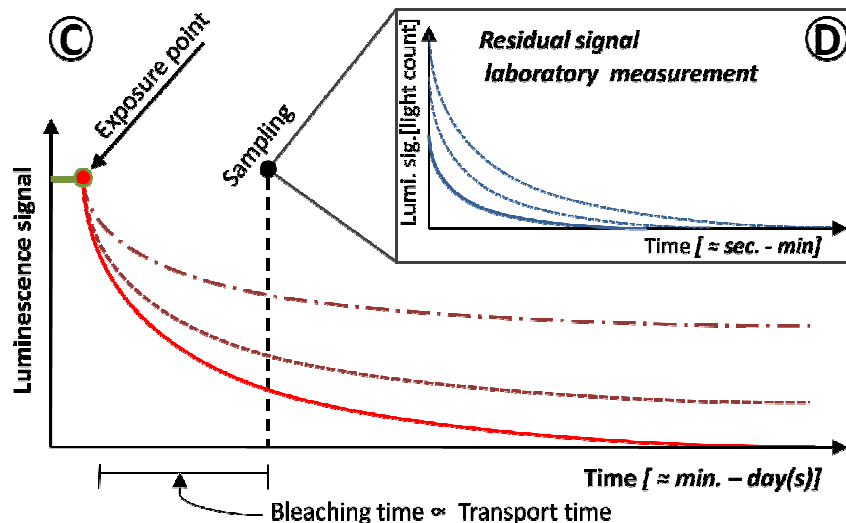


Figure II-7: Schematic sand transport time determination. (C) Bleaching curve with different signals (different bleaching rates). (D) Residual dose curves as a measure for transport time

In Figure II-7 a scheme is given how this would work in practise, the sampling is taken randomly here. This sampling on the bleaching curve depends on the duration of the exposure in its

transport history. A basic requirement is that the sediment under investigation needs a considerable initial luminescence signal. This residual dose (the level of signal leftover after a bleaching event) that is measured e.g. during suspended transport in the water column can act as a measure for e.g. transport distance from a (mega-)nourishment site.

2.3.2 Bleaching behaviour

Understanding the bleaching behaviour and measuring the residual doses will form a measure for the sediment transport (bleaching experiment; see 4.4.2). The bleaching behaviour is studied using controlled bleaching experiments using either a solar simulator or natural daylight exposure as a source of stimulation. The bleaching behavioural studies have developed alongside the introduction of each 'new' luminescence technique. Godfrey-Smith et al. (1988) were the first to study the bleaching behaviour of OSL in comparison to TL. They concluded that the bleaching rate of OSL is an order of magnitude faster than that of the TL signal in both feldspar and quartz.

OSL knows different types of light stimulation sources of which blue- (for quartz) and infrared (for feldspars) light stimulation are the most commonly used. All of these stimulation types are connected to different bleaching behaviour when exposed to daylight. Blue OSL in quartz is known to bleach very rapidly, within a matter of seconds-minutes (Bøtter-Jensen et al. 2003). IR light sensitive feldspars bleaches not as fast as the Blue OSL signal in quartz (Figure II-8; 1) but not nearly as slow as TL (Godfrey-Smith et al. 1988).

The stimulation of feldspar with IR light addresses only a distinct trap depth level in the feldspar mineral. Feldspars are common for their susceptibility to a phenomenon called anomalous fading (Wintle 1973). Anomalous fading is the self-emptying of electrons from their traps, hence losing signal without being exposed to light. In that case the ambient temperature under which the measurements are performed plays an important role in the sensitivity and effectiveness of stimulation and accordingly the natural bleaching rate. Bleaching experiments with this post-infrared infrared stimulation (pIRIR) in which two sequential elevated temperature IR stimulation shows in Figure II-8 (1) that this elevated temperature pIRIR signal at 290°C bleaches considerably slower than the IR signal at 50°C (Thomson et al. 2008, Buylaert et al. 2012). To understand firstly the stability of the IR/pIRIR signal in feldspar signals a multiple elevated temperature IR stimulation (MET-pIRIR) rounds are done on a single aliquot. Bleaching experiments on this show that the bleaching rates decrease with every sequential temperature step (Li & Li 2012, Fu & Li 2013). Indicated in Figure II-8 (2) are the unique bleaching characteristics per pIRIR signal. This is of interest to us, because we want to have a set of unique signals that could hypothetically represent multiple conditions in sediment transport for our luminescence tracing technique.

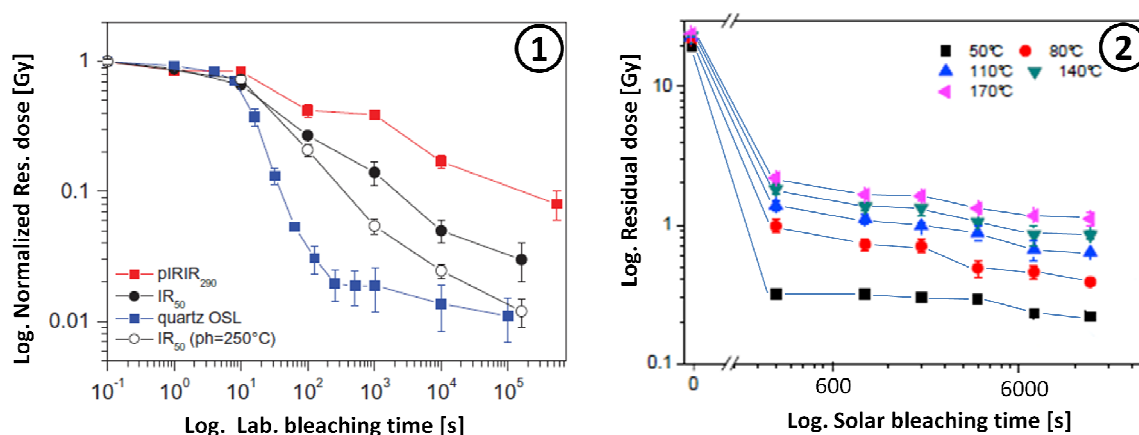


Figure II-8: Bleaching curve(s) (1) IR50-pIRIR290 protocol (modified from Buylaert et al 2012)(2) MET-pIRIR protocol: IR50-pIRIR80-110-140-170 (modified from Fu & Li 2013)

In the above bleaching experiments there is still the separation of the feldspar and quartz fraction. Unique in our study is the use of a polymineral sample (containing both fractions). Both

from the quartz as well as the feldspar fraction we intend to extract a signal. This means combining a sequential measurement with Blue OSL and IR/pIRIR.

In addition to all of the various OSL methods Bluszcz (2001) suggested that the simultaneous testing of OSL and TL might provide additional information on e.g. transport processes. Although Bluszcz (2001) acknowledges the difference in bleach ability there are no supporting bleaching experiments. In our bleaching research will also test the effect combining OSL measurements with TL measurements with supporting bleaching experiments.

2.3.3 Environmental bleaching

Ideal bleaching occurs under full sunlight conditions. Most bleaching tests are done using a solar simulator that mimics these ideal conditions and preferably amplifies it to shorten bleaching experiments. However, this is certainly not always the case in a natural situation. Clouds are the first source of reduction in bleaching effectiveness mainly due to the partial absorption of the light spectrum that is responsible for bleaching (Godfrey-Smith et al. 1988, Liritzis 2000).

During fluvial transport most transported sediment will stay submerged. Light is absorbed in water, especially water that is saline or laden with suspended particles (e.g. Berger & Luternauer 1987, Singrayer et al. 2005). Several experiments have proved the significance of this absorption in water and its effect on bleaching (e.g. Sanderson et al. 2007, Keisars et al. 2008).

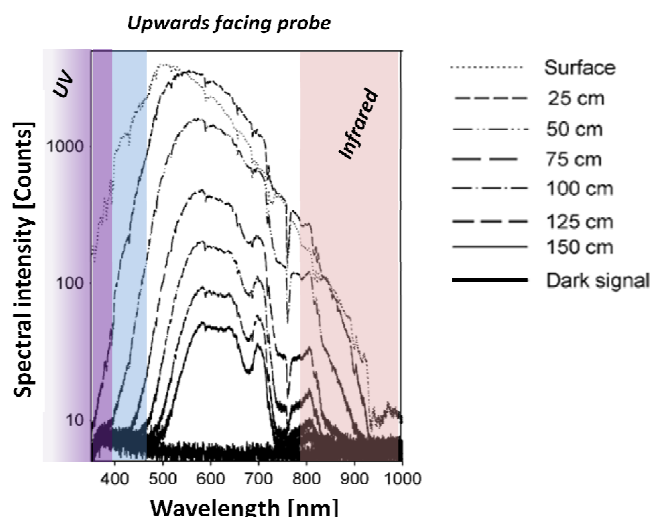


Figure II-9: Measured light spectrum in respect to water depth (from Sanderson et al. 2007)

In Figure II-9 an optic sensor has been used to measure the light spectrum at underwater depth intervals. The light intensity of the early part (UV, <400 nm) (purple/blue; superimposed) and the latter part (IR, >800) of the light spectrum attenuates very quickly whereas the middle part (blank) of the wavelength spectrum shows significantly less decrease in intensity with water depth (470nm-700nm).

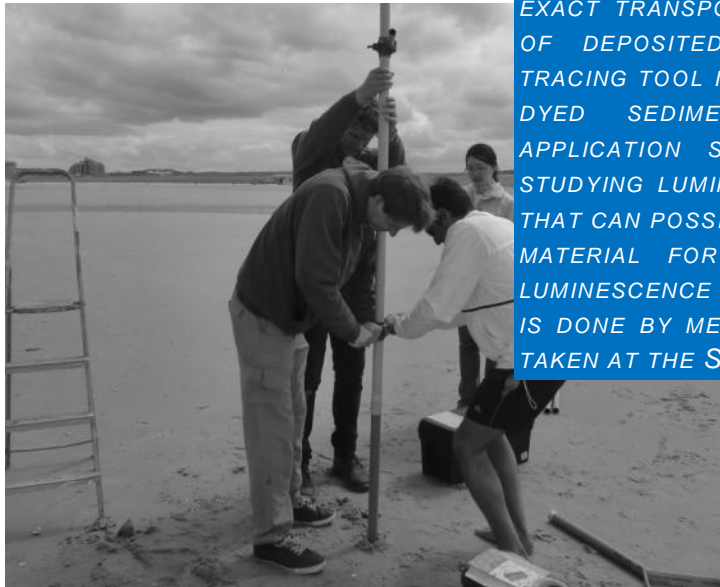
Keisars et al. (2008) made a comparison bleaching experiment measuring a TL signal with several samples bleached under dry conditions and with 1 mm of salt water. They concluded that salt water did filter out the necessary parts of the light spectrum that are responsible for the bleaching of sediment grains. Berger & Luternauer (1987) found a reduction of the luminescence signal at 4 m water depth with as much as 5×10^4 times the surface value.

For the age determination this means that there is a risk of a residual dose being present before burial (partial bleaching) making it hard to accurately determine an age for sediments that underwent water-lain transport. However for this study this might imply the possibility of making a distinction in transport mode, hence depth, by studying the ratio in measured OSL quartz (blue), feldspar (IR & pIRIR) signal and the TL signal.

Page left blank intentionally

CHAPTER 3: SAND ENGINE SITE & FIELD DATA

MONITORING OF GEO-MORPHOLOGY IS MAINLY BASED ON TOPOGRAPHIC MEASUREMENTS. TO INVESTIGATE THE SOURCE OF MATERIAL AND MORE EXACT TRANSPORT DATA AS TRANSPORT DISTANCE OF DEPOSITED MATERIAL A MORE POWERFUL TRACING TOOL IS NEEDED.. TRACING STUDIES USING DYED SEDIMENT GRAINS HAVE A LIMITED APPLICATION SCOPE. IN THIS THESIS WE ARE STUDYING LUMINESCENCE AS A TRACER TECHNIQUE THAT CAN POSSIBLY EXTEND THIS SCOPE. OBTAINING MATERIAL FOR TESTING THE APPLICABILITY OF LUMINESCENCE AS A SEDIMENT TRACING TECHNIQUE IS DONE BY MEANS OF CORE SAMPLES THAT WERE TAKEN AT THE SAND ENGINE.



Taking core samples at the Sand Engine, May 2012

The Netherlands, laying on the Northern hemisphere around 50° latitude, has to cope with severe storms driven by Westerly's winds. This is accompanied with high waves and an average tide of 2-3 meters. Coasts in the Netherlands are characterized by sandy beaches as well as sand nourishments on a regular base. Sand nourishments are the manual supply of sand to counteract the loss of sediment along the coast due to erosion. This erosion is mainly due to sea-level rise and cutting off the natural supply from rivers. The erosion along the Dutch coasts has been and is still increasing, therefore the sediment budget for nourishment has been steadily increasing since the start of nourishments in the 1970's. This erosion is a large problem for the hinterland, because this relies heavily on the coast and dunes for flood protection from sea. Today's coastal management strategies e.g. direct dumping of sediment on a coastal stretch require year-round coastal nourishments. A pilot project mega-nourishment, the Sand Engine, was constructed as a more sustainable and presumably better manageable alternative coastal management strategy (3).

Studying relative changes and provenance (=sedimentary origin) can only be done using a sediment tracer (1.1). In a (small) river this could be done with an artificial tracer e.g. dyed sediment particles. However, in coastal areas applying dyed artificial tracers encounter many problems e.g. dilution of the material. An average sand grain measuring a few hundred μm 's could easily travel kilometres per month along a coastal stretch under stormy weather conditions.

Luminescence measurements are done on quartz and feldspar sediment. The grain size fraction is an important factor in the results of the luminescence measurements. The grain size fraction and distribution are governing for the morphologic behaviour under hydraulic or aeolian forcing. Eventually the choice of the grain size fraction depends on the results from sample grain size analysis and dredge hopper grain size analysis (Rijkswaterstaat) that represents the nourished sediment (3.2.2). Field data for the present study were collected from this first ever mega-nourishment at the Dutch coast (3.3).

3.1 Sand Engine pilot project

The Sand Engine is a mega-nourishment pilot project involving the Dutch government, private parties and the Building with Nature program (BwN)³ in finding a better strategy for nourishing the coastal zone. This type and scale of nourishing has not been tried anywhere else in the world, therefore, and in combination with the Building with Nature program there is an extensive monitoring program and several (PhD) studies connected to it. These initiatives study e.g. the incorporation of nature's power to rework landscapes.

A mega-nourishment is a localized dump of millions of cubic metres $O(20 \text{ Mm}^3)$ instead of the broadening of the entire coastal stretch with a total sediment budget of 12 Mm^3 for the entire Dutch coast. In the Sand Engine pilot project mega-nourishment an amount of 21,5 million m^3 of sediment was dredged and dumped on a short 2.5 km stretch of beach as wide as 1,5 km out to sea at an average water depth 7,5 m (see Figure III-1). Immediate benefit here is that nourishment operations are more localized and on the deeper parts larger dredging vessels have enough keel clearance to be used. Using larger dredgers makes dredge operations more cost-efficient, because they can haul more material with each trip. Secondly the amount of sediment in one mega-nourishment is predicted to sustain the coast of sediment for 15-20 years, therefore increasing maintenance intervals. Another important motivator for building the Sand Engine is the potential to improve ecological values around the Dutch coasts. Because nature is doing all the work at a 'natural' pace marine life can adjust better to new circumstances. The design of the Sand Engine (see Figure III-1) also incorporates sheltered areas where species can breed.

Mega-nourishments are manmade coastal interventions. Building of the Sand Engine took only three months (March 2011 – July 2011). Sediment dynamics of large manmade coastal interventions are often unpredictable. The pilot project incorporates an elaborate monitoring program. Monitoring the mega-nourishment is a perfect opportunity to gain valuable insight and

³ Part of Ecoshape, an organisation that is closely involved with coastal research
http://www.ecoshape.nl/en_GB/overview-bwn.html

generated knowledge with respect to sediment dynamics and morphological processes (MER Sand Engine 2010; Table 0-2). This could improve future implications of mega-nourishments on coasts that suffer from structural erosion.

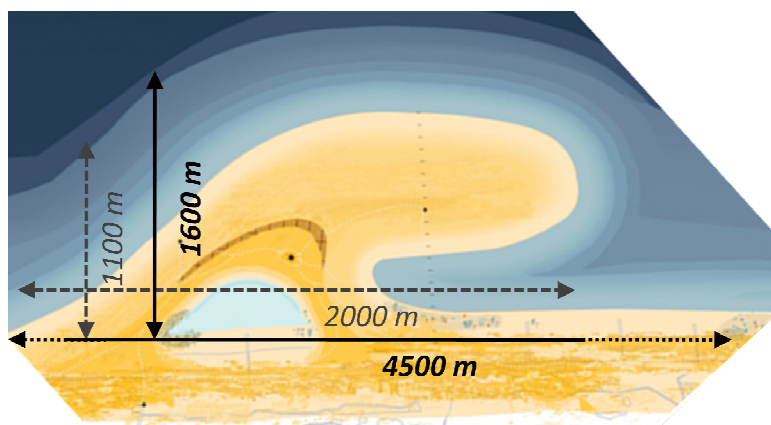


Figure III-1: Sand Engine dimensions (dashed) and monitoring area (solid), on concept drawing

The total area of the initial Sand Engine was approx. 128 ha. after reworking (20 year period) by nature this will result in a net gain of 35 ha land area alongshore to the existing beach. The initial dimensions of the Sand Engine were 2000m from North to South and measuring 1,5 km cross-shore (Figure III-1). The sand for the project was mined offshore in the North sea. This sand is collected in special sand pits that are designated by the government to be dredged. Geological studies have marked these sand mine pit as an old Rhine plateau dating back to the Holocene (0-11.700 years ago) when there still was a land bridge between the United Kingdom and the European mainland. This is an important fact to luminescence, because this 'old' material could contain a high luminescence value (2.3.1).

3.2 Bathymetric monitoring

The bathymetric model will be based on monthly bathymetry measurements done at the Sand Engine site. These near-shore bathymetry measurements were done on behalf of the BwN project. In the first place this model will act as a reference for the erosion- and deposition history of nourished sediment. Secondly it will act as a reference for the bored core samples that were taken for the purpose of luminescence measurements.

3.2.1 Bathymetry measurements

Each month a three day campaign is done to measure the bathymetry of 750 ha Sand Engine area. The monitoring data is collected using 3 types of equipment; a jet ski, 4wd quad and a wheelie or backpack (Figure III-2). For the shallow near shore (wet) measurements a normal measurement vessel's keel clearance would not suffice. However, a jet ski with a very low keel draft makes it deployable and very mobile in these shallow waters. The jet ski is equipped with a single beam echo sounder that takes sonar images of the bottom topography while navigating around the Sand Engine. The 4wd quad is equipped with a GPS with and is used to measure the dry parts and during low tide the intertidal areas of the Sand Engine. The GPS wheelie/backpack is used for the areas that are too wet for the quad and are unreachable by jet ski, such as tidal gullies.



Figure III-2: Bathymetry measurement equipment (source: Shore Monitoring & Research). Wheelie/Backpack GPS (left), 4wd quad with GPS (middle), Jet ski fitted with GPS and single beam echo sounder (right)

The GPS equipment in combination with the vessel and measurement equipment has an average error of about ± 0.10 m. On the jet ski the rolling and pitching of the vessel is partly compensated with the wide-angle beam of the echo sounder (Van Son et al. 2009). The echo registers the first echo of a reflection within the beam angle, thus some rolling inaccuracy is compensated by registering the first echoed signal. The measurements are defined on a gridded to an orthogonal grid of 10 by 10 m. The measurements have started in August 2011, the Sand Engine itself was finished in July 2011. For this study we will use the bathymetries starting from August 2011 to June 2012.

3.2.2 Bathymetry observations

Observing the bathymetry in Figure III-3 we observe that a spit is forming towards the beach in a Northern direction (green narrow arrows). Simultaneously the top of the Sand Engine is eroded away (wide red arrow). Comparing the first in Augustus 2011 bathymetry measurement we can conclude that the Sand Engine is slowly reattaching to the coastline and further evolves towards the North as a spit. Separated by a fast flowing channel that connects to the inner lagoon and the North Sea. Most logically the sediment from the top of the Sand Engine is diffusing towards adjacent coast.

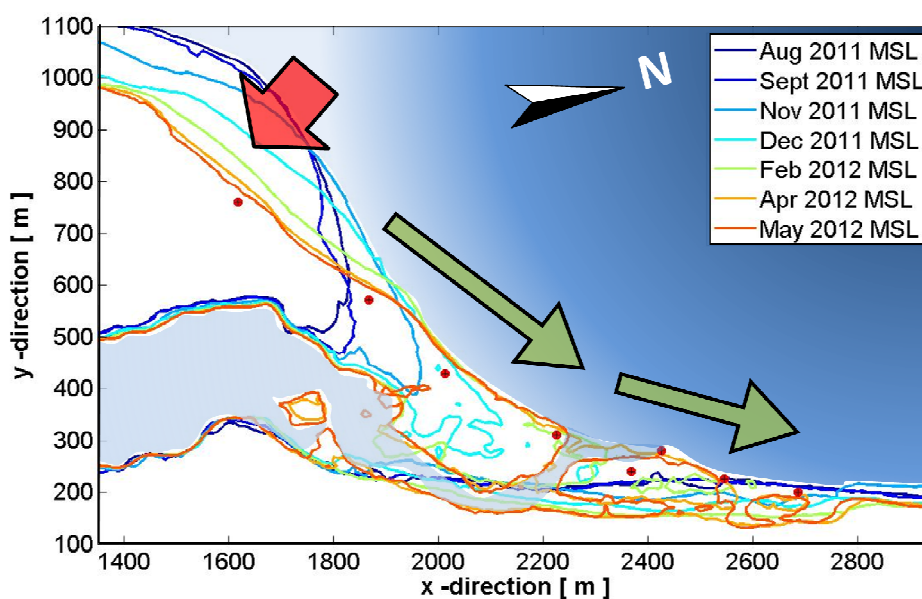


Figure III-3: General evolution of the Sand Engine spit

Studying the MSL contour lines we can assume that the average progress of the evolution is in the order of 200 m. However, at the adjacent coast we are also seeing an erosion of 50 m width, hence some of the sediment near the original coast the sediment is presumed to be a mixture of Sand Engine sand and pre-Sand Engine sand. This morphological evolution of this northward evolving spit is the part of the Sand Engine that is of interest to the project. In 3.3 where pointing out where along this spit we collected the sediment cores.

For the construction of the Sand Engine the contractor was required to fulfil the requirement that the D_{50} ⁴ of the dredged sediment was in between the 200-300 μm . Grain size analysis report were preformed for each 500.000 m^3 of dredged sediment. These samples were taken during the construction of the Sand Engine to check grain size values, to confirm to the client that requirements for grain sizes were met. A total of 63 grains size analyses were conducted. In Table III-1 the average values for the different parts of the distribution are shown. The measured average D_{50} value lay between 224 μm and 439 μm and the average for the whole Sand Engine is 301 μm . However, not all of the sediment that was dredged has yet been eroded and transported.

Sample	D ₁₀ [μm]	D ₅₀ [μm]	D ₉₀ [μm]	Type Sediment distribution	Sand content [%]
Average	164	301	564	-	-

Table III-1: Average grain size Sand Engine

After the first months of construction part of the Sand Engine has been eroding away (see Figure III-3). In this part of the Sand Engine 11 samples were taken for analysis. The results of these can be found in Table III-2.

Sample	D ₁₀ [μm]	D ₅₀ [μm]	D ₉₀ [μm]	Sample date	X-position* [m]**	Y-position* [m]**
1	224	399	760	23/05/2011	940	1098
2	139	281	567	01/06/2011	1140	1023
3	129	251	444	03/06/2011	1240	973
4	127	224	408	13/06/2011	1590	998
5	145	276	464	14/06/2011	1640	848
6	141	266	461	16/06/2011	390	948
7	144	265	432	17/06/2011	340	923
8	143	258	451	20/06/2011	290	948
9	154	285	480	23/06/2011	90	773
10	152	272	449	24/06/2011	40	798
11	181	316	555	25/06/2011	40	748
Average	152	281	497			

* Position is referenced to the rotated plot axis in Figure III-3

** The samples were taken from 25m*50m plots, this position is the bottom left corner coordinate of those plots

Table III-2: Sediment grain size samples from the eroded part of the Sand Engine

For the eroded part of the Sand Engine the values for the D_{50} values that were observed are between the 224 μm and 399 μm , with an average D_{50} value of 281 μm . For the luminescence measurements we will extract sediment samples from the newly formed spit at the northern part of the Sand Engine. Grain size analysis will also be performed on the selected samples to check their grain size distribution and how they compare to the nourished sediment.

⁴ D_{50} is the median grain size of a grain size distribution

3.3 Sediment sampling

Bored core samples were taken in the end of May 2012 and beginning of June 2012. The sediment cores were taken from the Sand Engine using a 'Van der Staay' suction-corer (Meene et al. 1979). Figure III-4, left, shows the coring process using the 'Van der Staay' suction-corer. The luminescence signal(s) are sensitive to contact with daylight. To achieve an accurate luminescence signal the sampling must be done under (near) dark circumstances. The samples were all taken under dry conditions, depending on the height of the tide.



Figure III-4: Sampling on the Sand Engine using the 'Van der Staay' suction corer. Coring using the corer(left), Samples in light tight containers (PVC-tube)(right).

A PVC pipe with a diameter of $\varnothing 50\text{mm}$ is driven into the ground and when retrieved cut in lengths of 400-500mm. From this 400-500mm the middle 200 mm is used for the luminescence measurements (Figure III-4, right). Keeping the upper and lower 100mm ensures that the sampled middle 200 mm stays free from exposure to direct daylight between coring and prior luminescence measurements.

3.3.1 Sediment core boring

To examine the potential of luminescence sediment tracing the cores were taken along the outer contour ranging from the seaward tip of the initial peninsula in a South (ZM-03) to North direction to the end of the spit (ZM-07) that was formed during the first eleven months (Figure III-5). From analysis of the monthly bathymetry in 3.2.2 this is the most sediment transport active zone. The first cores **ZM-03 to ZM-06** were taken on the **May 31st 2012**, the latter cores **ZM-07 to ZM-10** cores were taken on **June 5th 2012**.

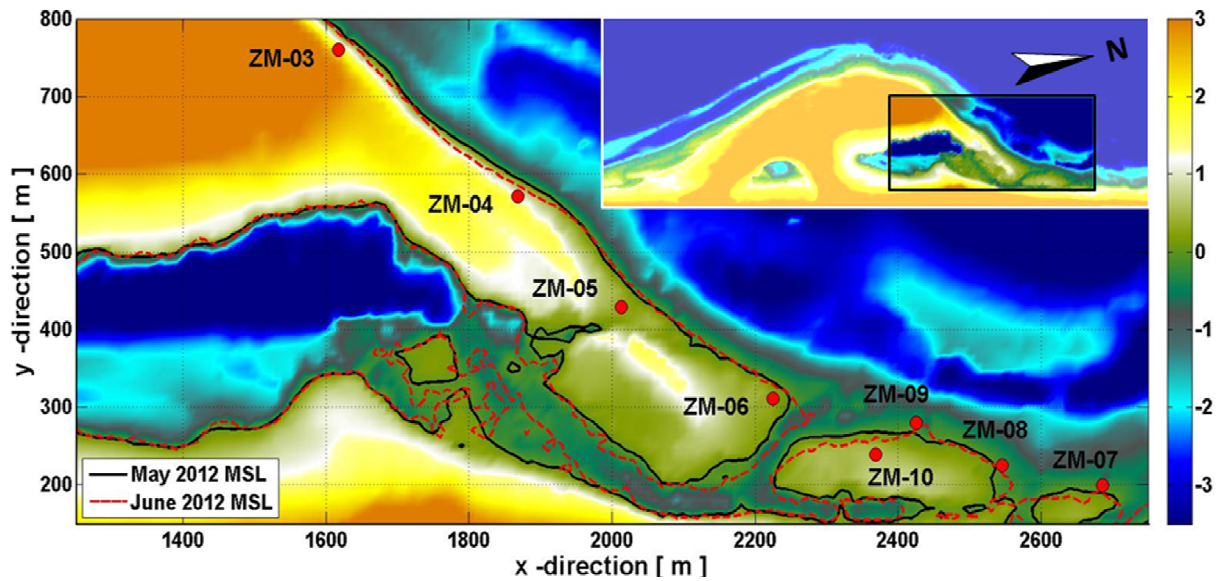


Figure III-5: Sampling core positions (May 2012 bathymetry)

From the Sand Engine 31 samples were taken, from eight different core locations with 1 to 7 samples per location. The idea was to collect samples up to 2 m depth measured from local field level. Coring in the shell rich sand of the Sand Engine proved to be hard by manual labour alone and thus at some sampling points this 2m depth was not reached (Figure III-6). All the samples with their data are described in Appendix 1.

3.3.2 Sample strategy

Because of time constraints and practical reasons only the most promising samples out of the 31 collected samples were chosen. Based on the morphological evolution in the months prior to the sampling seven samples were selected. The criteria being based on the thesis goal to study the feasibility of tracing sediment. In Figure III-6 the sample cores are plotted against bed level, see Figure III-5 for their positions. This bathymetry is linearly interpolated between the cores and the distance between the points is as the crow flies. This distance is about 1.2 km from the first sampling point at the Sand Engine towards the end of the spit. To distinct original from nourished sand a pre-Sand Engine level is plotted with data taken from JARKUS⁵ measurements done in 2010 before the construction of the Sand Engine.

⁵ JARKUS measurements are part of the yearly coastal measurements by Rijkswaterstaat (RWS), the Dutch ministry of Infrastructure and Environment

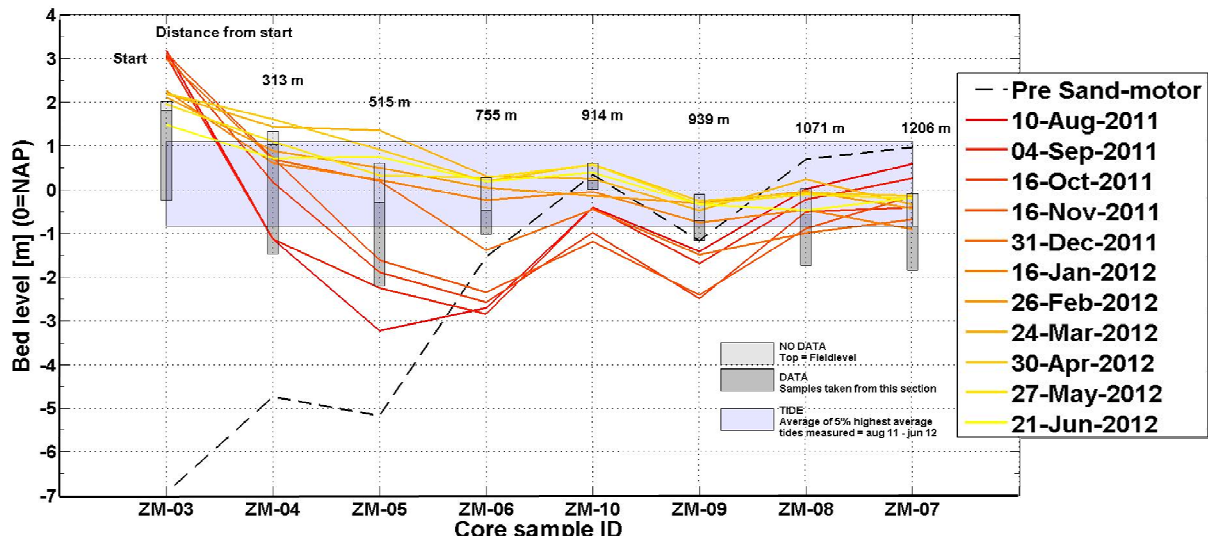


Figure III-6: Sample cores vs. monthly bathymetry (Aug-2011 - Jun 2012)

In Figure III-6 the 5% highest- and lowest tide level envelope averaged over the period Aug '11 until Jun '12 is plotted. We reckon that, if they have been deposited later than Aug '11, below this tide level the likelihood decreases that samples have fallen dry and have experienced full daylight exposure..

The first core (ZM-03) is located on the outer ridge of the initial Sand Engine and has not been eroded yet (although we are observing erosion of the bed level) the sediment in the core is assumed to be predominantly sand that is deposited during construction and has been buried ever since. In the following core positions (ZM-04 until ZM-06) we see a gradual accretion of the bed level, presumably consisting of transported Sand Engine sediment. At the core positions ZM-10 and ZM-09 we are observing the same gradual accretion, although in smaller quantities than at ZM-04 until ZM-05. This area at ZM-10 and ZM-09 is the tipping point between the accreting- and eroding part of the Sand Engine. In the first months after the implementation of the Sand Engine we observe erosion at the latter ZM-08 and ZM-07 core positions. However, after the month December this latter part of the adjacent coast starts to accrete again. Presumably this is because the nourishment starts to supply this part of the adjacent coast with a delay and that the Sand Engine in the first months after construction forms an obstruction to the littoral sediment drift from South of the Sand Engine.

In Figure III-7 each selected core was plotted separate with the tide, bathymetry change over the course of eleven months and all the samples per core. Plotting the separate core sample data against the bathymetry model more details on the monthly erosion/deposition process becomes visible.

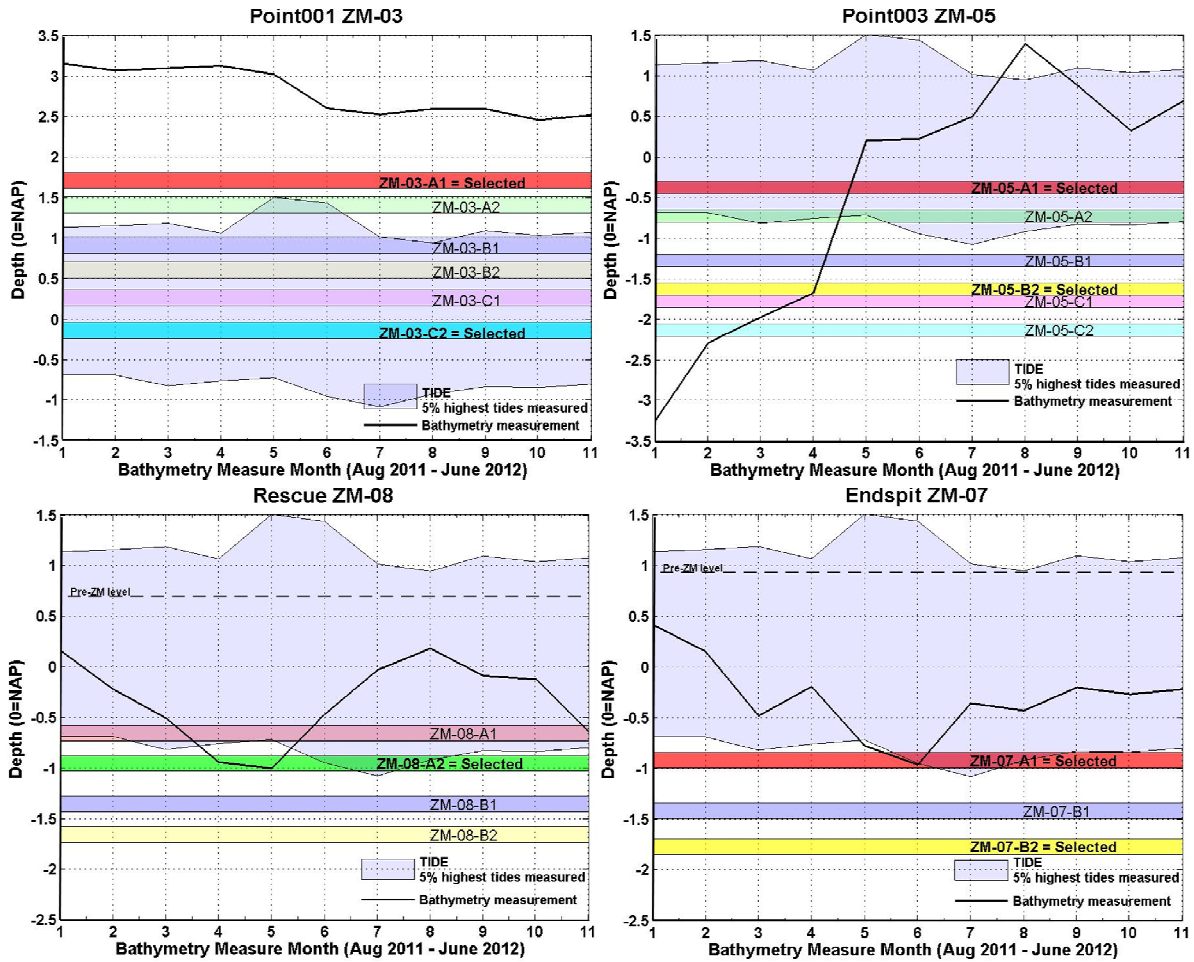


Figure III-7: Detailed bathymetry descriptions per core sample

The first hypothesis is that the luminescence signal changes in relation with and indicative transport distance. To test this we must select samples that on the one hand have not been transported or exposed to light (as a reference signal) and samples that have presumably been transported, thus potentially exposed to daylight. Determining whether the luminescence signal changes with distance we have selected samples from the first core (ZM-03) and samples from the last core (ZM-07). Secondly we study the effect of transport distance on three samples ZM-05, close to source sample and ZM-07 and ZM-08 as being transported further away. The third investigation are two samples that have been deposited at different locations under roughly the same conditions; month of deposition, depth with respect to MSL and erosion/deposition environment, to see whether the travel distance has a effect on the luminescence results. For this we selected samples from ZM-08 and ZM-07. The last is to study two samples that have been deposited at the same site during the same month. The only parameter being the depth difference and accordingly the chance of exposure to (full) daylight. In this last study sample(s) from ZM-05 fulfil these requirement. The samples for the luminescence measurements are highlighted and have the suffix '= selected' (Figure III-7). In Table III-3 an overview is given of these samples and how they relate to their hypothesis. Results from the luminescence measurements will be given 4.4.

Sample	Month of deposition (\pm)	Region	hypothesis
ZM-03-A1 (Point001)	< Augustus 2011 (Sand Engine)	Not reworked	<ul style="list-style-type: none"> • Act as a control sample, the sample presumably is not exposed to daylight. • Compare to other sample (<u>ZM-03-C2</u>) Point001, how much difference is there between both control samples
ZM-03-C2 (Point001)	< Augustus 2011 (Sand Engine)	Not reworked	<ul style="list-style-type: none"> • Act as a control sample, the sample presumably is not exposed to daylight. • Compare to other sample (<u>ZM-03-A1</u>) Point001, how much difference is there between both control samples
ZM-05-A1 (Point003)	November 2011	Only build-up (single cycle)	<ul style="list-style-type: none"> • Control sample deposition transport depth (high in water column) with sample <u>ZM-05-B2</u> • Control samples for transport distance, other conditions correspond to sample <u>ZM-07-A1</u> and <u>ZM-08-A2</u>
ZM-05-B2 (Point003)	November 2011	Only build-up (single cycle)	<ul style="list-style-type: none"> • Control sample deposition transport depth (low in water column) with sample <u>ZM-05-A1</u>
ZM-08-A2 (Rescue)	December 2011	Reworking (multiple cycles)	<ul style="list-style-type: none"> • Control samples for transport distance, other conditions correspond to sample <u>ZM-07-A1</u> and <u>ZM-05-A1</u>
ZM-07-A1 (Endspit)	January 2011	Reworking (multiple cycles)	<ul style="list-style-type: none"> • Furthest away sample, most chance of daylight exposure, measure and compare decrease with respect to the control sample(s) of <u>ZM-03</u> • Control samples for transport distance, other conditions correspond to sample <u>ZM-05-A1</u> and <u>ZM-08-A2</u>
ZM-07-B2 (Endspit)	< Augustus 2011 (pre-Sand Engine)	Not reworked	<ul style="list-style-type: none"> • Control sample for sediment from before the Sand Engine

Table III-3: Overview selected samples

The hypothesis assumptions are a relative simple approach in such a complex sediment system, since we are only taking the absolute distance between the samples. The bathymetry measurements for instance have a deviation of 0.1 m and are the average of a 10m x 10m area. Moreover, the sediment samples are spaced \pm 300 m apart as were the samples themselves only cover an area of a few square centimetres (coring area) and each sample is the average of 0.2 m in height. Relatively compared to the bathymetry measurements error and accuracy the very small samples the interpretation of results is therefore difficult.

3.3.3 Aeolian sample

In addition to the coring samples an aeolian sample was collected. This aeolian sample was taken on a windy day on which clear aeolian transport was visible. The sample was collected by placing down a sample PVC pipe with its opening directed in the prevailing wind direction. This sample was taken to see whether there exist a large difference between an aeolian transported sample and a water lain transport sample.

3.3.4 Sedimentology

High-resolution grain size analyses are obtained for each of the (selected) sample using a laser particle-size analyser (*Institut für Geophysik, University of Hamburg*). The results for the selected samples are in Table III-4.

Sample	D ₁₀ [µm]	D ₅₀ [µm]	D ₉₀ [µm]	Type Sediment distribution	Sand content [%]
ZM-03-A1	254.5	488.0	1159.8	Moderately Sorted Medium Sand	99.9
ZM-03-C2	199.8	369.4	697.6	Moderately Sorted Medium Sand	98.4
ZM-05-A1	216.4	350.6	524.6	Well Sorted Medium Sand	98.8
ZM-05-B2	205.7	346.3	640.1	Mod. Well Sorted Medium Sand	98.5
ZM-08-A2	255.3	398.3	587.8	Well Sorted Medium Sand	99.3

Table III-4: Grain size analysis results

Grain size results show that the grain size is between 350 µm and 480 µm. These values are coarser than the grain size of O (250 µm) typically found at this stretch of coast near the shoreline (Wijnberg, 2002) as well as the values measured during construction (average D₅₀ value 281 µm, eroded part). Grain size distributions can vary over depth, and D₅₀ values at a single core location can vary as much 119 µm (sample ZM-03, Table III-4). This heterogeneity at ZM-03 can be in part due to differences in the construction method, such as the distance from the outflow pipe, or reworking by dozers.

The measured D₅₀ value of the taken core samples are on average 40% larger than the average D₅₀ value of samples taken from the Sand Engine during construction, from the part that since has been eroded away. Core ZM-03 has not been transported, its values can be due to a dredged part with a coarse grain size. However, these D₅₀ values do not deviate that much considering the largest D₅₀ value found in the grain size analysis was 439 µm. The increasing D₅₀ value shift in the distributions (also noticeable in the D₁₀ and D₉₀ values) can be due to the transport capacity difference between coarse and fine(r) grains. Coarse grains tend to travel less far under the same forcing conditions than fine(r) grains would.

Our study area is relatively short taking into account the transporting forces under high waves (3+ m) and strong currents (1 m/s). In the natural transport situation there is a chance for the sediment to naturally sort over distance, hence higher percentage of heavier particles on a short distance from the Sand Engine and presumably more lighter material further away. This can result in a relatively high contribution of coarse grains in the first part of the Sand Engine spit and further away. Moreover the selected samples are also positioned relatively deep, increasing the chance of having more coarse grains in the sample.

Page left blank intentionally

CHAPTER 4: LUMINESCENCE MEASUREMENTS



MEASUREMENTS AND THE FINAL PREPARATIONS OF SAMPLES ARE CONDUCTED UNDER LABORATORY CONDITIONS I.E. IN A DARK ROOM AS IS USED FOR PHOTO DEVELOPMENT. THE MEASUREMENTS ARE PERFORMED ON A LUMINESCENCE READER. ALIQUOTS ARE THE STAINLESS STEEL DISKS ON WHICH A FEW HUNDRED GRAINS SIMULTANEOUSLY ARE PLACED. THE READER COUNTS THE LUMINESCENCE EVICTED FROM THE ALIQUOTS, WHICH IN TURN ARE THEN CALCULATED INTO A EQUIVALENT DOSE. IN THIS PART A PROTOCOL IS DEVELOPED FOR POLYMINERAL TEST SAMPLES TO AS AN ALTERNATIVE TO COMMON SEPARATED MEASUREMENTS. NEXT WILL BE THE TRANSLATION OF TEST RESULTS INTO A QUANTIFIABLE MEASURE UNIT, EQUIVALENT EXPOSURE TIME (EET).

The Sand Engine, October 2011⁶

⁶ Rijkswaterstaat / Joop van Houdt

In Chapter 0 the physical background of luminescence was treated. In this chapter measurements are presented from the samples that were selected in Chapter 1. First the measurement method is presented followed by the introduction of the newly developed PMS-SAR protocol. Last part of this chapter is the daylight bleaching experiment in an attempt to quantify the measured signal in the selected samples.

4.1 Signal measurement

On average 5% of all quartz grains give a good luminescence signal. At 20% this percentage is higher for feldspar(s). Still in one multigrain polymineral sample the actual percentage of grains – separate for the OSL (blue light = quartz, infrared light = feldspar(s)) and combined for the TL – giving a positive feedback in the measurement signals stays an unknown factor. Confirming this contribution ratio could be done with single grain analysis, though these are very laborious when handling multiple samples as we do. Secondly the luminescence signal, as does the sediment transport, depends on the extrinsic and intrinsic properties of grains, which are never exactly the same from grain to grain. For their first trials Huntley et al. (1985) used a green laser with a wavelength of 514.5 nm to evict the electrons out of their traps. Later infrared (IR) (= 870 nm) (Hütt et al. 1988) and blue (= 470 nm) light (Bøtter-Jensen et al. 1997) were used to improve OSL range and accuracy. The reason for changing from green to a shorter wavelength blue light stimulation is the increase in energy as well as the effective luminescence stimulation (Bøtter-Jensen et al. 1994b). Quartz is most effectively stimulated by blue light stimulation. However, quartz is not sensitive to infrared light stimulation. The opposite is true for feldspar(s), these are more sensitive to longer wavelength infrared light stimulation and less sensitive to blue light stimulation.

Signal measurements are carried-out on a luminescence reader (we are using the Risø TL/OSL DA-15 reader). This reader is fitted with several optical stimulation units e.g. blue and IR LED's (Light emitting diodes) as well as a heating element that heats the samples from below as well as being a TL stimulation unit. The two important acting components in a luminescence reader are the irradiation unit and the photomultiplier tube (PMT). The irradiation unit contains a radioactive β -source that gives samples a controlled dose for comparison with the naturally occurring radiation dose (important for measurement protocols for equivalent dose determination, see 4.2). The PMT monitors the luminescence light counts. The light spectrum detection window of the PMT can be controlled by putting in several different optical filters in front of it (see 4.2.1).

The main purpose of the detection filter is to prevent direct light (photons) from the stimulation source being measured (~430 nm for blue and ~870nm for IR) in the PMT. When using blue light (quartz fraction) stimulation a U-340 (340 nm) filter is fitted with a transmission window in the ultra violet region (measuring *in UV*). The IR and pIRIR (feldspar fraction) is preferably detected with an Interference-410 filter with a transmission window in the blue region (around 410 nm) (measuring *in blue*) (Balescu and Lamothe 1992). However, for simultaneous measurement of polymineral samples including quartz OSL and feldspar IRSL the detection window around 410 nm cannot be used because the quartz OSL stimulation is carried out in blue (~430 nm) i.e. the same wavelength region. Accordingly, for the measurement of polymineral samples we are restricted to the detection in UV using the U-340 filter. Using the U-340 filter has disadvantages for measuring feldspar signals, because it is well known that the most stable measurement signal from feldspar is emitted and measured with the blue transmission window. However, Preusser (1999b) found no significant differences between bleaching efficiency and signal stability for feldspars between measurements in blue or in UV.

4.1.1 Sample preparation

Luminescence tests are performed on aliquots, these are stainless steel discs with a single layer of grains adhered to it with silicon spray. In our case we were using an 8mm diameter mask size on which the grains are stuck. These discs are loaded on the sample carousel, which is placed in the luminescence reader.

Sieving

Before the start of any test the samples have to be separated into grain size fractions. In preparation all samples are wet sieved into the fractions 212-250 μm , 250-300 μm and 300-355 μm . The largest grain size fraction (**300-355 μm**) was chosen for further analysis. With this grain size fraction there are on average 150-200 grains on a 8 mm aliquot. This choice was taken firstly on the bases of sediment analyses pre-dating the Sand Engine. In the fall of 2010 Wijsman & Verduin (2011) found a characteristic D50 value for the Sand Engine area of 324 μm . Secondly, from sand analyse reports⁷ that were made of every 500.000 m^3 that was dredged for the Sand Engine (samples were taken from the sand on the dumping site) it can be concluded that this 300-355 μm fraction was well present in the material that was dumped at the Sand Engine.

Chemical treatment

The next step of the preparation process is chemical cleansing of the samples to remove and rinse out contaminations. Contaminations such as shell particles (carbonates) and organic material must be removed prior to measurement to avoid unwanted luminescence signal contributions. Some carbonates and organics emit a luminescence signal that could potentially bias the luminescence measurements. For the removal of carbonates hydrochloride acid (HCl) was used. The organics were removed by adding hydrogen peroxide (H_2O_2). Both these chemicals were diluted to a 10% concentration with distilled water. In between these steps the samples were rinsed with distilled water to reduce the reaction between both chemicals. An additional step was done to purify sample. Purifying or etching the sample helps to remove the outer alpha-irradiated rim (unwanted luminescence signal contribution) of the grains and any impurities in the larger feldspar grains. This last is done by leaving the sample for 15 minutes in a solution of 10% hydrofluoric acid (HF). The end product is a sample largely consisting of quartz and feldspar grains. This sample is called polymineral because no extra separation is performed on it.

For comparison two more extra steps were carried out on one exemplary sample (ZM-05-B2) to separate the quartz and feldspar fraction. For extraction of the quartz the poly mineral sample was treated with 40% HF for 40 minutes to dissolve all feldspars and purify the quartz fraction. To extract potassium rich (^{40}K), feldspar(s) a density separation is applied on a poly mineral sample. With density separation a sample is put in a liquid with an equal density to potassium rich feldspar (specific weight of 2.58 kN/m^3) and was left to settle. After some time the sample is separated in a ^{40}K -feldspar grain fraction, floating on the surface and a fraction of (heavier) rest materials that sank to the bottom (quartz has an average density of 2.65 kN/m^3).

4.2 Luminescence measurement protocol

The luminescence measurement protocol is a sequence of experiments that translates natural luminescence into equivalent dose. There are several types of protocols developed to make the translation of light counts to equivalent dose (e.g. Aitken 1998, Wallinga 2002). We are going to develop a new luminescence measurement protocol that is based on Murray and Wintle (2000) improved version of the SAR-procedure (**S**ingle **A**liquot **R**egeneration) protocol.

The underlying assumption of the SAR-protocol is that it is possible to measure a signal after each laboratory regenerative dose- and measurement stimulation cycle which acts as a reference measurement for the prior measurement cycle (in our case the natural signal). The

⁷ Source Rijkswaterstaat (RWS)

improved SAR procedure includes a test dose sensitivity correction. This test dose sensitivity correction is a small irradiation dose that is subordinately to the regenerative dose, which tests the luminescence response (luminescence per unit trapped charge), i.e. the luminescence output consistency of the sample with each luminescence measurement cycle and consecutive regeneration measurements.

The luminescence measurement plot is either called a glow curve, for TL or a shine down curve, for OSL/IRSL. In Figure IV-1 four examples are given of the measurement curves per type of signal. Figures are made with Luminescence Analyst (© University of Wales) a program used to analyse luminescence test data.

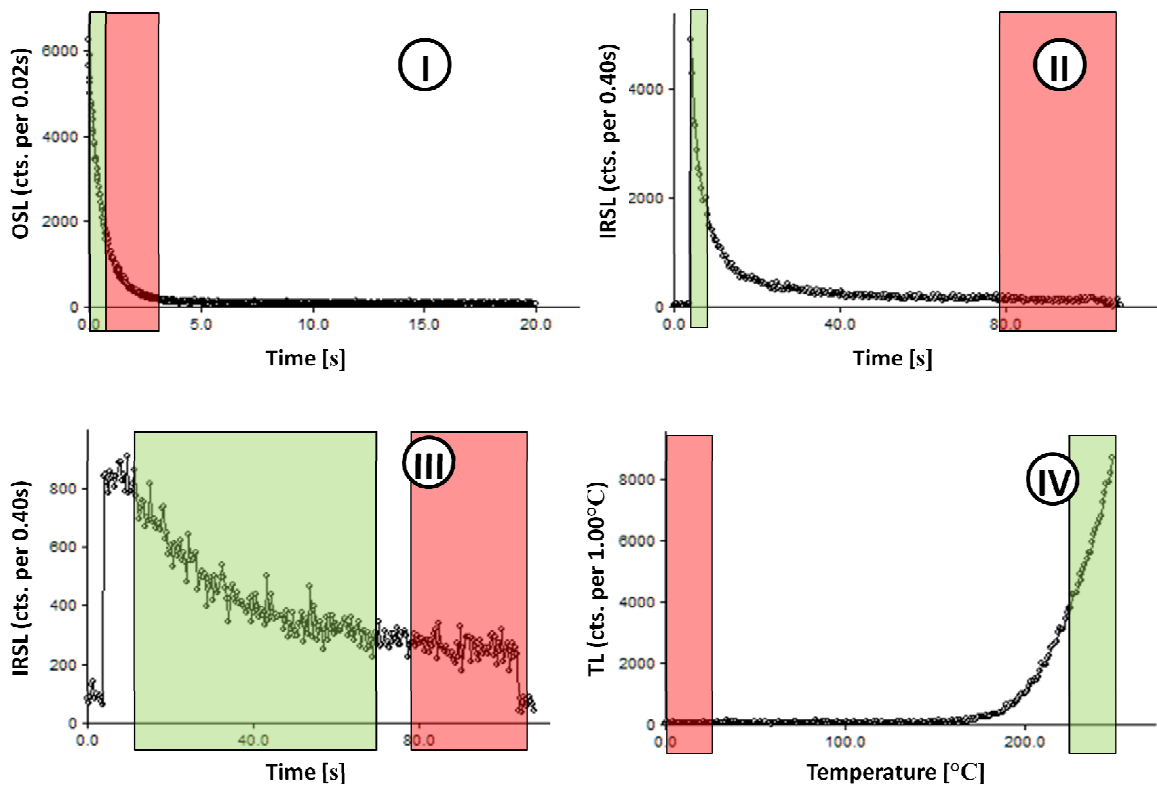


Figure IV-1: Luminescence curves (I) Shine down curve (Blue OSL; Quartz) (II) Shine down curve (IRSL; Feldspar) (III) Shine down curve (pIRIR-SL; Feldspar) (IV) Glow curve (TL; Feldspar + Quartz). The dots represent the light counts per set interval.

The information used from the curves is limited to the most readable bleachable component marked green in Figure IV-1, and a background component (e.g. dependent on the luminescence reader dark-count⁸) marked red in Figure IV-1. An OSL luminescence curve is generally assumed to consist of three separate components a fast, medium and a slow component. The most readable component according to Murray and Wintle (2003) is the fast one. In the early beginning of an OSL curve the highest OSL counts are measured. Using an early background subtraction (EBG) has two advantages. First a sensitivity problem is best understood in the early part of the OSL curve, hence one does not have to deal with a complex medium and slow component. Second the measurement does not have to continue until complete depletion for an accurate description of the slow component. In Table IV-1 and Figure IV-1 the integration intervals are given for the different signals.

⁸ Dark count (standard reader count) is the measured luminescence signal in absence of any stimulation

Stimulation	Signal (ch)	Background	Dimension
Infrared 25°C (IR 25)	10-15	200-250	(x 0.40[s])
Post-infrared infrared 90°C (pIRIR 90)	60-200	222-260	(x 0.40[s])
Post-infrared infrared 155°C (pIRIR 155)	60-200	222-260	(x 0.40[s])
Post-infrared infrared 225°C (pIRIR 225)	60-200	222-260	(x 0.40[s])
Blue 125°C (Blue 125)	1-24	25-80	(x 0.02[s])
Thermoluminescence 300°C (TL 300)	250-300	1-50	(x 1.00[°C])

Table IV-1: Signal intervals for the natural signal and test signal calculation

In the new protocol the natural luminescence signal ' L_n ' (including test dose sensitivity corrected signal ' T_n ') is measured first which is then compared to the luminescence signal from a known laboratory regenerative dose signal ' L_1 ' (and test dose sensitivity corrected signal ' T_1 ') and a second regenerative or recycle dose signal ' L_2 ' (and test dose sensitivity corrected signal ' T_2 '). The dose response curve is a linearly interpolated laboratory calibration curve that is used to translate natural luminescence to an equivalent dose (see Figure IV-2).

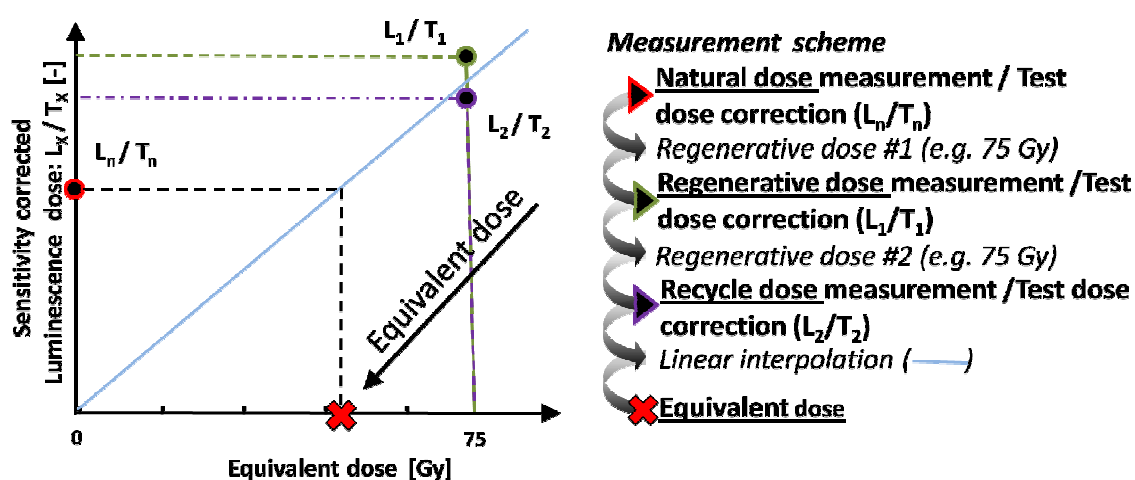


Figure IV-2: Equivalent dose determination scheme

In Figure IV-2 the ' L_n ' and ' T_n ' ratio represents the natural luminescence dose (on the vertical axis). A linear interpolation through the origin is constructed using the regenerative luminescence dose point (L_1 / T_1) and recycle dose point (L_2 / T_2). This linear interpolation is called the dose response curve. Via the curve an equivalent dose value is extracted (dark dashed line) corresponding to the natural luminescence signal.

4.2.1 Polymineral Multi-Signal Single Aliquot Regenerative dose protocol (PMS-SAR)

New in this study is the development of a Polymineral Multiple Signal Single Aliquot Regenerative dose protocol (PMS-SAR) (see Table IV-2). This protocol incorporates four stimulation types: blue OSL, infrared, post-infrared infrared and thermo luminescence. To use all of these stimulation types at once it is important to avoid consecutive signals to deplete the next signal to test. For that reason the TL measurement was measured in the end of each test cycle because the temperature was high enough to deplete other signals. The IRSL and pIRIR were stimulated prior to the blue OSL, the main reason for this is that the quartz fraction is not influenced by the IR-stimulation as were feldspar(s) are affected by the blue-stimulation (Thomsen et al. 2008). Preheating the sample is done to remove any unstable charge. This leaves the stable charge to be measured.

The protocol starts with measuring the IR and pIRIR signals from the feldspars. The IR measurement is done at just 25°C, subsequently pIRIR measurements are performed starting at a temperature of 90°C up to 225°C with intervals of 65°C, hence three pIRIR signals are measured. Compared to the IR signal these pIRIR signals are the harder to bleach luminescence components

in the feldspars. Bleaching rates lowering with each consecutive temperature elevation (Reimann & Tsukamoto 2012, Fu & Li 2013). Following the feldspar measurements the quartz is measured using a blue LED. This measurement is done at 125°C, because below 110°C the quartz signal is subject to re-trapping of evicted electrons in other traps instead of directly transferring to luminescence centres (Bailey 1997). Next a test dose is given to do a sensitivity correction assessment, following this the previous OSL/IRSL/pIR-IRSL measurements are repeated. Last to be measured during the cycle is the TL signal up to 300°C. After this a cleanout non-measurement (blue OSL at 280°C) is performed to make sure the sample is fully depleted and prepared to receive a regenerative dose. The regenerative dose is applied by irradiating the sample with β particles from a radioactive source before repeating the measurement procedure. The measurements are repeated three times. Once to obtain a natural luminescence dose measurement and twice to obtain respectively a first and second regenerative dose measurement. This second regenerative dose is called the recycling dose. The recycling dose tests the consistency of the first regenerative measurement cycle (i.e. a L_2 / T_2 point on the dose response curve).

Step(s)			Treatment	Temperature[°C] **	Duration [s]	Observed		
Cycle #1	Natural (-)			-	-	$\frac{L_{n(x)}}{T_{n(x)}}$		
	Cycle #2	Regen. dose (β -source)		-	750	-	$\frac{L_{1(x)}}{T_{1(x)}}$	
		Cycle #3	Recycling dose (β -source)		-	750	-	-
1.1	2.1	3.1	Preheat	250	0			
1.2	2.2	3.2	IRSL	25	100	$L_{n(25)}$	$L_{1(25)}$	$L_{2(25)}$
1.3	2.3	3.3	pIRIR	90	100	$L_{n(90)}$	$L_{1(90)}$	$L_{2(90)}$
1.4	2.4	3.4	pIRIR	155	100	$L_{n(155)}$	$L_{1(155)}$	$L_{2(155)}$
1.5	2.5	3.5	pIRIR	225	100	$L_{n(225)}$	$L_{1(225)}$	$L_{2(225)}$
1.6	2.6	3.6	OSL(blue)	125	20	$L_{n(125)}$	$L_{1(125)}$	$L_{2(125)}$
1.7	2.7	3.7	Test dose (β)	-	40	-	-	-
1.8	2.8	3.8	Preheat	250	0	-	-	-
1.9	2.9	3.9	IRSL	25	100	$T_{n(25)}$	$T_{1(25)}$	$T_{2(25)}$
1.10	2.10	3.10	pIRIR	90	100	$T_{n(90)}$	$T_{1(90)}$	$T_{2(90)}$
1.11	2.11	3.11	pIRIR	155	100	$T_{n(155)}$	$T_{1(155)}$	$T_{2(155)}$
1.12	2.12	3.12	pIRIR	225	100	$T_{n(225)}$	$T_{1(225)}$	$T_{2(225)}$
1.13	2.13	3.13	OSL (blue)	125	20	$T_{n(125)}$	$T_{1(125)}$	$T_{2(125)}$
1.14	2.14	3.14	TL	300	150 [2°C/s]	$T_{n(TL)}$	$T_{1(TL)}$	-
1.15*	2.15*	***	OSL (blue)	280	100	-	-	-

* Next Aliquot (After all aliquots → Next Cycle)

** Between every step the sample is cooled with liquid nitrogen (N_2) to 60°C if needed

*** End of luminescence sequence

Table IV-2: Luminescence measurement protocol (PMS-SAR)

The main reason for the development of such a complex luminescence measurement protocol is to measure different luminescence signals with different bleaching properties from the same sub-sample (i.e. a similar set of mineral grains). In addition, it is more time-effective

measuring different minerals in the same aliquot than measuring quartz and feldspar fraction separately.

4.3 Performance test of PMS-SAR protocol

The performance of the PMS-SAR protocol was tested to prove whether the use of a polymineral sample instead of separated quartz- and feldspar fractions is justified. Furthermore, the use of two different detection windows namely a U-340 filter and Interference-410 (I-410) filter are compared. These filters detect luminescence light around 340 nm (in the UV light region) and 410 nm (in the blue light region), respectively.

The PMS-SAR performance test contains different combinations of the two filters (U-340 and I-410) and mineral fractions: polymineral fraction, quartz- and feldspar fraction. The assumption for doing this is that we know that quartz is most reliably measured as quartz-rich fraction in the UV and feldspar as K-rich feldspar fraction is in the blue. During one measurement only a single detection window can be applied. Simultaneously measuring quartz (blue) and feldspar (IR) is impossible with a I-410 detection window. The I-410 filter is near the blue light wavelength (~430 nm), hence if one would measure quartz blue OSL with the I-410 filter a part of the light emitted by the blue LED would as well be measured. To measure with the full PMS-SAR protocol proposed in Table IV-2 only the U-340 detection window can be used, this is the purple '<' sign in Figure IV-3 and Figure IV-4.

To solve heterogeneousness problems (balance of quartz and feldspars grains in the subsample) we use large (8mm mask) poly mineral samples (Sawakuchi et al. 2012). For the test we are using sample ZM-05-B2. Summaries of the data for the PMS-SAR test measurements can be found in Appendix 2. The signal values comprise of a mean value (based on a number of subsample measurements) and a standard deviation.

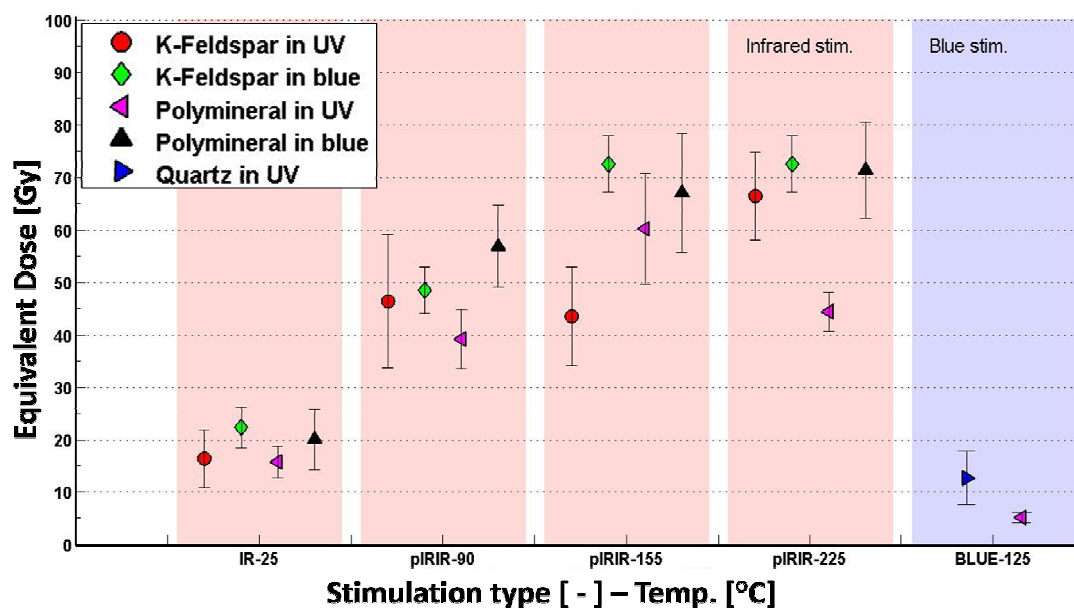


Figure IV-3: PMS-SAR test results OSL signal

Five combinations of sample fractions and detection filters were tested. Figure IV-3 gives the OSL signals of the PMS-SAR test. The IR and pIRIR signals stimulate the k-feldspar fraction, in a polymineral sample. The goal here is to see whether the PMS-SAR polymineral in UV (purple '<') result corresponds with the separate tests on k-feldspar in UV as well as Blue. Studying the results were seeing that in the IR-25 and pIRIR-90 signal these measurements show a similar result, taking into account the standard deviation. At the pIRIR-155 signal we observe a dip in the equivalent dose between the polymineral in UV and the k-feldspar in UV, a possible explanation for this is that the pIRIR-155 is a low(er)-sensitive feldspar trap, because the (optimal) k-feldspar in Blue shows an

relative high equivalent dose. This is sound if we consider that the k-feldspar is best observed in blue, though there is still no significant difference. Comparing the k-feldspar in blue, in ideal conditions with the I-410 filter, and the polymineral in UV for the pIRIR-155 signal we observe that both these do overlap each other. However, In the pIRIR-225 the signals of the k-feldspar and polymineral both in blue show a comparable equivalent dose, though the PMS-SAR condition (purple left triangle) shows a considerable lower value. In the blue-125 signal a noticeable difference is observed between the blue stimulated quartz fraction measured in UV in comparison with the polymineral in UV. This is presumably due to contributions from some (blue light sensitive) feldspars grains. In the TL results part of the PMS-SAR test (Figure IV-4) the lowest equivalent dose values are measured in the k-feldspar fraction in blue, this could presumably be attributed to the anomalous fading. Quartz in UV shows the highest equivalent dose values, though with a large standard error. The polymineral equivalent dose mean-value is intermediate between those from quartz- and feldspar suggesting that both quartz and feldspar contribute to this signal.

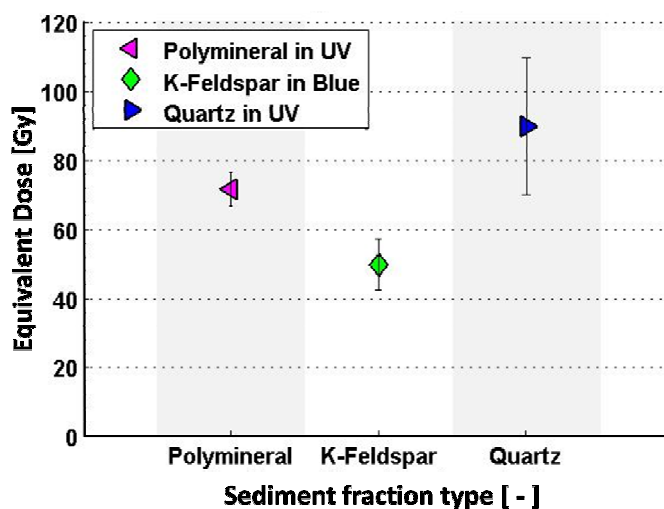


Figure IV-4: PMS-SAR test results TL signal

The PMS-SAR protocol in combination with polymineral samples performs, compared to separated measurement of quartz and feldspar. In both the OSL and TL part of the PMS-SAR test results using a polymineral mostly agree within uncertainty with the target values of the separate measurements. Considering the relatively large measurement uncertainties we can consider that the use of the PMS-SAR protocol (i.e. U-340 filter and the use of polymineral sample) is validated, with the exception of the pIRIR-225 signal, which has substantially deviating values between the separate mineral measurements and the polymineral.

4.4 Sand Engine luminescence results

Using the PMS-SAR protocol we examined the samples that were selected in 3.3. Figure IV-5 shows the results of the luminescence measurements of the seven samples, with the summary of the data found in Appendix 4. The value per sample and signal are based on a number of aliquots (8-24), in Figure IV-5 are mean values (see Appendix 4 for the exact number of aliquots) with their standard deviation. Analysing the results we are observing the largest loss in signal over distance in the IR-25 and Blue-125 signal, which is in agreement with our expectation from literature literature (see section 4.2.1). The pIRIR signals show less pronounced signal losses over distance compared to the IR-25 and Blue-125 because these signals bleach significantly slower under the same exposure conditions. The TL (TL-300) signal is the least effectively bleached by exposure to daylight (presumably attenuated by water).

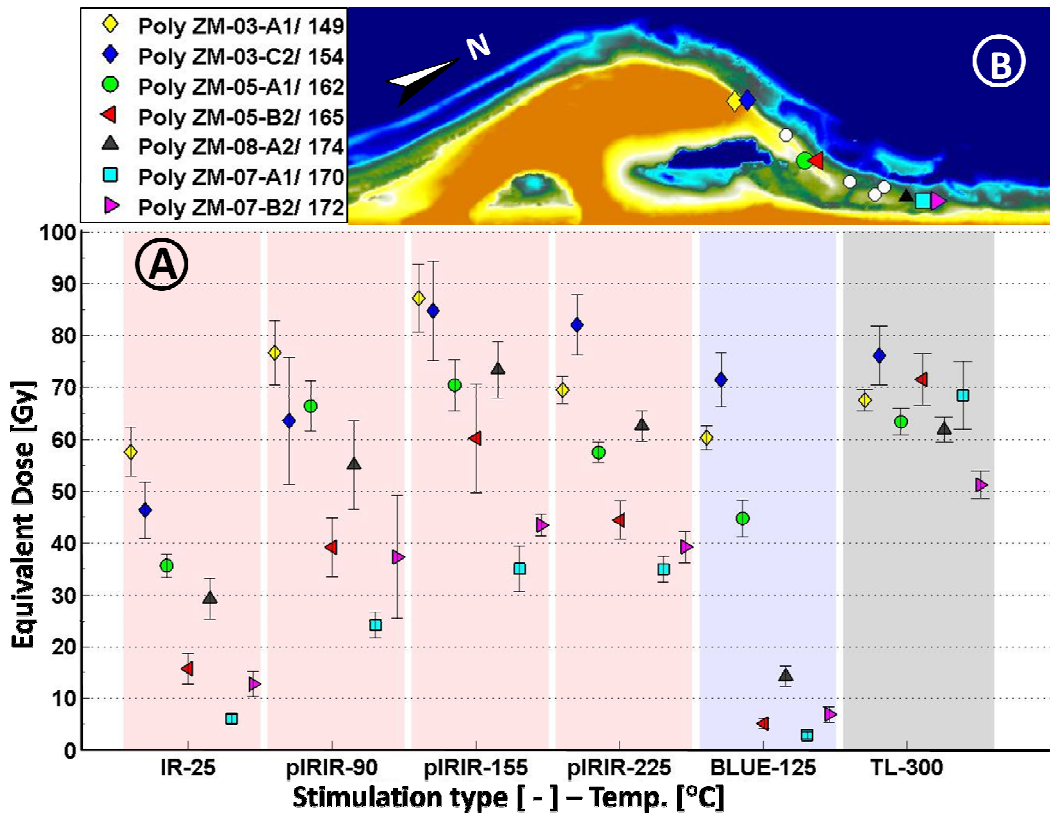


Figure IV-5: (A) Equivalent dose values, and standard error for all seven samples and (B) the sample positions (equal to graph signs) relative to the Sand Engine (contour June 2012)

Observing these results in Figure IV-5 and the signal lose rates in each sample we can state that the luminescence sequence potentially provides a monitor for short-, mid- and long term processes defining short term as <1 year and <1500 m coastal sediment transport, long term as >10 years and >10 km (based on the superimposing of the measured signals). Respectively these are the Blue-125 (OSL) & IR-25 (IRSL) signals for the short term. The pIRIR-90 and 155 signals for midterm studies and the pIRIR-225 & TL for the longer term.

4.4.1 Signal characteristics

The mean equivalent dose values for the separate samples and signals are based on a equivalent dose distribution from 20-24 aliquots. In the observations of Figure IV-5 a loss in equivalent dose over distance is observed. However this is not yet related to any of the morphologic processes in the nourishment e.g. daylight exposure time. Before we can do so we need to analyse the mean equivalent dose values more closely. Studying the Equivalent dose value distributions rather than the mean value could potentially provide additional information on the inter-aliquot scatter, which on its turn can act as an indicator for e.g. heterogeneous bleaching history of a sample. The bleaching is mostly never evenly spread over a sample, hence there can be a large variability between the separate subsamples of a single sample due to transport activity or a difference in provenance. Instead of an observed decrease in the mean equivalent dose value a shape of a distribution could give a much better indication of the (partial) daylight exposure durations and/or intensities. In Figure IV-6 in distribution (B) the problem of taken a mean equivalent dose value. For here the mean value here will be primarily influenced by the high value peak in the distribution masking the low value peak. The degree of scatter of bleaching within a sample is indicated with it being (A)/(C) homogeneously (low inter-aliquot scatter, narrow distribution) or (B) heterogeneously (high inter-aliquot scatter, wide distribution). Apart from this indicator there is also an indication if the sample were to be well bleached (low equivalent dose

values) or poorly bleached (high equivalent dose values) and partially bleached if both are present. Both of this indicators can be graded by skewness and kurtosis.

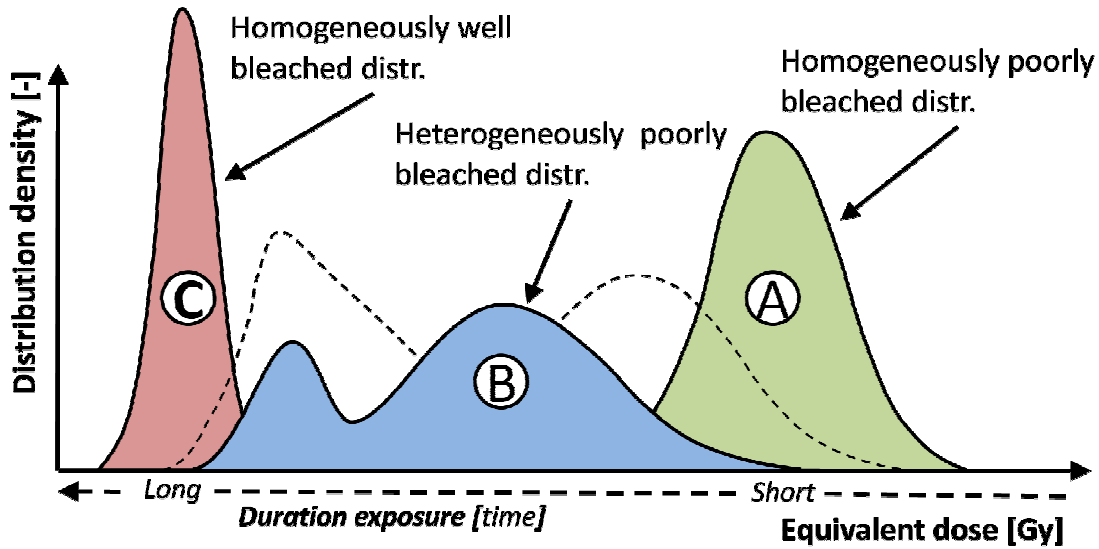


Figure IV-6: (A) homogeneously poorly bleached (B) heterogeneously mixed bleached (right skewed distr.) (C) homogeneously well bleached. The dotted contours are distribution shapes in between A, B and C.

The kernel density estimation (KDE) is a distribution function that fits as a continuous histogram over the luminescence results per sample (Galbraith and Roberts, 2012). Four signal KDE with the seven samples are plotted in Figure IV-7 (fast-to-bleach) and Figure IV-8 (slow-to-bleach).

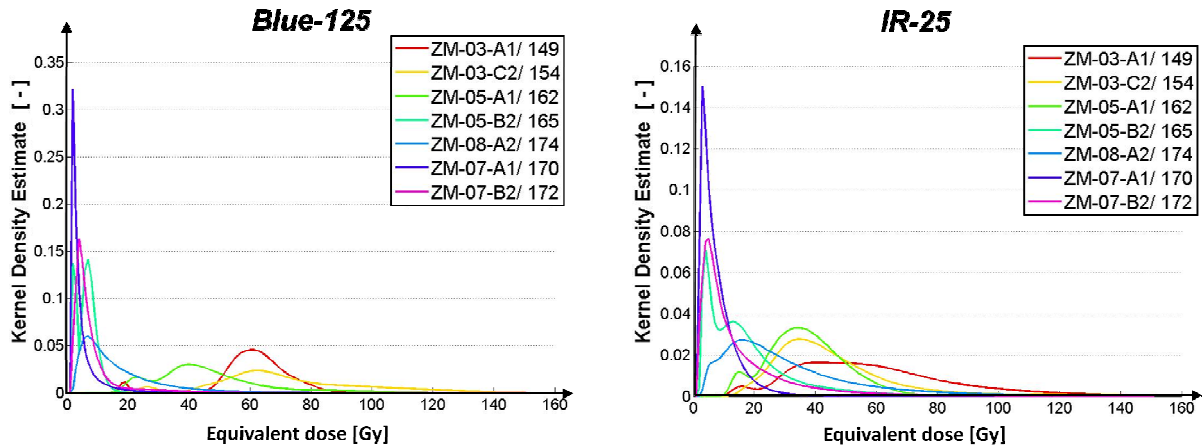


Figure IV-7: Kernel density estimation plots from fast-to-bleach signals of all selected samples

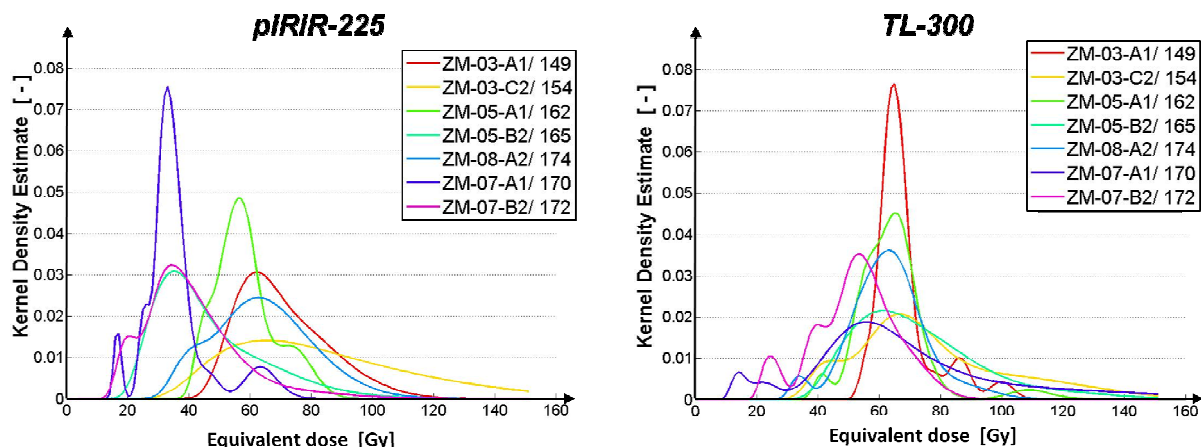


Figure IV-8: Kernel density estimation plots from slow-to-bleach signals of all selected samples

The Blue-125 and IR-25 are the signals that bleach most rapid. The pIRIR-225 and TL-300 are the hardest to bleach signals. To get these plots in perspective with Figure IV-6 we assume that distributions concentrating around 70 Gy are comparable to a homogeneously poorly- /un-bleached sample (A), a sample that has not or barely been bleached since its last burial. In the Blue-125 signal the plot shows more clearly the different shifting stages: homogeneously un-bleached (sample: ZM-03-A1 / 149), heterogeneously partial-bleached (sample: ZM-05-A1 / 162) and homogeneously well bleached (sample: ZM-07-A1 / 170). However the TL-300 does show a spread of the D_e values from a more homogeneous (sample: ZM-03-A1 / 149) to a heterogeneously (sample: ZM-07-A1 / 170) partial-bleached distribution without the shift towards lower equivalent dose values. Observed from the signal distribution evolution per sample is that within the fast-to-bleach signals we can see a distinctive change in distribution as where in the TL-300 samples this is much more obscured.

We can conclude that the mean equivalent values in combination with the distribution information for the fast-to-bleach as well as the slow-to-bleach are usable for Sand Engine scale morphological studies. However, for the TL-300 signal this information must be sought in the diffusion or spreading of the (KDE) distribution working with these temporal- and spatial scales and environments.

4.4.2 Bleaching experiment

During e.g. suspended transport in the water column the sediment comes into contact with daylight. The difference in bleaching behaviour of the different signals and effect of environmental circumstances on bleaching can be of considerable influence (see 2.3.2 and 2.3.3). A bleaching experiment was carried-out to translate equivalent dose values and transport distance into an equivalent in light exposure, related to the morphology.

During the exposure experiment we have used natural daylight in December 2012 (based on sunrise and sundown charts, minus dawn and dusk times) and with minimal influence of artificial lighting. Noted must be that this daylight conditions do correspond with the period with the most morphological activity (storm season). The bleaching was done with intervals ranging from 5 to 300.000 seconds, the latter is equivalent to 1.5 weeks of daylight.

The results are given in Figure IV-9 which are based on 6-8 aliquots (see Appendix 4), and fitted with a stretched hyperbolic- (OSL, IR and pIRIR) or stretched exponential (TL) function. On the horizontal axis the logarithmic bleaching time is plotted and on the vertical axis a normalization of the equivalent dose is given to emphasize the rate of bleaching for the different signals. As expected the Blue-125 and IR-25 show the fastest decrease in signal, though the IR-25 bleached an order of magnitude slower than the Blue-125. Both the pIRIR-90 and pIRIR-150 in the beginning show similar bleaching rates. However after 60 seconds the pIRIR-155 becomes one order of

magnitude slower in bleaching rate than the pIRIR-90 signal. For both the pIRIR-225 and TL-300 the bleaching rates are much slower than the other signals in which the TL-300 seems to have a threshold in resetting at 45% present of the starting values.

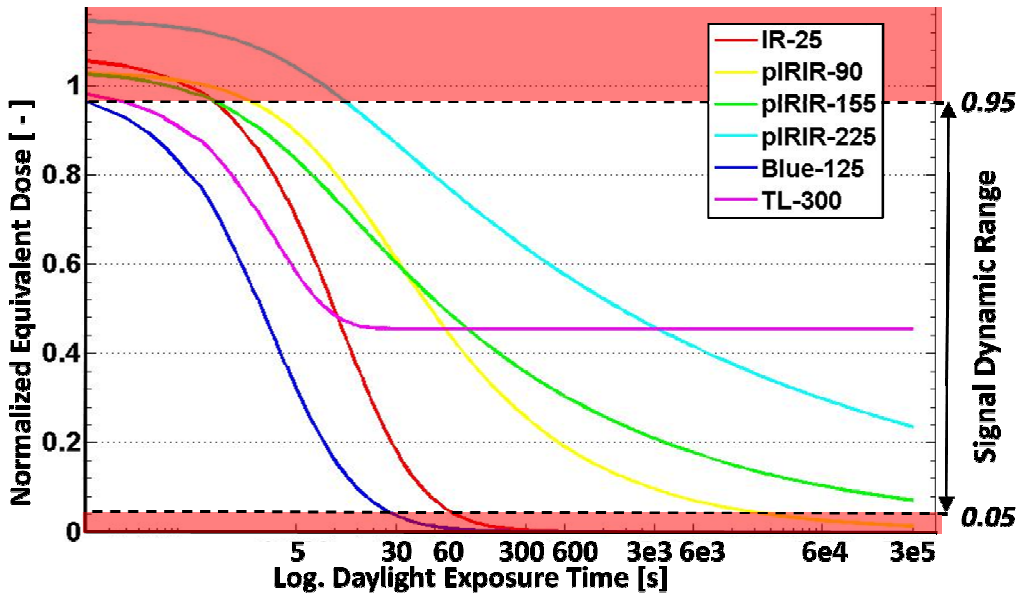


Figure IV-9: Bleaching experiment curves for the five different signals

The dynamic range in which the signal can be effectively used is what we assume between 5% lowest and 5% highest values, comparable to a normalized equivalent dose level of 0.05 and 0.95. in Table IV-3.

Stimulation bleach curve	Start [s]	End [s]	Dynamic range	
	0.95	0.05		
Blue 125°C (Blue 125)	0	24	24 s	Short
Infrared 25°C (IR 25)	1	78	77 s	Short
Post-infrared infrared 90°C (pIRIR 90)	3	14.100	14.097 s	Mid
Post-infrared infrared 155°C (pIRIR 155)	0	± 1.500.000	1.500.000	Long
Post-infrared infrared 225°C (pIRIR 225)	14	>5.000.000	>5.000.000	Long
Thermoluminescence 300°C (TL 300)	0.5	>5.000.000	>5.000.000	Long

Table IV-3: Dynamic range per luminescence signal

The bleaching experiment KDE results for fast-to-bleach signals (Figure IV-10) and slow-to-bleach signals (Figure IV-11) show distributions of the different subsamples on which the fitted curves of the bleaching experiment in Figure IV-9 are based.

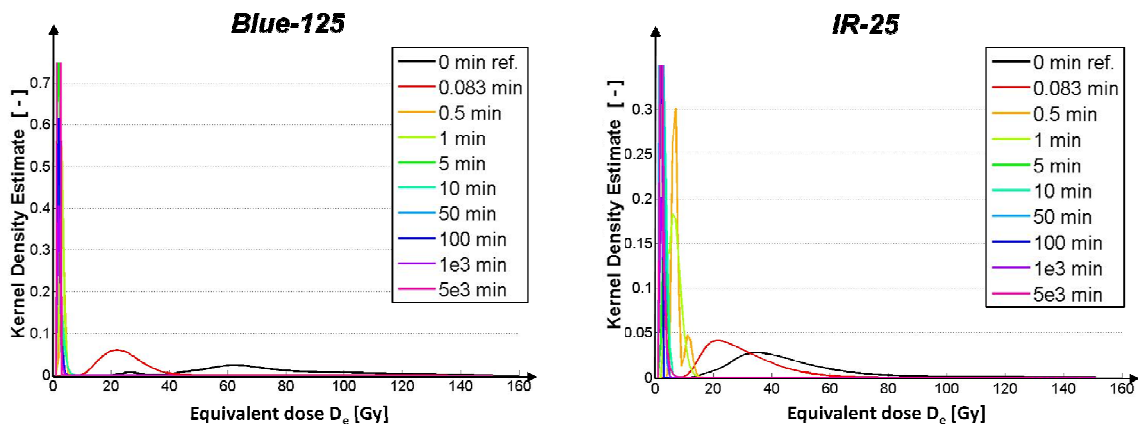


Figure IV-10: Kernel density estimation graphs of the bleaching experiment fast-to-bleach signals

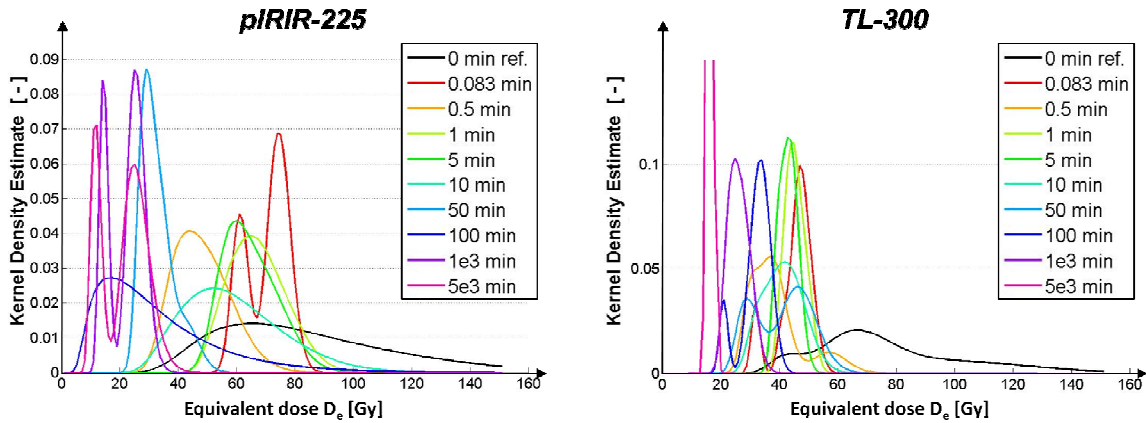


Figure IV-11: Kernel density estimation graphs of the bleaching experiment slow-to-bleach signals

These distributions can act as another method of quantifying the Sand Engine samples. In the Blue-125, IR-25 and partially the TL-300 plot, the distribution seem to go from a heterogeneously poorly bleached distribution (as in (B) Figure IV-6) to a homogeneously well bleached distribution (as in (C) Figure IV-6). However, the pIRIR-225 first goes to a homogeneously poorly bleached (as in (A) Figure IV-6). This difference in course displays that what we ought to expect from the samples (homogeneously un-bleached → heterogeneously partially bleached → homogeneously well bleached). However this seems to miss in the faster signal KDE distribution course, although not yet proven we expect this to come from the minimal exposure during dredging operations.

4.4.3 Effective Exposure Time (EET)

The measured luminescence signals are connected into a measurable effective exposure time (EET) through interpolation of the mean value onto the bleaching curves of (Figure IV-12).

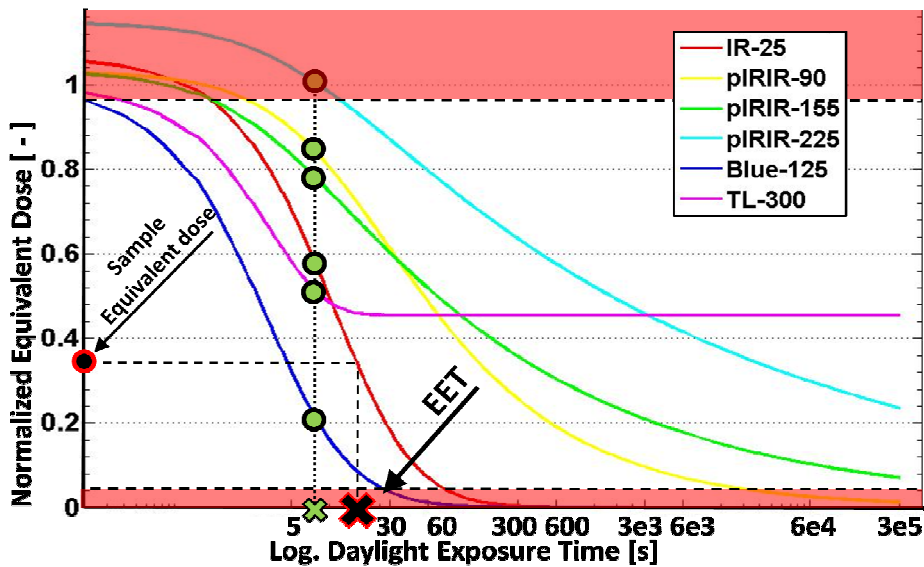


Figure IV-12: Effective Exposure Time (EET) interpolation

We expect that the observed difference in the signal lose rate is explained by connecting these equivalent dose values to a EET value. We hypothesize (depicted in Figure IV-12 with green symbols with black rim dots connected with dotted line) that the values of the equivalent dose differ per sample but that their EET values per signal are more or less uniform, provided that the equivalent dose value lays within the dynamic range of the sample. The underlying assumption here is that every grain has presumably been exposed to an equal amount of equivalent daylight.

Page left blank intentionally

CHAPTER 5: APPLICATION SYNTHESIS

BEFORE APPLYING A NEW TRACER TECHNIQUE ONE MUST FIRST UNDERSTAND THE INTERNAL DYNAMICS OF THE TRACER WHEN EXPOSED TO A TEST SITUATION. ONCE THESE INTERNAL DYNAMICS ARE UNDERSTOOD THE TRACER CAN BE IMPLEMENTED INTO A SEDIMENT TRACING STUDY. TO STUDY THE INTERNAL DYNAMICS OF THE LUMINESCENCE TRACER IT IS EVALUATED AGAINST A BATHYMETRIC MODEL COMPRISED OF SAND ENGINE DATA WHICH INCLUDES MONTHLY SURVEYS OF THE TOPOGRAPHY.



Rapid flowing channel mouth at Sand Engine , March 2012⁹

⁹ Rijkswaterstaat / Joop van Houdt

A powerful sediment tracing technique must fulfil certain requirements regarding the representation of morphologic change. We are interested whether luminescence properties of sediment can infer sediment transport and changes in the morphology and how they are deduced from a range of luminescence signals. We now will study the signals separately and how to apply these (5.1) and also the relation between signal and morphological change/ bathymetry data (5.1.3 and 5.1.4) Last will be a discussion on the (possible) capabilities of the technique for sediment tracing studies and whether the technique proves feasible (5.2).

5.1 Luminescence signal analysis

The principle of the luminescence sediment tracing technique is based on the bleaching behaviour of multiple luminescence signals (2.3.1). This bleaching behaviour was quantified with a controlled experiment with set bleaching times (4.4.2). We measured bleaching rate(s) with several orders of magnitude differences between the respective luminescence signals. These measurement equivalent dose results of the selected samples are then reflected onto the bleaching curve(s) (4.4.3).

5.1.1 Equivalent Exposure Time (EET) results

The bleaching curves represent bleaching under ideal full daylight exposure. However, from the bathymetry analysis of the selected samples the chance of a prolonged full daylight exposure occurring without the involvement of e.g. seawater to decrease the light intensity is minimal. First analysis of Figure V-1, where the mean EET values (4.4.3) are plotted on a logarithmic scale, shows a large scatter in values per sample. Studying this plot we notice that between the samples (except for the aeolian sample) most sample mean EET values stay within 0-100 seconds range. The Blue-125, IR-25, pIRIR-90, pIRIR-155 and TL-300 signals show a gradual rise of mean EET with distance from the starting point of sediment transport. Over the distance of 1.2 kilometre a difference in mean EET of a few seconds to a minute is measured. In 2.3.3 the significant influences of water on the light spectrum and intensity was illustrated. The samples are assumed to have been transported in submerged conditions, either as suspended- or bed load.

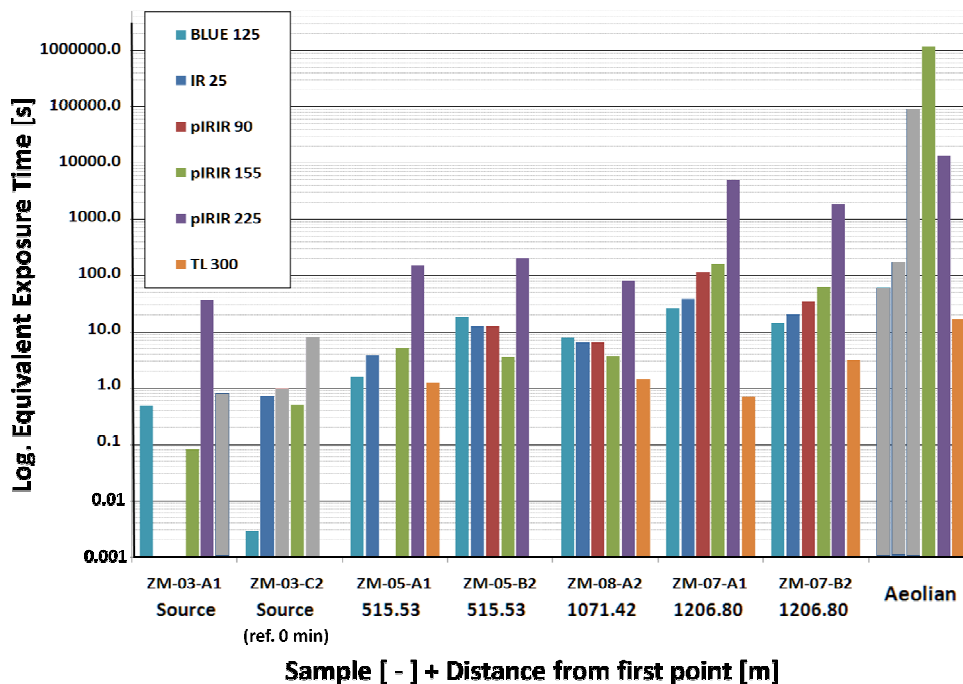


Figure V-1: Mean Equivalent Exposure Time (negative values cannot be shown)

The robustness of the fitted functions of the bleaching experiment curves is expressed in a number between 0 for poor fitting and 1 for a perfect fit. All the fits of the bleaching experiment are between 0.7 and 0.85, indicating a reasonably good fit. The faster signals are completely depleted after a certain duration of daylight exposure. The dynamic range of the fast-to-bleach signals is shorter and earlier than for the slow-to-bleach signals (Figure IV-9). In the bleaching curves a lower level under which the signal is to be assumed depleted and also an upper level to indicate where the bleaching starts to deplete is plotted (measurement limit, calculation error etc.). In this case we are using a 5% and 95% residual signal threshold (Figure IV-9). For the Blue-125 this limit is reached after 25 seconds of full daylight exposure and for IR-25 this is after 80 seconds. In case of the pIRIR-90 signal the 5% threshold is reached after 14.100(!) seconds because the main dynamic range of pIRIR-90 is considerably longer. In Figure V-1 the gray marked EET values are not within this dynamic range and are therefore rejected. Plotting three fast-to-bleach signals in a separate plot (Figure V-2) we observe that for the water lain transported samples the threshold is not yet reached even for the fast-to-bleach signals. However, the aeolian sample shows mean EET values that are twice or more this threshold level for the Blue-125-, IR-25- and pIRIR-90 signals.

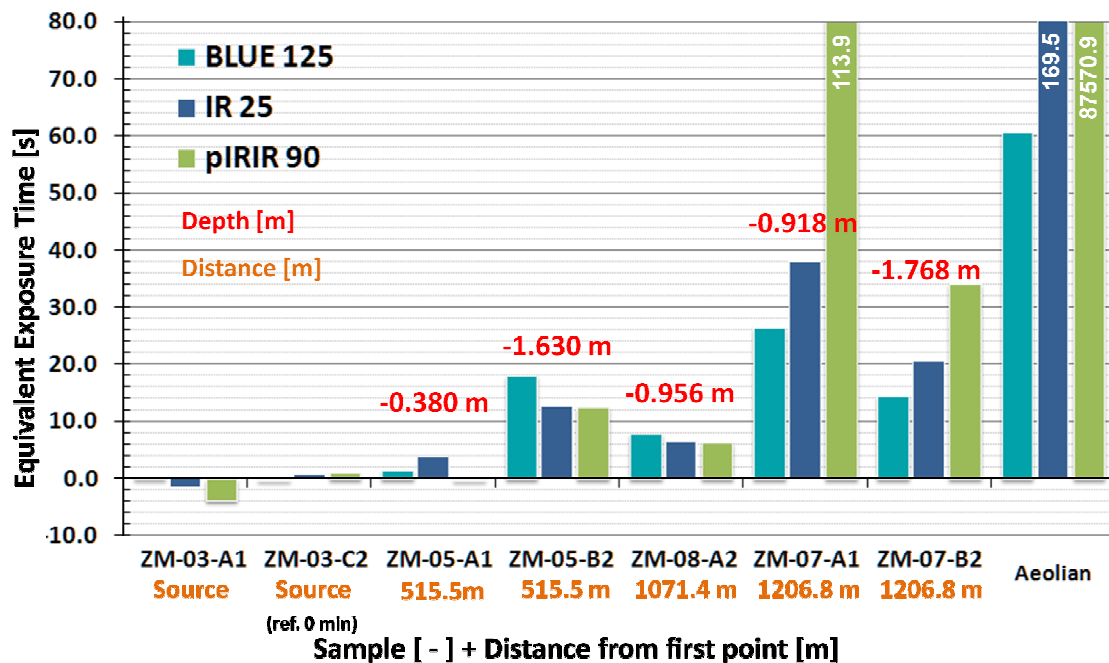


Figure V-2: Mean Equivalent Exposure Time (fast-to-bleach signals)

This plot suggests a number of things, first is that for the (presumable) water lain transported samples ZM-05, ZM-07 and ZM-08 over this distance (1200 m) the fast signals (*Blue-125*, *IR-25* and *pIRIR-90*) could be used for luminescence sediment tracing. For the aeolian transported sample the fast-to-bleach signals already are well below the 5% threshold as well as the slow-to-bleach pIRIR-155 signal. The only signals in the aeolian sample that are not yet outside the dynamic range are the pIRIR-225 and TL-300 signal. For aeolian sediment transport measurements these slow-to-bleach signals show the biggest potential.

5.1.2 Sediment source

First requirement for a luminescence study is the abundant presence of mineral that is luminescence sensitive. The second requirement, since we are studying the decay over transport, is that the sediment at the start of the transport has a considerable luminescence charge. The higher this starting luminescence equivalent dose in the mineral the longer the bleaching process will take and in theory the further we might be able to trace the sediment. These two requirements are crucial for the presence of a strong and suitable luminescence signal in the dredged/dumped

material. In the case of the Sand Engine the sand is mined from an old river Rhine terrace on the North Sea (see *MER: Aanleg en zandwinning Sand Engine Delflandse kust, February 2010*) 7 km out of the coast of The Hague, the Netherlands. These sediment deposits at this location presumably have not been disturbed for over 50.000 years. This is a good indicator for the presence of a strong initial luminescence signal, because it has potentially accumulated signal over the completely undisturbed, buried period. Second indicator, although no further research concerning this is available at the moment, is the dredging and dumping method. Some of the luminescence signals are bleached within minutes thus any exposure to daylight of the material can result in a strong depletion of signal. We reckon that during nourishment operations there are moments that sediment is fully exposed to daylight for short amounts of time e.g. in the barge or during rainbowing the sediment on the (underwater) beach face. However, this is most of the time in combination with water that, as we have seen, reduces the bleaching effectiveness considerably, hence the bleaching process is limited during the construction of the Sand Engine.

The samples from core ZM-03 act as control on the starting value of the nourished sand and whether these contain a strong and suitable luminescence signal. Two separate subsamples were selected to study the variability in luminescence starting value. ZM-03-A1 is a sample from the top (+1.709m NAP) of the selected ZM-03 core, ZM-03-C2 (-0.141m NAP) is the lowest samples of this core. These samples are either dumped by rain bowing or by pipe out flowing. In both cases there is a realistic chance of exposure to daylight. Figure V-3 gives the luminescence measurement results for the two ZM-03 samples. Both samples show a large equivalent dose (and thus strong luminescence signals) despite the possibility of exposure during nourishment operations. However, the mean values of both samples differ 10% - 15% from sample to sample with changing standard error.

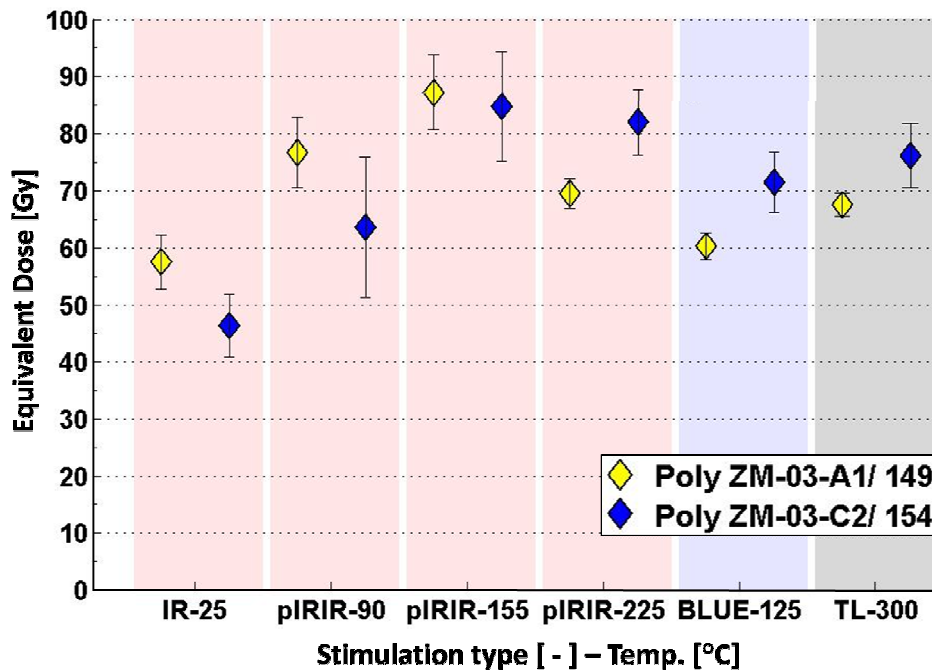


Figure V-3: Source control samples

Observing the underwater light spectrum from Figure II-9, we see that the blue part of the light spectrum penetrates the water losing less of its light intensity than the IR part. The value of the Blue-125 signal in Figure V-3 confirms this fact. The bottom sample (ZM-03-C2) has a higher luminescence value compared to the top sample (ZM-03-A1). This can be attributed by the fact that the Blue-125 signal only needs a short amount of light exposure to bleach. Since the chance of fallen dry and being fully exposed to daylight is higher in the top sample (+1.709m NAP) it should (as it is the case) be that the top sample has the lowest mean equivalent dose Blue-125 signal.

Interpreting the findings and their historical setting is hard or even impossible to verify at this moment.

5.1.3 Transport distance

In Figure V-2 we observe a clear trend of increasing EET with distance. This measure for transport distance of sediment can be connected to the dynamics in a mega-nourishment. The hypothesis here is that with distance from the original position of the nourished Sand Engine there is a decrease in luminescence signal and accordingly equivalent dose, because of the potential exposure to daylight while being transported. To test this hypothesis a selection of three samples is used (ZM-05-A1, ZM-08-A2 and ZM-07-A1). From the bathymetry analysis these three samples share the most commonalities as in deposition month, transport probability etc. In Figure V-4 the EET values are plotted (on a logarithmic scale) on the vertical scale as where the distance between them is plotted on the horizontal axis. The EET values are linearly connected to each other. First observation (in this case the ZM-03 samples are assumed 'EET = 0') from this plot is an increase of EET value with distance from the first transported sample ZM-05-A1 (A) as where point ZM-08-A2 (B) and ZM-07-A1 (C) both show higher values. However, studying the absolute EET values between A and B the difference is just a few seconds as where C is a multiple in seconds EET higher than B at just a quarter of the distance between A and B.

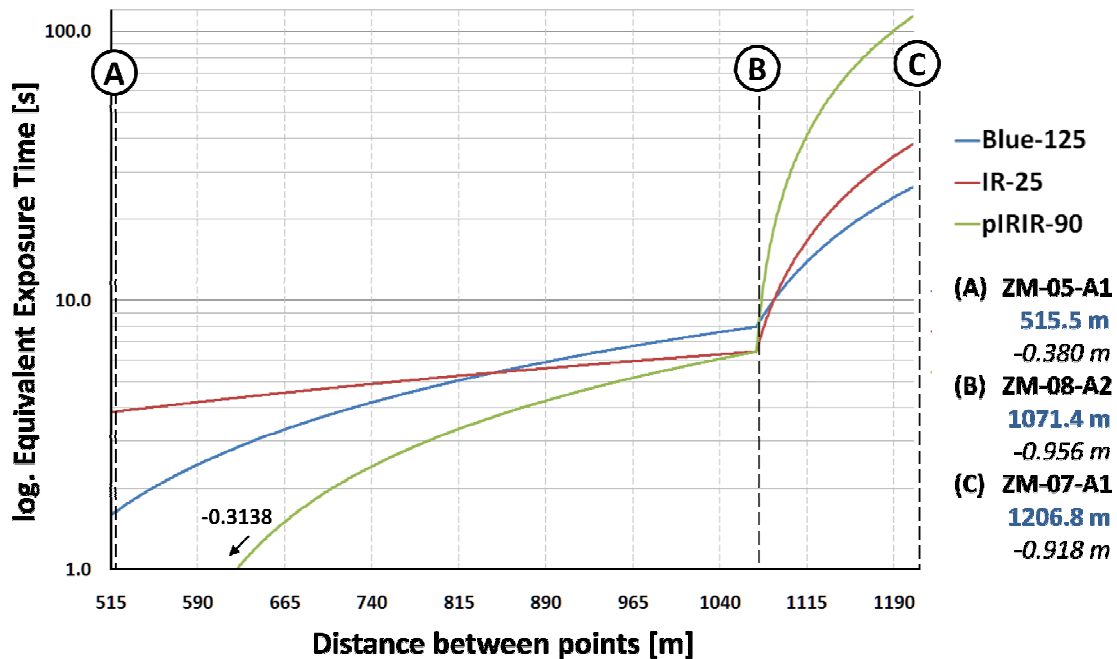


Figure V-4: Distance vs. mean equivalent exposure time ('distance', 'depth')

Studying the Kernel density estimation of the calculated EET values for every measurement result and bearing in mind that the every mean equivalent dose is based on the measurement of 20-24 sub-samples (aliquots) the following can be derived. Although the mean EET values in Figure V-4 do not differ strongly from one and another for sample ZM-05-A1 and ZM-08-A2 the shape of the EET KDE distributions do (Figure V-5). For example the shape of the ZM-05-A1 distribution(s) is considerably tighter than the ZM-08-A2 distribution(s). This would imply that looking at the inter-aliquot ratio, sample ZM-05-A1 has a higher contribution of samples that haven't seen any light or very little (between 5s-10s EET), since ZM-08-A2 has a wider distribution the contribution of aliquots between 5s-10s EET is lower and there is also some contribution of aliquots with higher EET values. In ZM-07-A1 there is much more scatter and contribution from aliquots with EET values between 15s-25s. This is what actually we would expect from samples that have crossed a larger distance from the eroded part of the Sand Engine. Thus having a larger transport distance.

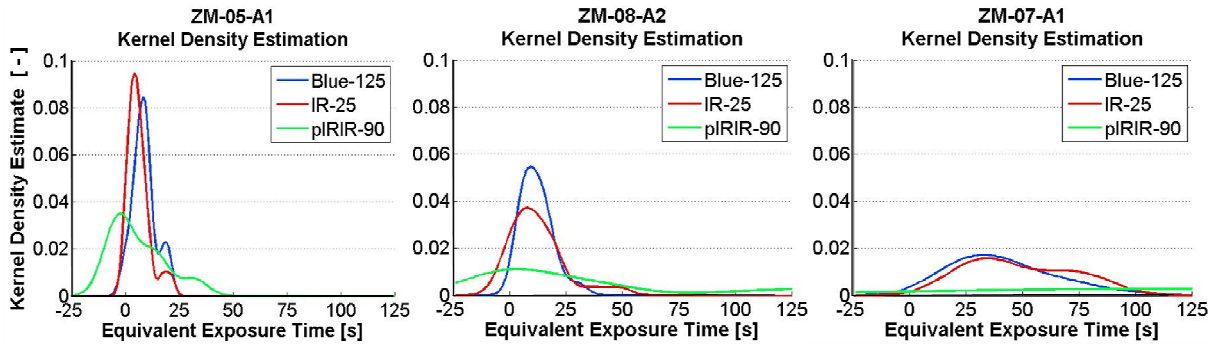


Figure V-5: Kernel Density Estimation EET values (ZM-05-A1, ZM-08-A2 and ZM-07-A1)

The scatter in the EET distributions is also signal dependent. However, a similar conclusion can be drawn in these signals. Taking a mean value does not consider this spread in the distribution, in this case a statistical treatment could possibly give us better EET estimates in the future.

Studying the course of EET values or the distributions still gives no satisfying explanation for the jump in EET values between ZM-08-A2 and ZM-07-A1 and the minimal gain in EET value between ZM-05-A1 and ZM-08-A2 where you would expect that ZM-08-A2 EET values would closer resemble to those of ZM-07-A1. Further inspection of the bathymetry data reveals a possible explanation for this observation. Studying the monthly morphological change at core position ZM-08 it becomes visible (Figure V-6) that a channel mouth migrates trough this point in northern direction. The migration is indicated by the continuous line (December 2011) and the dashed line (January 2012).

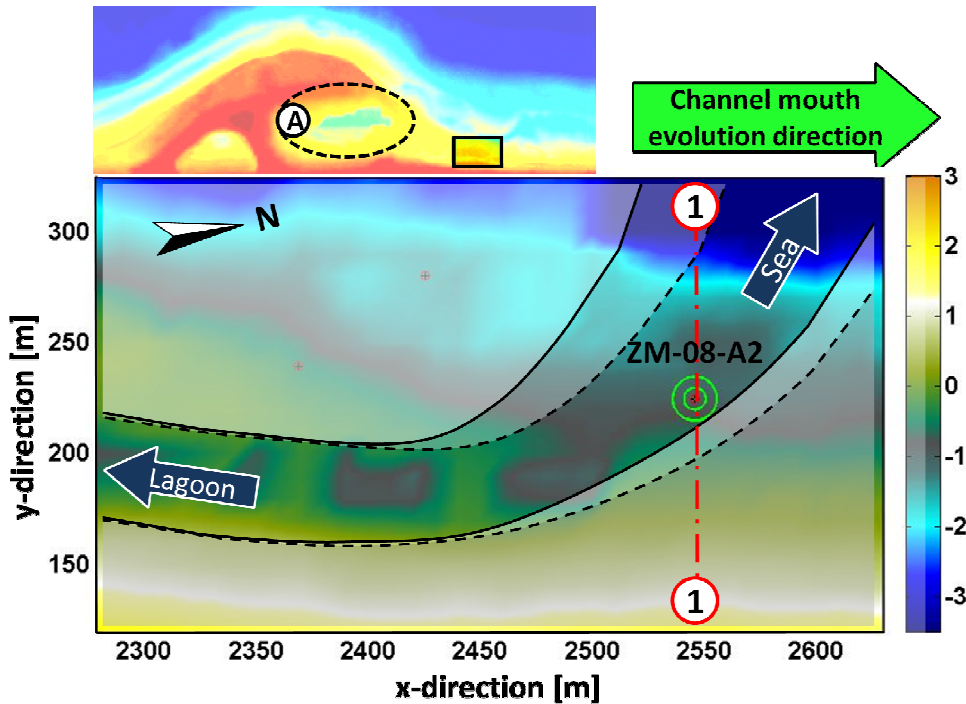


Figure V-6: Top view of ZM-08-A2. Marked is the long shore channel that was formed between the inner lagoon and the sea

In Figure V-6 a cross section is made, indicated by the '1-1' line. This cross section is plotted in Figure V-7 together with the sample core and sample position. The area marked with A is a linear interpolated trajectory of the bottom morphology in between the months. Going straight through sample position ZM-08-A2.

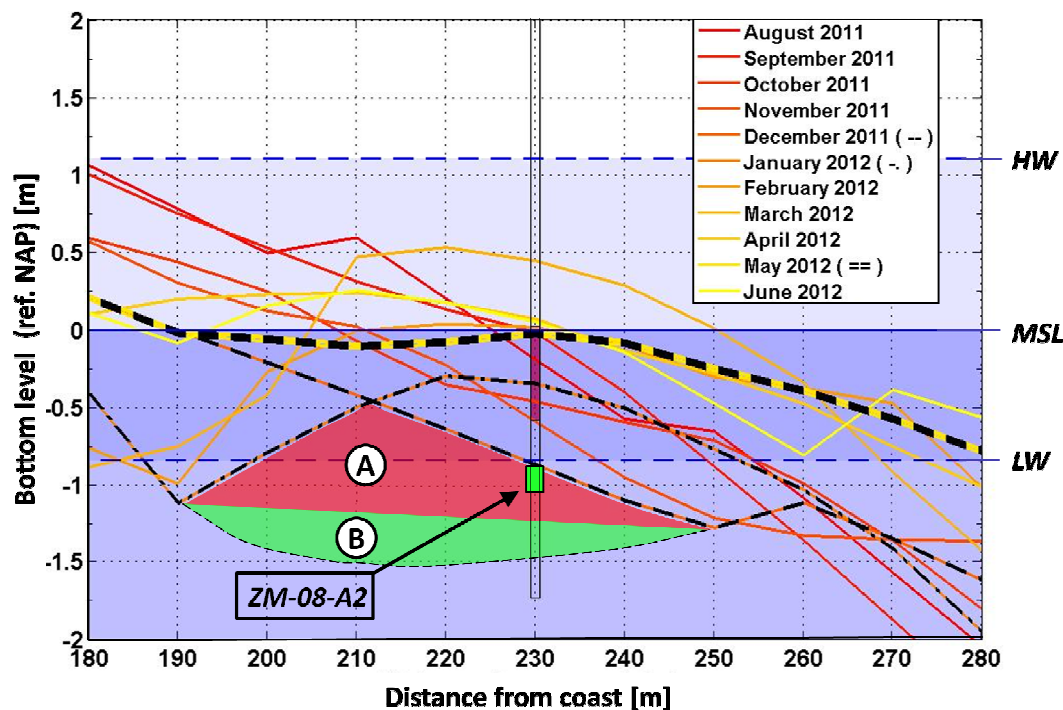


Figure V-7: Cross section (1 -- 1) of core ZM-08-A2. (A) Presumable erosion path (B) Case of severe erosion between monthly bathymetry surveys

This in itself is not the reason we reckon that low EET values are measured. We think that in this channel high flow velocity were measured which is connected to high transport capacity of sediment. This rapid flow between the inner lagoon (see Figure V-6; A, dashed circle) and the sea acts as a highway for transporting 'fresh' nourished sediment from the inner lagoon to the adjacent coast. This lagoon sediment is presumably sediment that resembles behaviour of 'short' transported sediment, as is the case for ZM-05-A1. Thus explaining our relative low EET values in sample ZM-08-A2.

5.1.4 Mode of transport

Generally we distinct 3 types of sediment transport modes: Aeolian (wind driven), suspended load (floating)- and bed load (rolling/bouncing) water lain transport. The aeolian transport has already become evidently from Figure V-2 having much higher EET values compared to the water lain transported sediment samples. The latter two are harder to distinct given the measured EET values. We assume here that a distinction between the latter two can be observed between two samples, preferably of the same core, deposited at different depths. A hypothesis here is that suspended particles that are transported and presumably deposited at an average higher bed level contain higher EET values. As where a sample that has been deposited at a deeper level should contain a lower average EET value, because during the bed load transport of sediment the chance of exposure to light is smaller than the suspended load transported sediment.

Studying the measurement results an increase of EET with depth is found (Figure V-8). However, expected is that this had shown an adverse result with the highest EET values measured in the top sample and the lower values in the bottom sample. It seems that here our very simple assumption is not right. Looking at the Samples from the ZM-07 core would seem to meet with our assumption. However, the bottom sample of core ZM-07 here presumably consists of pre-Sand Engine sediment (see Figure III-6) which in turn could have a different EET value because for it being pre-Sand Engine making it incompatible with core ZM-05. This is an important finding because it does say something of the mode of transport, although further study is needed to prove this latter.

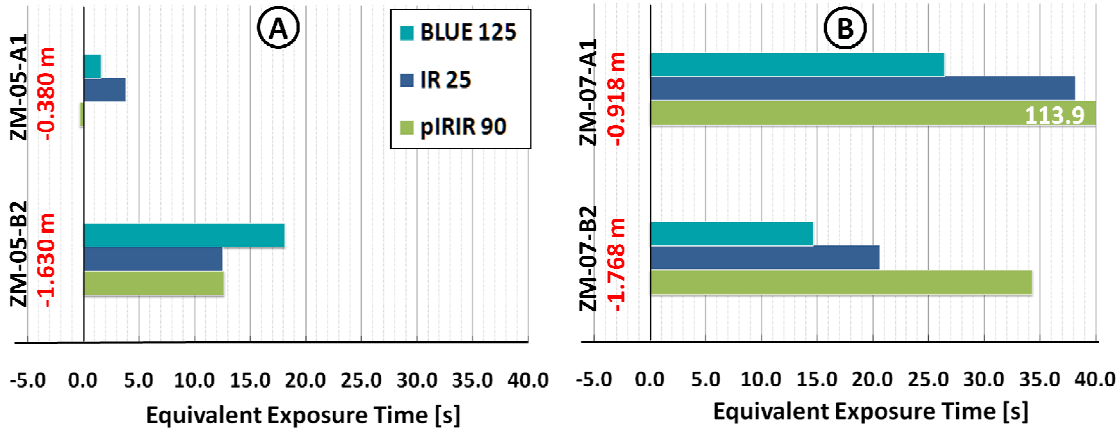


Figure V-8: (A) EET values ZM-05-A1 and ZM-05-B2 (B) EET values ZM-07-A1 and ZM-07-B2

In Figure V-9 (A,B) a first deduction is made towards a possible explanation for what we found in Figure V-8 (A). We know that the bleaching of water lain transported grains is dependent on the time and intensity of light penetrating into the water column (Figure V-9, B). Solely studying the transport profile (A) and the intensity decay curve (B) we expect that suspended sediments in the higher regions of the profile have been exposed to a higher intensity of light, and accordingly better bleaching conditions than the suspended or even as bed load sediments travelling in lower regions. This effect becomes stronger when turbidity is added and the light intensity is further diminished by sediments attenuating light.

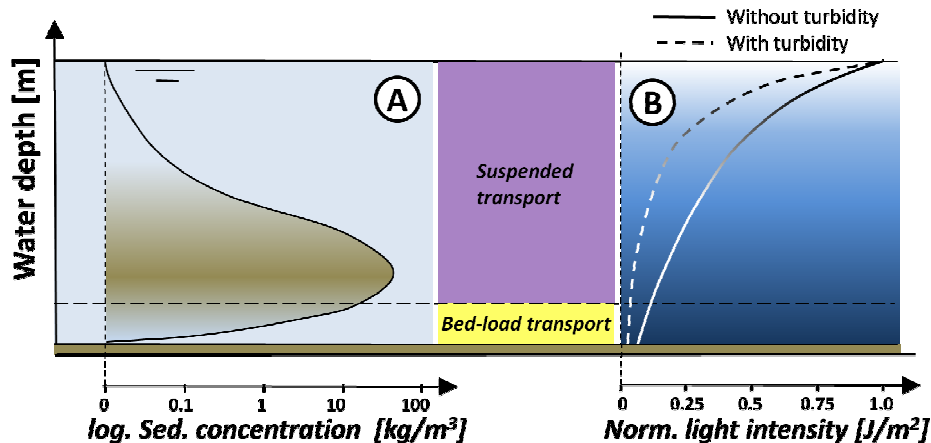


Figure V-9: Typical long shore sediment transport concentration depth profile (Modified from Bosboom & Stive 2011; Figure 6-8) (B) Schematically interpreted light penetration vs. water depth, without and with the turbidity by sediment in suspension (Modified from Boyd 2000; Figure 1.6)

However, water lain suspended sediment grains travel in turbulent chaotic swirls distributed over the entire water column. Here sediments are being constantly exchanged between different depths (Figure V-9, A). This makes the likelihood smaller that sediments travel at a constant level and refutes our earlier assumption when we only looked at the transport profile.

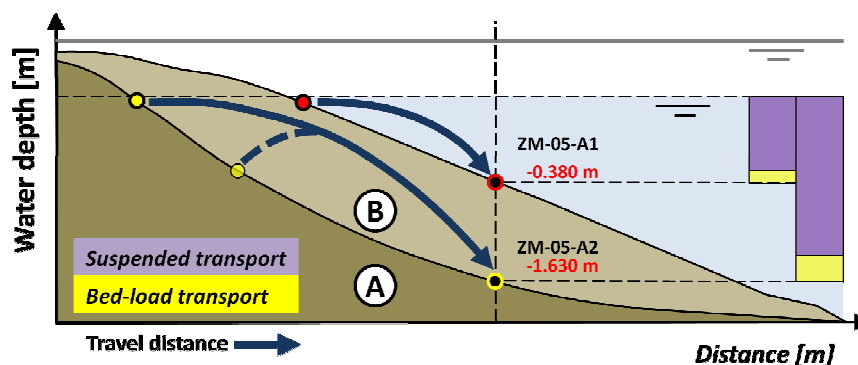


Figure V-10: Schematic representation of transport distance vs. mode of transport

We reckon that at this moment the (presumable) distance travelled – in combination with depth – is much more governing the luminescence EET value in this case of water lain transport than the actual mode of transport. This is schematically drawn in Figure V-10. The aeolian sample in comparison with the water lain samples displays EET levels that are 1-5 orders of magnitude higher. Despite having only one aeolian sample to compare to the difference from the water lain samples is substantial in a way that we can conclude that a distinction can be made between the water lain transported samples and aeolian transported samples on the bases of luminescence measurements with the PMS-SAR protocol..

5.2 Discussion

Luminescence measurements from the Sand Engine samples show promising results. Observed are indicators that endorse the potential of luminescence applied to coastal morphology monitoring. However, there are some critical points of discussion that are not yet covered by this investigation. One is the validity of the results in relation to the area that is covered by the sampling. These two points will form the motivation for the feasibility.

5.2.1 Capabilities

This study unmistakably shows the potential of the luminescence technique in morphological studies. We do not only measure a signal, a quantifiable difference is observed in the general transport direction of the newly formed spit at the Sand Engine. The luminescence technique potentially can be used as an hind cast tool to study the morphological history of a redistributing nourishment with spit forming. This case deals with the spit forming of a mega-nourishment along a North Sea coastal area. Observed in the experimental results is that some of the signals have a limited dynamic range, hence the applicability per signal is limited. However were using a multiple array of signals from a single sample each with an increasing dynamic range solving this problem partially. For the Sand Engine i.e. over a water lain transport distance of 1200m between the different samples only the fastest-to-bleach signal (blue OSL) of the six in total measured signals has reached its dynamic range limit. The faster-to-bleach signals (blue-OSL, IR25) are very sensitive to seconds of bleaching increasing for the slow-to-bleach signals (pIRIR-225, TL-300) to hours-days of bleaching under full daylight conditions.

The PMS-SAR protocol can be used to study morphology within a 1000m range for the fast-to-bleach signals to several kilometres and further for the slower bleachable signals. The bleaching rates of the different signals are influenced by the environmental conditions (e.g. light intensity, presence of water etc.). Depending on the test settings in which the bleaching curve experiments are conducted. We reckon that by doing experiments under different environmental conditions it is possible to deduce a detailed sedimentary history from the luminescence measurements and rather than absolute values of sedimentation and erosion also produce relative details as sediment provenance of, in our case, nourished sediment or whether the sediment is coming from other sources like offshore or the original beach face.

5.2.2 Pitfalls

We have observed a difference in dynamic bleaching range for the measured signals. This dynamic range for the fast-to-bleach signals is within the first 10-30 seconds (Blue-125) and for the slow-to-bleach signals this is well past a week of natural daylight bleaching. This however holds closely to the experimental conditions in comparison with the natural circumstances. The bleaching experiment has been conducted under test conditions comparable to aeolian transport and we are applying these to water lain conditions. However, doing more comprehensive bleaching experiments that are able to mimic turbid underwater conditions will also increase the complexity of the interpretation. We do also not know what number of test conditions (i.e. how many morphological scenarios do we need to mimic) are necessary to realistically represent the relation(s) between coastal morphodynamics and luminescence bleaching behaviour

The highest resolution in transport distance/equivalent exposure times etc. depends firstly on the accuracy and precision of measuring. There will always be an error margin whether this is naturally or artificial induced. The mean equivalent dose values are based on the average of ± 20 aliquot sample. However, we have shown that the mean value does leave out important details on how the values are distributed amongst these 20 aliquots. This inter-aliquot difference could potentially provide more insights about sediment transport processes, however, the development of a more sophisticated statistical procedure is still outstanding. In addition, one could question whether this number of aliquots could suffice in representing the distribution insight a core subsample. Secondly there is the use of the polymineral sampled aliquots as described earlier. We observed that these measurement values do not deviate much for the measured luminescence signal from separated quartz and feldspar fraction. Still the measured feldspar- (IR-part) or quartz (Blue-part) signal whether this is in a polymineral sample or not depends on two things, the sensitivity of the grains (i.e. giving a bright or dim signal) and the ratio to the two mineral being present in the polymineral sample.

Third is the (in)homogeneity of the starting signal of the different sediments. We saw that on a small scale this could be as much as 10% to 15% between samples. However, this not necessarily has to be a downside, because for identifying the source one could use a very stable signal that is not effected so much by bleaching and this could then be passed into the calculation with the faster bleachable signals.

Feldspars are common for their susceptibility to a phenomena called anomalous fading (Wintle 1973). Anomalous fading is the self-emptying of electrons from their traps, hence losing signal without being exposed to light. This phenomena might express itself in the lower temperature IR and pIRIR. The higher temperature pIRIR signals are known to be more stable and do not suffer as much from this phenomena (Thomsen et al. 2008).

5.2.3 Feasibility

The goal of this whole thesis was to investigate the feasibility using luminescence technique to study morphological processes. The development of the luminescence protocol with multiple signals is a big contribution to both the luminescence community as for morphological research. The results have been surpassing our own expectations in representing general morphology dynamics on the scale of the newly formed spit of the Sand Engine. However, the results are not conclusive enough to fully relate them to detailed morphological processes, hence for practical applications the technique is not yet fully understood. Still the technique shows a great potential for applications in sediment tracing. Not only in the case of (mega-)nourishments we also reckon that this luminescence technique is applicable to all types of sandy coasts, provided that the site meets the luminescence requirements (5.1.2).

CHAPTER 6: CONCLUSION & RECOMMENDATIONS

THIS THESIS IS FINALIZED WITH SOME CONCLUSIONS AND RECOMMENDATIONS CONCERNING THE USE, IMPLICATION AND SUGGESTIONS THAT COULD AND NEED TO BE ADDRESSED IN FOLLOW UP RESEARCH. THE MEASUREMENT RESULTS REVEAL THE POTENTIAL OF THE TECHNIQUE AND THE USE OF IT IN MORPHOLOGICAL STUDIES. DISTINCT LUMINESCENCE MEASUREMENT RESULTS CAN BY APPOINTED TO MORPHOLOGICAL EVOLUTION DETAILS THAT ARE INHERENT TO SEDIMENT TRANSPORT DYNAMICS AT THE SAND ENGINE.



Sand Engine, July 2012¹⁰

¹⁰ *Rijkswaterstaat / Joop van Houdt*

Concluding this master thesis the research questions, introduced in 1.3, will be discussed. This is preceded by a conclusion, based on insights that were obtained during this thesis. A final remark is formed by recommendations towards related- and future research .

6.1 Conclusion

This thesis is one of the first studies combining natural sediment luminescence properties as a technique to investigate coastal morphological processes on a short timescale by utilizing the luminescence bleaching characteristics as a measure to trace sediment. Bored core field samples on the north-eastern side sand spit of the Sand Engine were obtained to test our hypothesis towards the applicability of the luminescence technique on (recently) transported samples.

For this purpose a new custom-made luminescence protocol was developed appropriate to match the complexity of the coastal morphology dynamics. Obtained from experiments the effectiveness of our newly developed PMS-SAR (*Polymineral Multiple Signal - Single Aliquot Regenerative*) luminescence protocol proved itself able to give results, while simultaneously increasing practicality, comparable with the current measuring methods using separated mineral samples of quartz and feldspar.

Through controlled bleaching experiments we conclude that with this multi-step multi-signal protocol we can observe a difference in bleaching behaviour per signal from a single polymineral sediment aliquot sample. Proceeding this results we also found that these bleaching rates differ several orders of magnitude with an equal amount of daylight exposure. The signal depletion is a finite process where the quartz sensitive 'blue-125' signal (blue light stimulation) has the shortest effective bleaching- or dynamic range such that the signal is depleted after less than 30 seconds. However, the feldspar(s) sensitive 'pIRIR-225' signal (post-infrared infrared light stimulation) has a dynamic range of >100 hours daylight exposure. This difference could hold possibilities to use a set of signals for short-term processes and others for long(er)-term studies forming a unique luminescence fingerprint for each measured sample.

Based on data from bathymetrical surveys and the GPS position of the bored cores a selection of subsamples was done. With the selection of the subsamples assumptions regarding the possible sedimentary history were done preceding the measurement of the luminescence equivalent dose. By subsequently relating the latter measured equivalent dose values to the bleaching curves yielded a new measurement unit; equivalent exposure time (EET). In these EET values we observed an quantifiable increase with distance from the original contour of the Sand Engine. Matching our expectation that with transport distance a rise in EET would be measured. Strikingly within our study area the water lain transported samples show just seconds to minutes EET where the one aeolian transported sample in general shows much larger values of up to day(s) of EET.

Concluding the main research question, whether it is possible to apply a multi signal luminescence protocol as an accurate technique for tracing sediment particles and sedimentary transport history within a mega nourishment. The results of the measurements in Chapter I reveal the potential of the technique and the use of it in morphological studies. Distinct, though quantitatively, luminescence measurement results can be appointed to morphological evolution and processes.

6.2 Recommendations

Primarily this thesis has taken the first steps towards the development of a measurement technique that coastal engineers or luminescence researchers could use to investigate morphological evolution on a coastal stretches or other morphological active areas (sub-aqueous as well as aeolian transport studies). Due to the complexity of the coastal system, firm conclusions cannot be made yet on either the transport distance or provenance of the selected sediment samples. Recommendations are therefore made below to improve the qualitative value of the measurement results in relation to the morphodynamics.

Cores have been taken during a sampling campaign of 2 days representing a snapshot of the morphology. However, comparison of samples is in this way harder because the sediment that is measured has not only been transported but might also have a totally different source or starting luminescence value. Sediment for the nourishment has been dredged from several offshore sites and is subsequently nourished in one spot. During these dredging operations the sediment is reworked and mixed a couple of times and possibly has, to some degree, been exposed to daylight. This might induce an extra variable in the measured luminescence signal(s) values. Assessing the dredging and dumping methods e.g. rain bowing for potential exposure might produce a more accurate view on the measured luminescence values after it has been transported by natural processes. In the case of the Sand Engine there were reasonable estimations on where the most erosion would occur. At the same moment this piece could have been cored just after completion of the Sand Engine to actually have a more representative overview of starting values. Since this sediment would later be eroded, transported and deposited at the newly formed spit.

The selection of samples has been done on the bases of criteria as distance from original contour, depth and (presumable) deposition month. The results of these samples give us a good indication of the morphological evolution in relation to luminescence signal. However, only seven subsamples, of a total of thirty, were used to make such an impression. Advisable is it to select a number of extra samples to see how these, with bathymetric description, stand in proportion to the already measured samples.

Observed in the water lain samples are low EET values. This seems to be out of line considering that with an average current velocity of 1 m/s one does expect that bleaching times would be higher for at least the samples at the end of the studied area. We reckon that this is due our bleaching experiment that was conducted under non-obstructed full daylight conditions. Since *Keisars et al. (2008)* in his experiment shows the impact of water on bleaching rates of respectively a TL signal. Investigating the effect on the bleaching rates/ behaviour of the signals in our protocol when samples are submerged is an important step in improving our understanding of luminescence behaviour in (water lain) transported sediment.

The smallest scale in sediment system is a single sediment grain. In this study we are using 'bulk' samples that consist of 100-150 grains with a size in the range of 300 μ m - 355 μ m. It is well possible that the sedimentary history of each grain differs greatly from one and another. Since luminescence measurements can be applied to measure such single grains. By measuring single grains one could recover much more detailed information on the composition of sediment samples luminescence signals with varying sedimentary histories. However, this needs to be a practical consideration since this is a very laborious method of measuring.

Morphology is a very dynamic phenomenon with many complex interactions between (hydraulic) forcing and sediment. Sediment transport in an environment as the Sand Engine is not a straightforward process in which a bulk of sediment is transported entirely at a set rate from A to B. To investigate the behaviour of luminescence signals, small scale sediment transport experiment could be created in a research flume in which the forcing and transport conditions are more controlled and can vary according to mimic natural conditions.

REFERENCES

- Aitken, M. J., Tite, M. S., and Reid, J., (1964) *Thermoluminescent dating of ancient ceramics*. *Nature*, 202: p. 1032–1033.
- Aitken, M.J. (1985) *Thermoluminescence Dating*. Academic Press, London
- Aitken, M.J. (1998) *Introduction to Optical Dating*. Oxford University Press ISBN13: 9780198540922
- Bailey, R.M. (1997) *Optical detrapping from the 110°C quartz TL region*. *Ancient TL* 15: p. 7-10
- Balescu, S. and Lamothe, M. (1992) *The blue emission of K-feldspar coarse grains and its potential for overcoming TL age underestimation*. *Quaternary Science Reviews* 11: p. 45-51.
- Ballarini, M., Wallinga, J., Murray, A.S., Heteren, S. van, Oost, A.P., Bos, A.J.J., Eijk, C.W.E. van (2003) *Optical dating of young coastal dunes on a decadal time scale*. *Quaternary Science Reviews* 22: p. 1011-1017.
- Black, K.S., Athey, S., Wilson, P. and Evans, D. (2007) *The use of particle tracking in sediment transport studies: a review*. In Balson, P., and Collins, M.B., *Coastal and Shelf Sediment Transport*. Geological Society of London, Special Publication 274: p.73-91
- Bosboom, J and Stive M.S.F (2011) *Coastal Dynamics I: Lecture notes CT4305*. VSSD publishing, Delft
- Bøtter-Jensen, L., Duller, G.A.T. and Poolton, N.R.J. (1994b) *Excitation and emission spectrometry of stimulated luminescence from quartz and feldspars*. *Radiation Measurements* 23: p. 613-616
- Bøtter-Jensen, L., Agersnap Larsen, N., Markey, B.G. and McKeever, S.W.S. (1997) *Al₂O₃:C as a sensitive OSL dosimeter for rapid assessment of environmental photon dose rates*. *Radiation Measurements* 27: p. 295-298.
- Bøtter-Jensen, L., Andersen, C.E., Duller, G.A.T., Murray, A.S. (2003) *Developments in radiation, stimulation and observation facilities in luminescence measurements*. *Radiation Measurements* 37: p. 535–541.
- Bluszcz, A. (2001) *Simultaneous OSL and TL dating of sediments*. *Quaternary Science Reviews* 20: p. 761-766.
- Buylaert, J.-P., Jain, M., Murray, A.S., Thomsen, K.J., Thiel, C. and Sohbaty, R. (2012) *A robust feldspar luminescence dating method for Middle and Late Pleistocene sediments*. *Boreas*, 10.1111/j.1502-3885.2012.00248.x. ISSN 0300-9483.
- Boyd, C.E. (2000) *Water quality: An introduction*. Springer, ISBN-13: 978-0792378532
- DHV BV., H+N+S landschapsarchitecten (2010) *Kust Visie Zuid-Holland: Projectnota/ MER Sand Engine Delflandse kust*. Dossier C6158-01.001, registratienummer WA-WN20090054
- Dronkers, J. (2005) *Dynamics of Coastal Systems*. Advanced series on Ocean Engineering, vol. 25. World Scientific, Singapore.
- Foster, I.D.L. (2000) *Tracers in Geomorphology*. Wiley, Chichester.
- Fu, B., Field, J.B., Newham, L.T. (2006) *Tracing the source of sediment in Australian coastal catchments*. *Regolith* 2006: p.100
- Fu, X., Li, S.-H., (2013) *A modified multi-elevated-temperature post-IR IRSL protocol for dating Holocene sediments using K-feldspar*. *Quaternary Geochronology* (2013), **IN PRESS**, doi: 10.1016/j.quageo.2013.02.004.
- Galbraith, R.F., Roberts, R.G. (2012) *Statistical aspects of equivalent dose and error calculation and display in OSL dating: An overview and some recommendations*. *Quaternary Geochronology* 11: p. 1-27

- Godfrey-Smith, D.I., Huntley, D.J. and Chen, W.H. (1988) *Optical dating studies of quartz and feldspar sediment extracts*. Quaternary Science Review 7: p. 373-380
- Grasso, F., Michallet, H., Barthélemy, E. (2011) *Experimental simulation of shoreface nourishments under storm events: A morphological, hydrodynamic, and sediment grain size analysis*. Coastal Engineering 58, Issue 2: p.184-193
- Hansen, L., Funder, S., Murray, A.S. and Mejdahl, V. (1999) *Luminescence dating of the last Weichselian Glacier advance in East Greenland*. Quaternary Science Review 18: p. 179-190
- Huntley, D.J., Godfrey-Smith, D.I., and M.L.W. Thewalt. (1985) *Optical Dating of Sediments*. Nature 313: p. 105-107
- Hütt, G., Jeak, I. and Tchonka, J. (1988) *Optical Dating: K-Feldspars optical response stimulation spectra*. Quaternary Science Review 7: p. 381-386
- Keizars, K.Z., Forrest, B.M. and Rink, W.J. (2008) *Natural Residual Thermoluminescence as a Method of Analysis of Sand Transport along the Coast of the St. Joseph Peninsula, Florida*. Journal of Coastal Research, 24(2): p. 500-507.
- Li, B., Li, S.-H., (2011) *Luminescence dating of K-feldspar from sediments: a protocol without anomalous fading correction*. Quaternary Geochronology 6: p. 468-479.
- Liritzis, I (2000) *Advances in thermo- and opto-luminescence dating of environmental materials (sedimentary deposits). Part I: Techniques*. Global Nest: the Int. J. Vol. 2, No 1: p 3-27
- Liu, H., Hamamoto, A., Sato, S. (2011) *Monitoring the nourished sand alongshore movement base on feldspar luminescence measurement*. University of Tokyo, Tokyo 113-8656, Japan.
- Meene E.A. van de, Staay J. van der, Teoh Lay Hock (1979) *The Van Der Staay Suction Corer*, ISBN 90 1202 3874
- Preusser, F. (1999b) *Bleaching characteristics of some optically stimulated luminescence signals*. Ancient TL 17: p. 11-14.
- Post, K.D. van der, Oldfield, F. and Voulgaris, G. (1995) *Magnetic tracing of beach sand: preliminary results*. Coastal Dynamics '94, Proceedings of International Conference: p. 323-334.
- Poolton, N.R.J., Ozanyan, K.B., Wallinga, J., Murray, A.S., Bøtter-Jensen, L., (2002a) *Electrons in feldspar II: a consideration of the influence of conduction band-tail states on luminescence processes*. Physics and Chemistry Minerals 29: p. 217-225.
- Reimann, T. and Tsukamoto, S. (2012) *Dating the recent past (<500 years) by post-IR IRSL feldspar e Examples from the North Sea and Baltic Sea coast*. Quaternary Geochronology 10: p. 180-187
- Richardson, N.M. (1902) *Experiment on the movements of a Load of Brickbats Deposited on the Chesil Beach*, Proceedings of the Dorset Natural History and Archaeological Society 23: p.123-133
- Rink, W.J. (1999) *Quartz luminescence as a light-sensitive indicator of sediment transport in coastal processes*. Journal of Coastal Research, 15(1): p. 148-154.
- Rotman, R., Naylor, L., McDonnell, R. and MacNiocaill, C. (2008) *Sediment transport on the Freiston Shore managed realignment site: An investigation using environmental magnetism*. Geomorphology 100 (2008): p. 241-255
- Sanderson, D.C.W., Bishop, P., Stark, M., Alexander, S., Penny, D. (2007) *Luminescence dating of canal sediments from Angkor Borei, Mekong Delta, Southern Cambodia*. Quaternary Geochronology 2: p. 322-329
- Sawakuchi, A.O., Kalchgruber, R., Giannini, P.C.F., Nascimento Jr., D.R., Guedes, C.C.F., Umisedo, N.K. (2008) *The development of blowouts and fore dunes in the Ilha Comprida*

- barrier (South-eastern Brazil): the influence of Late Holocene climate changes on coastal sedimentation. Quaternary Science Reviews 27: p. 2076 - 2090.*
- Sawakuchi, A.O., Blair, M.W., DeWitt, R., Faleiros, F.M., Hyppolito, T.N., Guedes, C.C.F. (2011) *Thermal history versus sedimentary history: OSL sensitivity of quartz grains extracted from rocks and sediments. Quaternary Geochronology 6: p. 261 - 272.*
- Sawakuchi, A.O., Guedes, C.C.F. , DeWitt, R., Giannini, P.C.F., Blair, M.W., Nascimento Jr., D.R., Faleiros, F.M. (2012) *Quartz OSL sensitivity as a proxy for storm activity on the southern Brazilian coast during the Late Holocene. Quaternary Geochronology 13: p. 92-102*
- Singarayer, J.S., Bailey, R.M., Ward, S., Stokes, S. (2005) *Assessing the completeness of optical resetting of quartz OSL in the natural environment. Radiation Measurements 40: p. 13-25*
- Son, S. van, Lindenbergh, R., Schipper, M.A. de, Vries, S. de, Duijnmayr, K., 2009. *Using a personal watercraft for monitoring bathymetric changes at storm scale. International Hydrographic Conference. Cape Town, South Africa.*
- Stokes, S., Bray, H.E. and Blum, M.D. (2001) *Optical resetting in large drainage basins: tests of zeroing assumptions using single-aliquot procedures. Quaternary Science Reviews 20: p. 879-885.*
- Thomsen, K.J., Murray, A.S., Jain, M., Bøtter-Jensen, L., (2008) *Laboratory fading rates of various luminescence signals from feldspar-rich sediment extracts. Radiation Measurements 43: p. 1474-1486.*
- Ventura Jr., E., Nearing, M.A., Norton, L.D. (2001). *Developing a magnetic tracer to study soil erosion. Catena 73: p. 277-291.*
- Walling, D. E. (2003) *Using environmental radionuclides as tracers in sediment budget investigations, erosion and sediment transport measurement in rivers. Technological and Methodological Advances, Proceedings of the Oslo Workshop, June 2002 : p. 57-78.*
- Wallinga, J. (2002) *Optically stimulated luminescence dating of fluvial deposits: a review. Boreas Vol. 31: p. 303-322, Oslo. ISSN 0300-9483*
- White, T.E. (1998) *Status of measurement techniques for coastal sediment transport. Coastal Engineering 35: p. 17-45.*
- Wijnberg, K.M. (2002) *Environmental controls on decadal morphologic behaviour of the Holland coast. Marine Geology 189: p. 227-247.*
- Wijsman J.W.M., Verduin E. (2011). *T₀ monitoring Sand Engine Delflandse kust: benthos ondiepe kustzone en natte strand. IMARES, Yerseke. (in Dutch)*
- Wintle, A.G. (1973) *Anomalous fading of thermoluminescence in mineral samples. Nature 245: p. 143-144.*
- Wintle, A.G. (2008) *Luminescence dating: where it has been and where it is going. Boreas, Vol. 37: p. 471-482. 10.1111/j.1502-3885.2008.00059.x. ISSN 0300-9483.*
- Wintle, A.G., Huntley D.J. (1979b) *Thermoluminescence dating of sediments. PACT, 3: p. 374-380*
- Wintle, A. G. & Murray, A. S. (2000) *Quartz OSL: Effects of thermal treatment and their relevance to laboratory dating procedures. Radiation Measurements 32: p. 387-400.*

LIST OF FIGURES

Figure I-1: Coloured plastic tracers in an experimental flume (www.florentgrasso.com)	3
Figure II-1: Microscopic picture of minerals (luminescence test sub-sample)	9
Figure II-2: Different components contributing to accumulation of luminescence signal (modified from Preusser et al. 2008)	10
Figure II-3: Energy level diagram (modified from Aitken 1998).....	11
Figure II-4: Energy level diagram (modified from Aitken 1998)	11
Figure II-5: Schematic sediment age determination. (A) Burial cycles; accumulation and resetting. (B) Example of bleaching curve(s) during exposure.	12
Figure II-6: Coastal phenomena time- and length scales (Modified from Dronkers 2005)	13
Figure II-7: Schematic sand transport time determination. (C) Bleaching curve with different signals (different bleaching rates). (D) Residual dose curves as a measure for transport time	13
Figure II-8: Bleaching curve(s) (1) IR50-pIRIR290 protocol (modified from Buylaert et al 2012)(2) MET-pIRIR protocol: IR50-pIRIR80-110-140-170 (modified from Fu & Li 2013).....	14
Figure II-9: Measured light spectrum in respect to water depth (from Sanderson et al. 2007).....	15
Figure III-1: Sand Engine dimensions (dashed) and monitoring area (solid), on concept drawing	19
Figure III-2: Bathymetry measurement equipment (source: Shore Monitoring & Research). Wheelie/Backpack GPS (left), 4wd quad with GPS (middle), Jet ski fitted with GPS and single beam echo sounder (right)	20
Figure III-3: General evolution of the Sand Engine spit.....	21
Figure III-4: Sampling on the Sand Engine using the 'Van der Staay' suction corer. Coring using the corer(left), Samples in light tight containers (PVC-tube)(right).	22
Figure III-5: Sampling core positions (May 2012 bathymetry)	23
Figure III-6: Sample cores vs. monthly bathymetry (Aug-2011 - Jun 2012)	24
Figure III-7: Detailed bathymetry descriptions per core sample.....	25
Figure IV-1: Luminescence curves (I) Shine down curve (Blue OSL; Quartz) (II) Shine down curve (IRSL; Feldspar) (III) Shine down curve (pIRIR-SL; Feldspar) (IV) Glow curve (TL; Feldspar + Quartz). The dots represent the light counts per set interval.....	32
Figure IV-2: Equivalent dose determination scheme.....	33
Figure IV-3: PMS-SAR test results OSL signal	35
Figure IV-4: PMS-SAR test results TL signal.....	36
Figure IV-5: (A) Equivalent dose values, and standard error for all seven samples and (B) the sample positions (equal to graph signs) relative to the Sand Engine (contour June 2012).....	37
Figure IV-6: (A) homogeneously poorly bleached (B) heterogeneously mixed bleached (right skewed distr.) (C) homogeneously well bleached. The dotted contours are distribution shapes in between A, B and C.	38
Figure IV-7: Kernel density estimation plots from fast-to-bleach signals of all selected samples.....	38
Figure IV-8: Kernel density estimation plots from slow-to-bleach signals of all selected samples	39
Figure IV-9: Bleaching experiment curves for the five different signals	40
Figure IV-10: Kernel density estimation graphs of the bleaching experiment fast-to-bleach signals... ..	40
Figure IV-11: Kernel density estimation graphs of the bleaching experiment slow-to-bleach signals ..	41

Figure IV-12: Effective Exposure Time (EET) interpolation	41
Figure V-1: Mean Equivalent Exposure Time (negative values cannot be shown).....	44
Figure V-2: Mean Equivalent Exposure Time (fast-to-bleach signals)	45
Figure V-3: Source control samples	46
Figure V-4: Distance vs. mean equivalent exposure time ('distance', 'depth')	47
Figure V-5: Kernel Density Estimation EET values (ZM-05-A1, ZM-08-A2 and ZM-07-A1).....	48
Figure V-6: Top view of ZM-08-A2. Marked is the long shore channel that was formed between the inner lagoon and the sea	48
Figure V-7: Cross section (1 -- 1) of core ZM-08-A2. (A) Presumable erosion path (B) Case of severe erosion between monthly bathymetry surveys.....	49
Figure V-8: (A) EET values ZM-05-A1 and ZM-05-B2 (B) EET values ZM-07-A1 and ZM-07-B2.....	50
Figure V-9: Typical long shore sediment transport concentration depth profile (Modified from Bosboom & Stive 2011; Figure 6-8) (B) Schematically interpreted light penetration vs. water depth, without and with the turbidity by sediment in suspension (Modified from Boyd 2000; Figure 1.6)	50
Figure V-10: Schematic representation of transport distance vs. mode of transport	51

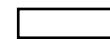
LIST OF TABLES

Table I-1: Assumptions on the use of tracers in particle tracing studies (after Foster 2000).....	2
Table III-1: Average grain size Sand Engine	21
Table III-2: Sediment grain size samples from the eroded part of the Sand Engine.....	21
Table III-3: Overview selected samples.....	26
Table III-4: Grain size analysis results.....	27
Table IV-1: Signal intervals for the natural signal and test signal calculation.....	33
Table IV-2: Luminescence measurement protocol (PMS-SAR).....	34
Table IV-3: Dynamic range per luminescence signal	40

APPENDIX 1: SUMMARY RECENT STUDIES

Author	Nature of research	Methodology
Keisars et al. (2008)	Natural residual thermoluminescence (NTRL) as a method of analysis of sand transport along the coast of the St. Joseph Peninsula, Florida	Quartz Thermo Luminescence 8mm mask aliquot 90-150 µm & 150-212 µm
	Site area: 19.2 km along shore, St. Joseph Peninsula, Florida	Sampling strategy: Underwater (1 m), top first 2-3 cm.(~km(s) spatial diff.)
Conclusion(s):	<ul style="list-style-type: none"> The NTRL signal decreases with distance travelled. With bleaching experiments an empirical estimation is given for the exposure duration. This exposure cannot be a measure for the velocity of sand transport a alongshore only with confidence a measure is given for the swash/littoral zone residence times in salt water; <i>Significant difference using 90-150 µm or 150-212µm</i> implies that for shorter studies using TL it is better to use smaller grain size fractions and for larger areas using larger grain size fractions is recommended. 	
Liu et al. (2011)	Monitoring the nourished sand long shore movement based on luminescence measurement	Feldspar Thermo Lumi.& Optical Stimulated Lumi. 10 mm mask aliquot 180-300 µm
	Site area: 13 km alongshore, Miyazaki Coast, 17 km alongshore, Shounan Coast, Japan	Sampling strategy: Surface, 10 cm beneath the top level.(~100 m(s) spatial diff.)
Conclusion(s):	<ul style="list-style-type: none"> The nourished sediment exhibited high luminescence values compared to the native beach sediment. Between the measurement erosive spots were identified in this was because of low values measured there inside the nourishment area; After a storm event between measurements traces of this high signal grains were found further alongshore of the nourishment. Proving the capability to monitor the movement of nourished sand 	
Sawakuchi et al. (2012)	Quartz OSL sensitivity as a proxy for storm activity on the southern Brazilian coast during the late Holocene	Quartz Optical Stim. Lumi. Single grain aliquot 180-250 µm Multi grain aliquot (10 mm) 120-150 µm
	Site area: 55 km alongshore, Ilha Comprida barrier, Brazil	Sampling strategy: Surface (~10 km(s) spatial diff.)
Conclusion(s):	<ul style="list-style-type: none"> The more bleaching cycles a quartz grain has undergone the more sensitive it becomes (sensitive meaning the light intensity emitted per unit radiation dose [per Gy], the higher the output the more sensitive is quartz grain); A sensitivity increase is measured pre-storm in south-west direction because of the low sensitivity quartz grains supplied by the Ribeira de Iguape River on the southern end of the study area and after the storm this increase was in northeast direction because of the supplying of high sensitive grains from the coastal area. Proven the provenance (or spatial sourcing) capability. 	

Appendix 1: Summary of recent geomorphologic luminescence studies



APPENDIX 2: CORE SAMPLE DETAILS

		Sample name	Upper [m]	Lower [m]	Deposition month***
Location	Point001	ZM-03-A1	1.809	1.609	Augustus 2011
Sampling date	31/05/2012	ZM-03-A2	1.509	1.309	Augustus 2011
		ZM-03-B1	1.009	0.809	Augustus 2011
xRD [m]*	72939.640	ZM-03-B2	0.709	0.509	Augustus 2011
yRD [m]*	453036.500	ZM-03-C1	0.359	0.159	Augustus 2011
zRD [m]**	2.009	ZM-03-C2	-0.041	-0.241	Augustus 2011
<hr/>					
Location	Point002	ZM-04-A1	1.024	0.824	May 2012
Sampling date	31/05/2012	ZM-04-B1	0.574	0.374	October 2011
		ZM-04-B2	0.174	0.024	September 2011
xRD [m]	73247.300	ZM-04-C1	-0.276	-0.426	September 2011
yRD [m]	453096.800	ZM-04-C2	-0.626	-0.776	September 2011
zRD [m]	1.324	ZM-04-D1	-0.926	-1.076	September 2011
		ZM-04-D2	-1.326	-1.476	Augustus 2011
<hr/>					
Location	Point003	ZM-05-A1	-0.305	-0.455	November 2011
Sampling date	31/05/2012	ZM-05-A2	-0.655	-0.805	November 2011
		ZM-05-B1	-1.205	-1.355	November 2011
xRD [m]	73450.140	ZM-05-B2	-1.555	-1.705	November 2011
yRD [m]	453108.300	ZM-05-C1	-1.705	-1.855	October 2011
zRD [m]	0.595	ZM-05-C2	-2.055	-2.205	September 2011
<hr/>					
Location	Point004	ZM-06-A1	-0.474	-0.624	December 2011
Sampling date	31/05/2012	ZM-06-A2	-0.824	-1.024	December 2011
xRD [m]	73679.670				
yRD [m]	453188.000				
zRD [m]	0.276				
<hr/>					
Location	Onspit	ZM-10-A1	0.202	0.002	February 2012
Sampling date	05/06/2012				
xRD [m]	73829.230				
yRD [m]	453246.800				
zRD [m]	0.602				

Location	Rescue south	ZM-09-A1	-0.711	-0.861	January 2012
Sampling date	05/06/2012	ZM-09-A2	-1.011	-1.161	December 2011
xRD [m]	73836.750				
yRD [m]	453316.200				
zRD [m]	-0.111				

Location	Rescue	ZM-08-A1	-0.581	-0.731	December 2011
Sampling date	05/06/2012	ZM-08-A2	-0.881	-1.031	December 2011
		ZM-08-B1	-1.281	-1.431	Augustus 2011
xRD [m]	73958.320	ZM-08-B2	-1.581	-1.731	Augustus 2011
yRD [m]	453368.500				
zRD [m]	0.019				

Location	Endspit	ZM-07-A1	-0.843	-0.993	January 2012
Sampling date	05/06/2012	ZM-07-B1	-1.343	-1.493	Augustus 2011
		ZM-07-B2	-1.693	-1.843	Augustus 2011
xRD [m]	74071.020				
yRD [m]	453456.400				
zRD [m]	0.602				

- * GPS data (RD means Rijksdriehoekmeting, Dutch standard coordinate system)
- ** Bathymetry data [m]
- *** Data from Figure III-7, Estimated(!)

Appendix 2: Core sample details, samples

APPENDIX 3: POLYMINERAL PERFORMANCE TEST

Stimulation		Temperature [°C]	Mineral	Mask size [mm]	Filter	No. aliquots*	Eq. dose value	
							Mean dose [Gy]	Mean Error [Gy]
Infrared	IR	25	Polymineral	8	U-340	8	12.009	0.305
Infrared	pIRIR	90	Polymineral	8	U-340	8	31.985	1.439
Infrared	pIRIR	155	Polymineral	8	U-340	5	38.987	1.221
Infrared	pIRIR	225	Polymineral	8	U-340	8	33.669	0.888
Blue	OSL	125	Polymineral	8	U-340	8	5.252	0.451
Heat	TL	300	Polymineral	8	U-340	8	85.024	0.658
Infrared	IR	25	Polymineral	8	I-410	6	20.104	1.739
Infrared	pIRIR	90	Polymineral	8	I-410	5	56.756	2.553
Infrared	pIRIR	155	Polymineral	8	I-410	6	66.962	3.288
Infrared	pIRIR	225	Polymineral	8	I-410	6	71.280	8.151
Blue	OSL	125	Polymineral	-	I-410	-	-	-
Heat	TL	300	Polymineral	-	I-410	-	-	-
Infrared	IR	25	K-Feldspar	2.5	U-340	7	16.443	1.502
Infrared	pIRIR	90	K-Feldspar	2.5	U-340	5	46.343	3.352
Infrared	pIRIR	155	K-Feldspar	2.5	U-340	4	43.460	2.449
Infrared	pIRIR	225	K-Feldspar	2.5	U-340	6	66.359	8.797
Blue	OSL	125	K-Feldspar	-	U-340	-	-	-
Heat	TL	300	K-Feldspar	-	U-340	-	-	-
Infrared	IR	25	K-Feldspar	2	I-410	17	22.374	0.658
Infrared	pIRIR	90	K-Feldspar	2	I-410	17	48.422	1.491
Infrared	pIRIR	155	K-Feldspar	2	I-410	17	72.412	2.978
Infrared	pIRIR	225	K-Feldspar	2	I-410	17	83.607	1.844
Blue	OSL	125	K-Feldspar	-	I-410	-	-	-
Heat	TL	300	K-Feldspar	2	I-410	4	49.664	1.058
Infrared	IR	25	Quartz	-	U-340	-	-	-
Infrared	pIRIR	90	Quartz	-	U-340	-	-	-
Infrared	pIRIR	155	Quartz	-	U-340	-	-	-
Infrared	pIRIR	225	Quartz	-	U-340	-	-	-
Blue	OSL	125	Quartz	2.5	U-340	15	12.735	0.788
Heat	TL	300	Quartz	5	U-340	12	89.556	1.971

* Rejection criteria: Recycling ratio difference <20%, Test dose error <20% and Signal min.>3 times the Background level

Appendix 3: Summation Polymineral performance test measurements (300-355 μm)

APPENDIX 4: CORE SAMPLE MEASUREMENTS

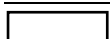
Stimulation		Temp [°C]	Mineral	Filter	No. aliquots*	Eq. dose value		
Sample	NCL-code			Mask size [mm]		Mean dose [Gy]	Mean Error [Gy]	
ZM-03-A1		13 12 149			24 (total)			
Infrared	IR	25	Polymineral	8	U-340	24	57.496	4.758
Infrared	pIRIR	90	Polymineral	8	U-340	20	76.575	6.133
Infrared	pIRIR	155	Polymineral	8	U-340	20	87.064	6.532
Infrared	pIRIR	225	Polymineral	8	U-340	24	69.417	2.661
Blue	OSL	125	Polymineral	8	U-340	24	60.260	2.338
Heat	TL	300	Polymineral	8	U-340	24	67.475	2.053
ZM-03-C2		13 12 154			24 (total)			
Infrared	IR	25	Polymineral	8	U-340	19	46.334	5.380
Infrared	pIRIR	90	Polymineral	8	U-340	9	63.528	12.192
Infrared	pIRIR	155	Polymineral	8	U-340	11	84.636	9.514
Infrared	pIRIR	225	Polymineral	8	U-340	19	81.927	5.726
Blue	OSL	125	Polymineral	8	U-340	17	69.602	5.422
Heat	TL	300	Polymineral	8	U-340	19	76.037	5.672
ZM-05-A1		14 12 162			24 (total)			
Infrared	IR	25	Polymineral	8	U-340	24	35.644	2.265
Infrared	pIRIR	90	Polymineral	8	U-340	18	66.326	4.791
Infrared	pIRIR	155	Polymineral	8	U-340	22	70.357	4.913
Infrared	pIRIR	225	Polymineral	8	U-340	24	57.422	1.974
Blue	OSL	125	Polymineral	8	U-340	24	44.743	3.489
Heat	TL	300	Polymineral	8	U-340	24	63.301	2.519
ZM-05-B2		14 12 165			24 (total)			
Infrared	IR	25	Polymineral	8	U-340	16	15.820	2.985
Infrared	pIRIR	90	Polymineral	8	U-340	14	39.166	5.710
Infrared	pIRIR	155	Polymineral	8	U-340	13	60.132	10.466
Infrared	pIRIR	225	Polymineral	8	U-340	16	44.365	3.690
Blue	OSL	125	Polymineral	8	U-340	8	5.252	1.079
Heat	TL	300	Polymineral	8	U-340	8	85.024	6.583
ZM-08-A2		14 12 174			24 (total)			
Infrared	IR	25	Polymineral	8	U-340	23	29.270	3.931
Infrared	pIRIR	90	Polymineral	8	U-340	15	54.998	8.506
Infrared	pIRIR	155	Polymineral	8	U-340	20	73.304	5.454
Infrared	pIRIR	225	Polymineral	8	U-340	22	62.514	2.940
Blue	OSL	125	Polymineral	8	U-340	23	14.363	1.983
Heat	TL	300	Polymineral	8	U-340	23	61.818	2.471
ZM-07-A1		14 12 170			24 (total)			
Infrared	IR	25	Polymineral	8	U-340	24	6.180	0.807
Infrared	pIRIR	90	Polymineral	8	U-340	22	24.243	2.516
Infrared	pIRIR	155	Polymineral	8	U-340	23	35.023	4.331
Infrared	pIRIR	225	Polymineral	8	U-340	20	34.973	2.518



Blue	OSL	125	Polymineral	8	U-340	24	3.056	0.692
Heat	TL	300	Polymineral	8	U-340	24	68.336	6.544
ZM-07-B2						24 (total)		
Infrared	IR	25	Polymineral	8	U-340	23	12.682	2.539
Infrared	pIRIR	90	Polymineral	8	U-340	6	37.295	11.808
Infrared	pIRIR	155	Polymineral	8	U-340	11	43.422	2.121
Infrared	pIRIR	225	Polymineral	8	U-340	17	40.139	3.557
Blue	OSL	125	Polymineral	8	U-340	24	7.030	1.479
Heat	TL	300	Polymineral	8	U-340	24	51.163	2.603
ZM-01						24 (total)		
Infrared	IR	25	Polymineral	8	U-340	22	0.536	0.120
Infrared	pIRIR	90	Polymineral	8	U-340	3	1.402	1.524
Infrared	pIRIR	155	Polymineral	8	U-340	7	4.350	1.077
Infrared	pIRIR	225	Polymineral	8	U-340	19	30.181	1.707
Blue	OSL	125	Polymineral	8	U-340	24	0.811	0.130
Heat	TL	300	Polymineral	8	U-340	24	33.325	0.577

* Rejection criteria: Recycling ratio difference <20%, Test dose error <20% and Signal min.>3 times the Background level

Appendix 4: Summation sample measurements (300-355 μm)



APPENDIX 5: BLEACHING EXPERIMENT MEASUREMENTS

Stimulation		Temperature [°C]	Mineral	Filter	No. aliquots*	Eq. dose value		
Bleaching time						Mean dose [Gy]	Mean Error [Gy]	
0.05 min				Mask size [mm]	24 (total)			
Infrared	IR	25	Polymineral	8	U-340	8	33.547	1.167
Infrared	pIRIR	90	Polymineral	8	U-340	2	58.909	3.148
Infrared	pIRIR	155	Polymineral	8	U-340	3	75.005	8.400
Infrared	pIRIR	225	Polymineral	8	U-340	8	92.296	4.020
Blue	OSL	125	Polymineral	8	U-340	8	22.481	0.821
Heat	TL	300	Polymineral	8	U-340	8	44.297	1.557
0.5 min						24 (total)		
Infrared	IR	25	Polymineral	8	U-340	7	5.689	0.145
Infrared	pIRIR	90	Polymineral	8	U-340	1	30.000	2.000
Infrared	pIRIR	155	Polymineral	8	U-340	4	44.284	4.298
Infrared	pIRIR	225	Polymineral	8	U-340	6	48.151	2.331
Blue	OSL	125	Polymineral	8	U-340	8	1.789	0.200
Heat	TL	300	Polymineral	8	U-340	8	35.346	0.859
1 min						24 (total)		
Infrared	IR	25	Polymineral	8	U-340	8	5.465	0.184
Infrared	pIRIR	90	Polymineral	8	U-340	3	28.861	2.789
Infrared	pIRIR	155	Polymineral	8	U-340	3	45.873	4.869
Infrared	pIRIR	225	Polymineral	8	U-340	7	65.801	2.196
Blue	OSL	125	Polymineral	8	U-340	8	1.903	0.172
Heat	TL	300	Polymineral	8	U-340	8	44.408	1.214
5 min						24 (total)		
Infrared	IR	25	Polymineral	8	U-340	8	1.839	0.140
Infrared	pIRIR	90	Polymineral	8	U-340	3	18.601	1.269
Infrared	pIRIR	155	Polymineral	8	U-340	3	34.732	3.006
Infrared	pIRIR	225	Polymineral	8	U-340	8	66.524	2.483
Blue	OSL	125	Polymineral	8	U-340	8	1.139	0.215
Heat	TL	300	Polymineral	8	U-340	8	41.952	1.281
10 min						24 (total)		
Infrared	IR	25	Polymineral	8	U-340	8	1.729	0.175
Infrared	pIRIR	90	Polymineral	8	U-340	3	11.444	0.784
Infrared	pIRIR	155	Polymineral	8	U-340	5	25.363	1.710
Infrared	pIRIR	225	Polymineral	8	U-340	8	57.156	2.183
Blue	OSL	125	Polymineral	8	U-340	8	0.912	0.197
Heat	TL	300	Polymineral	8	U-340	8	39.984	1.360
50 min						24 (total)		
Infrared	IR	25	Polymineral	8	U-340	8	1.110	0.069
Infrared	pIRIR	90	Polymineral	8	U-340	5	8.505	0.880

Infrared	pIRIR	155	Polymineral	8	U-340	6	23.935	1.913
Infrared	pIRIR	225	Polymineral	8	U-340	8	31.677	1.012
Blue	OSL	125	Polymineral	8	U-340	8	0.662	0.156
Heat	TL	300	Polymineral	8	U-340	8	39.720	1.247
100 min						24 (total)		
Infrared	IR	25	Polymineral	8	U-340	8	0.481	0.102
Infrared	pIRIR	90	Polymineral	8	U-340	5	1.748	0.651
Infrared	pIRIR	155	Polymineral	8	U-340	4	5.809	0.994
Infrared	pIRIR	225	Polymineral	8	U-340	8	29.215	1.724
Blue	OSL	125	Polymineral	8	U-340	8	0.775	0.108
Heat	TL	300	Polymineral	8	U-340	8	31.048	1.451
1000 min						24 (total)		
Infrared	IR	25	Polymineral	8	U-340	8	0.671	0.193
Infrared	pIRIR	90	Polymineral	8	U-340	2	0.938	0.910
Infrared	pIRIR	155	Polymineral	8	U-340	1	3.345	1.048
Infrared	pIRIR	225	Polymineral	8	U-340	3	20.977	1.597
Blue	OSL	125	Polymineral	8	U-340	8	0.552	0.122
Heat	TL	300	Polymineral	8	U-340	8	25.104	1.383
5000 min						24 (total)		
Infrared	IR	25	Polymineral	8	U-340	7	0.275	0.241
Infrared	pIRIR	90	Polymineral	8	U-340	1	-	-
Infrared	pIRIR	155	Polymineral	8	U-340	1	7.089	0.740
Infrared	pIRIR	225	Polymineral	8	U-340	6	20.100	1.846
Blue	OSL	125	Polymineral	8	U-340	8	1.172	0.213
Heat	TL	300	Polymineral	8	U-340	8	15.248	2.392

* Rejection criteria: Recycling ratio difference <20%, Test dose error <20% and Signal min.>3 times the Background level

Appendix 5: Summation bleaching experiment measurements (300-355 μm)